

Original Article

Integrative revision of the *Lygodactylus gutturalis* (Bocage, 1873) complex unveils extensive cryptic diversity and traces its evolutionary history

Javier Lobón-Rovira^{1,2,3,*}, Aaron M. Bauer⁴, Pedro Vaz Pinto^{1,2,3,5}, Jean-Francois Trape⁶, Werner Conradie^{7,8}, Chifundera Kusamba^{9,10}, Timóteo Júlio⁵, Garin Cael¹¹, Edward L. Stanley¹², Daniel F. Hughes¹³, Mathias Behangana¹⁴, Franck M. Masudi¹⁵, Olivier S.G. Pauwels¹⁶, Eli Greenbaum¹⁷

¹CIBIO, Centro de Investigação em Biodiversidade e Recursos Genéticos, InBIO Laboratório Associado, Campus de Vairão, Universidade do Porto, 4485-661 Vairão, Portugal

²Departamento de Biologia, Faculdade de Ciências, Universidade do Porto, 4099-002 Porto, Portugal ³BIOPOLIS Program in Genomics, Biodiversity and Land Planning, CIBIO, Campus de Vairão, 4485-661 Vairão, Portugal ⁴Department of Biology and Center for Biodiversity and Ecosystem Stewardship, Villanova University, Villanova, PA 18947, United States ⁵Fundação Kissama, Rua 60 Casa 560, Lar do Patriota, Luanda, Angola

⁶Laboratoire de Paludologie et Zoologie Médicale, Institut de Recherche pour le Développement, UMR MIVEGEC, 10200 Dakar, Senegal

⁷Port Elizabeth Museum (Bayworld), P.O. Box 13147, 6013 Humewood, South Africa

⁸Department of Nature Conservation Management, Natural Resource Science and Management Cluster, Faculty of Science, George Campus, Nelson Mandela University, 6031 George, South Africa

⁹Laboratoire d'Herpétologie, Département de Biologie, Centre de Recherche en Sciences Naturelles, Lwiro, République Démocratique du Congo ¹⁰Laboratory of Ecology and Wildlife Resources Management, Department of Biology, Faculty of Sciences, National Pedagogical University, Kinshasa, Democratic Republic of the Congo

¹¹Royal Museum for Central Africa, Leuvensesteenweg 13, 3080 Tervuren, Belgium
 ¹²Division of Digital Imaging, Florida Museum of Natural History, University of Florida, Gainesville, FL 32611, United States
 ¹³Department of Biology, Coe College, Cedar Rapids, IA 52402, United States

¹⁴Department of Environmental Sciences, Makerere University, P.O. Box 7062, Kampala, Uganda
¹⁵Department of Ecology and Biodiversity of Earth Resources, Centre de Surveillance de la Biodiversité of the University of Kisangani, Democratic Republic of the Congo

¹⁶Département des Vertébrés Récents, Royal Belgian Institute of Natural Sciences, 1000 Brussels, Belgium
¹⁷Department of Biological Sciences, University of Texas at El Paso, El Paso, TX 79968, USA

http://zoobank.org/E44C651C-4485-44B8-9B86-B05C9CBF57CC

'Corresponding author: CIBIO, Centro de Investigação em Biodiversidade e Recursos Genéticos, InBIO Laboratório Associado, Campus de Vairão, Universidade do Porto, 4485-661 Vairão, Portugal. E-mail: j.lobon.rovira@cibio.up.pt

ABSTRACT

Lygodactylus is the most speciose gekkonid group in Africa, with several additional, candidate species already identified from previous studies. However, in mainland Africa, several groups remain only partially resolved, and there are several taxonomic inconsistencies. Lygodactylus gutturalis was described from Guinea-Bissau in the 1870s and since then, the species has been recorded from West to East Africa, and it is widely distributed through different biomes and ecoregions. However, this taxon has never been studied in detail. In this work, we use an integrative approach, including molecular phylogenetic analysis, morphometrics, skull osteology, and biogeography to provide the first systematic revision of the L. gutturalis species complex. The L. gutturalis complex is a subgroup within the L. picturatus group and includes nine well-differentiated species. We elevate Lygodactylus gutturalis dysmicus to full species status, recognize Lygodactylus depressus as the sister species to L. gutturalis, describe five new species (Lygodactylus kibera sp. nov., Lygodactylus karamoja sp. nov., Lygodactylus mirabundus sp. nov., Lygodactylus leopardinus sp. nov., and Lygodactylus gamblei sp. nov.), and propose an additional candidate species that requires further research. Also, in order to shed light on some taxonomic inconsistencies between the L. gutturalis and Lygodactylus angularis groups, we revisit the L. angularis group, within

which we elevate *Lygodactylus angularis heeneni* and *Lygodactylus angularis paurospilus* to full species status. The *L. gutturalis* subgroup diversified during the Late Miocene (between 5–15 Mya), probably as a consequence of multiple vicariant events driven by the expansion of the African savannahs and the establishment of climatic refugia.

Keywords: Africa; biogeography; climatic refugia; CT-scan; Gekkonidae; Miocene; phylogeny; systematics

INTRODUCTION

Lygodactylus Gray, 1864 is a genus of day geckos commonly referred to as African dwarf geckos, which represent the most speciose group of Gekkonidae in Africa and the fifth-most diverse genus in the world, with 82 recognized species (Röll et al. 2010, Gippner et al. 2021, Vences et al. 2022) and more than 20 new candidate species (Puente et al. 2009, Conradie et al. 2016, Lanna et al. 2018, Belluardo et al. 2021, Gippner et al. 2021, Vences et al. 2022). With a probable Malagasy origin (Röll et al. 2010, Mezzasalma et al. 2017, Gippner et al. 2021), Lygodactylus has an important area of diversification in south-eastern Africa, from Kenya to eastern South Africa, with over 40 species from this region (Röll et al. 2010, Travers et al. 2014, Malonza et al. 2016, 2019, Gippner et al. 2021). However, more than 15 species from mainland Africa have never been included in a phylogenetic analysis (including species from all different phylogenetic groups identified by Gippner et al. 2021) and, therefore, evolutionary patterns in this group remain incompletely understood.

A recent revision of Lygodactylus (Gippner et al. 2021) resolved this speciose genus into four main monophyletic clades: two strictly Malagasy clades (Clade A and B), an Afro-American clade (Clade C), and an Afro-Malagasy clade (Clade D). Whereas clades A and B have been mostly resolved, the species-level taxonomy of the mainland Africa clades is still in need of revision (Gippner et al. 2021, Vences et al. 2022). The Afro-American clade (Clade C) is characterized by having some representatives with vivid dorsal coloration and gular patterning in central and eastern Africa, and some dull-coloured species in South America. This clade includes four well-differentiated groups: the Lygodactylus picturatus group (14 species), the Lygodactylus fischeri group (five species), the Lygodactylus klugei group (two species + three candidate species), and the Lygodactylus angularis group (two species). Below, we focus on the *L. picturatus* and *L. angularis* groups.

The L. picturatus group is a species complex and one of the most diverse mainland African groups with 14 nominal taxa (Röll et al. 2010, Malonza et al. 2016, 2019, Gippner et al. 2021). Nevertheless, as mentioned above, some species within this group have never been included in a molecular phylogenetic analysis, and therefore, their evolutionary relationships remain unknown (e.g. Lygodactylus depressus Schmidt, 1919; Lygodactylus inexpectatus Pasteur, 1965 (1964); Lygodactylus manni Loveridge, 1928; Lygodactylus scortecii Pasteur, 1959; Lygodactylus picturatus sudanensis Loveridge, 1935; and Lygodactylus gutturalis dysmicus Perret, 1963) (Röll et al. 2010, Malonza et al. 2016, 2019, Gippner et al. 2021). Some Lygodactylus cf. gutturalis sequences from Uganda (obtained from Röll et al. 2010) and Tanzania (obtained from the specimen PEM R16817) were included in Gippner et al. (2021) as L. manni. However, the species was previously identified as L. cf. gutturalis and mislabelled in Gippner et al. (2021) as L. manni 'in error', recovering L. manni as the sister species to *Lygodactylus gutturalis* (Bocage, 1873). Thus, the placement of *L*.

manni remains to be molecularly confirmed and its phylogenetic relationships remain unclear. Furthermore, previous molecular analyses have shown minor genetic differences between some described species (e.g. Lygodactylus mombasicus Loveridge, 1935 and Lygodactylus kimhowelli Pasteur, 1995), calling into question the taxonomic status of some taxa (Röll et al. 2010, Castiglia and Annesi 2011, Malonza et al. 2016, 2019, Gippner et al. 2021).

The L. picturatus group can be subdivided into four main subgroups based on coloration and molecular affinities (Röll et al. 2010, Gippner et al. 2021): (1) the L. picturatus subgroup (including L. depressus, L. inexpectatus, Lygodactylus keniensis Parker, 1936, L. kimhowelli, L. manni, L. mombasicus, Lygodactylus picturatus picturatus (Peters, 1870), L. picturatus sudanensis, L. scortecii, Lygodactylus tsavoensis Malonza, et al. 2019, and Lygodactylus wojnowskii Malonza, Granthon & Williams, 2016). This subgroup is characterized by males with bright yellow to white heads with blueish to grey dorsal coloration on the dorsum (Loveridge 1947); (2) Lygodactylus williamsi Loveridge, 1952 (with only one representative) is characterized by its bright blue dorsal coloration from the snout to tip of the tail (Loveridge 1952); (3) Lygodactylus chobiensis FitzSimons, 1932 (with only one representative) and (4) the L. gutturalis complex that are characterized by their dull brown dorsal coloration and unique gular patterning (Bocage 1873, FitzSimons 1932).

Lygodactylus depressus is remarkable because it is only known from century-old specimens, and is a biogeographic outlier compared to its hypothesized closest relatives. Whereas all the other members within the L. picturatus subgroup are known from the Kenyan Rift and relatively dry areas east of it, and have vivid yellowish-blueish coloration, L. depressus is the only representative of lowland rainforest west of the Albertine Rift. It was described from Medje, Haut-Uele Province [Democratic Republic of the Congo (DRC)] and has a distinct dark blueish-grey dorsal coloration (Schmidt 1919). The only diagnostic feature provided by Schmidt (1919: 185) to distinguish this species from L. gutturalis (found in sympatry) was 'ventral and subcaudal scales yellow in life', which is a character frequently found in L. gutturalis individuals (Trape et al. 2012).

Lygodactylus gutturalis has the widest distribution of any Lygodactylus, occurring from Senegal in West Africa to Ethiopia and south-west Somalia and south to the former Katanga region of DRC (de Witte 1953, Håkansson 1981, Lanza 1990, Broadley and Cotterill 2004, Bauer et al. 2006, Chirio and Ineich 2006, Largen and Spawls 2006, Chirio and LeBreton 2007, Auliya et al. 2012, Trape et al. 2012, Segniagbeto et al. 2015, Spawls et al. 2018, Behangana et al. 2020). The species was described in 1873 by Bocage, as part of the genus Hemidactylus, based on the divided toepad of the type series. The type series was collected from Bissau, Guinea-Bissau by Mr Sá Nogueira, a naval employee from Cape Verde in 1870. In 1885, Boulenger moved the species to Lygodactylus. Unfortunately, part of the type series was lost in a fire that devastated the Lisbon Museum of Bocage (MBL) in

1978. However, two specimens from this series had been sent by Bocage to the Natural History Museum of London (BMNH) and Museum für Naturkunde Berlin (ZMB), where they were assigned the registration numbers BMNH 1875.4.26.8 and ZMB 7771, respectively. Bocage (1873) provided an accurate and concise description of L. gutturalis, which has contributed to the unequivocal identification of the species. Thus, L. gutturalis is characterized by its large size, gular patterning with two or three dark \cap -shaped chevrons, dull brown to grey colour on the dorsum, and 6–8 precloacal pores (Bocage 1873, Boulenger 1885, Spawls *et al.* 2018). Nevertheless, morphological similarities to another species group, the L. angularis group, have caused some taxonomic confusion between these clades.

Lygodactylus angularis was described by Günther (1893) 20 years after Bocage (1873) described L. gutturalis, based on a specimen from the Shire Highlands, Nyassaland (now Malawi). The two species were geographically separated with clear morphological differences between them. Whereas L. angularis exhibited, as described by Günther (1893: 556), a 'throat with three or four concentric V-shaped blue lines, the angles being directed backwards', whereas *L. gutturalis* had two or three dark ∩-shaped chevrons that converged anteriorly (Bocage 1873: 211). Between 1933 and 1969, four nominal taxa (species or subspecies) within the L. angularis group were described (Lygodactylus angularis heeneni de Witte, 1933; Lygodactylus angularis paurospilus Laurent, 1952; Lygodactylus angularis dysmicus Perret, 1963; Lygodactylus angularis grzimeki Bannikov & Darevsky, 1969). However, the brief descriptions of some taxa, combined with the lack of molecular data, have led to some taxonomic misidentifications among these two groups of Lygodactylus with ornamented throats (Pasteur, 1965(1964)).

In 1933, de Witte described L. heeneni from Kapiri, Lualaba Province, DRC, as a full species, based on the gular patterning and number of precloacal pores which differ from L. angularis. However, Loveridge (1947: 222), treated it as a subspecies of *L*. angularis, stating it '... differs from the typical form only in the obsolescent gular markings of the female which, in typical form, are equally well developed in both sexes' Nevertheless, Loveridge (1947) did not examine any male specimens of L. heeneni and disregarded the original description provided by de Witte (1933). Surprisingly, this taxonomic change was followed by de Witte (1953) without any further comment. However, Pasteur, 1965(1964), in his detailed revision of Lygodactylus, strongly criticized Loveridge's action and suggested that L. heeneni should be recognized as a valid species. Nonetheless, Perret (1963) and Broadley (1991) treated *L. heeneni* as a subspecies of *L. angularis* without further explanation. Subsequently, Broadley (1998) and later Haagner et al. (2000) treated it as a full species, again without justification. In their review of reptiles of the former Katanga region of DRC, Broadley and Cotterill (2004: 41) included the first taxonomic remarks: 'This form was described as a subspecies of L. angularis Günther, common in buildings on the Zambian copperbelt, but there is no indication of intergradation in throat pattern, and they are best regarded as sister species'. Since then, some authors have considered L. heeneni as a valid species (Haagner et al. 2000, Pietersen et al. 2021) or as a subspecies (Rösler 2000), without further evidence.

Laurent (1952) named L. angularis paurospilus based on an insufficient description of two specimens (one male and one

female) from Haute Lubitshako (1900-2000 m a.s.l.), South Kivu Province, DRC, which is located on the Kabobo Plateau (sensu Hirschfeld et al. 2015). He identified some morphological similarities of L. a. paurospilus to both L. heeneni and L. angularis, such as 'typical gular pattern, however, the line that constitutes the chevrons resembles irregular spots', 'three postmentals as in heeneni Witte but seven precloacal pores as in angularis Günther ...' (translated from original in French; Laurent 1952: 18). However, Pasteur, 1965(1964) questioned the validity of this taxon based on the inadequate description provided by Laurent, which seemed to overlap morphologically with L. a. heeneni. The following year, Wermuth (1965) included L. a. paurospilus as a valid taxon. Greenbaum and Kusamba (2012) suggested a species-level status for this taxon because of its distribution in isolated highlands, and the substantial distance (over 1000 km) from the nominate type locality in southern Malawi (Günther 1893).

In 1963, Perret described L. a. dysmicus as the western subspecies of *L. angularis*, differentiating it from the nominate form based on gular patterning. Interestingly, Perret mentioned that the gular patterning resembles L. picturatus or L. thomensis, but it is opposite to the 'V-shaped chevron' patterning of L. angularis. However, he did not compare L. a. dysmicus to L. gutturalis, which occurs in neighbouring areas. Kluge (1991, 1993, 2001) considered L. a. dysmicus as a subspecies of L. gutturalis, but did not provide justification. This interpretation was followed by LeBreton (1999); however, Chirio and LeBreton (2007) considered L. dysmicus as a full species without justification. Nevertheless, none of these authors provided morphological or molecular comparisons between material of L. dysmicus and L. gutturalis. Finally, Bannikov and Darevsky (1969) described L. a. grzimeki, restricted to Lake Manyara, Manyara Region, Tanzania, based on differences in the gular patterning that seemed to differentiate it from *L.* angularis sensu stricto (s.s.).

Given the taxonomic problems with these two groups and the need for molecular data for certain critical taxa, we set out to revise the *L. gutturalis* complex with an integrative taxonomic approach using morphological, molecular, biogeographic, and ecological data. We compared the type material of most nominal taxa within *L. gutturalis* and *L. angularis* to shed light on the taxonomic status of these poorly understood species complexes.

MATERIAL AND METHODS

Sampling

Specimens and tissue samples of the *L. gutturalis* complex were collected across the distributional range (from Angola, Benin, Burundi, DRC, Ghana, Guinea-Bissau, Mali, Senegal, Tanzania, and Uganda) between 2000 and 2021. Some specimens were fixed in 10% formalin and others in 96% ethanol, after which they were transferred to 70% ethanol for long-term storage in the Museo Nacional de Ciencias Naturales (MNCN), Spain, University of Texas at El Paso Biodiversity Collections (UTEP), USA, Port Elizabeth Museum at Bayworld Complex (PEM), South Africa, and the Institut de Recherche pour le Développement (IRD), Senegal. For molecular analyses, liver or muscle samples were collected and stored in 95–99% ethanol. For each sample collected, its location was recorded using precise coordinates.

Collections), and WC (Werner Conradie field numbers). Where material was not collected, references are stated as Missing Data (-). New GenBank numbers provided in this work are shown in Table 1. List of material used for the genetic analyses with information on catalogue numbers, field numbers, localities (country—province/region/department, locality), GenBank accession numbers, and sources. Abbreviations: BRZC (Beate Röll field numbers), CFS (Congo field series, used by C.K.), DFH (Daniel F. Hughes field numbers), DRC (Democratic Republic of the Congo), EBG and ELI (Eli Greenbaum field numbers), IRD (Institut de Recherche pour le Développement, Dakar), MNCN (Museo de Ciencias Naturales de Madrid), NMK (National Museums of Kenya), Port Elizabeth Museum (PEM), P1 (Pedro Vaz Pinto field numbers), TR (Jean-François Trape field numbers), UTEP (University of Texas at El Paso Biodiversity

bold face.

Species	Catalogue number	Field number	Locality	S91	RAGI	c-mos	Source
L. chobiensis	ı	BRZC 13-1	Zimbabwe—Matabeleland North Province, Victoria Falls	GUS93456	GU593580	I	Röll et al. 2010
L. chobiensis	I	BRZC 13-2	Zimbabwe—Matabeleland North Province, Victoria Falls	GUS93457	GU593581	ı	Röll et al. 2010
L. chobiensis	PEM R27402	WC-7098	Angola—Cuando Cubango Province	OR211689	1	I	This work
L. keniensis	ı	BRZC 21-1	- 1	GU593474	1	ı	Röll et al. 2010
L. keniensis	ı	BRZC 21-1b	Kenya—Baringo Province, Lake Bogoria	GUS93475	GU593598	ı	Röll et al. 2010
L. keniensis	I	BRZC 21-2	Kenya—Baringo Province, Lake Bogoria	GUS93476	GUS93S99	ı	Röll et al. 2010
L. kimhowelli	I	BRZC 22-1	Tanzania (captive specimen)	GU593479	GUS93600	ı	Röll et al. 2010
L. kimhowelli	I	BRZC 22-1b	Tanzania (captive specimen)	GUS93477	I	ı	Röll et al. 2010
L. kimhowelli	I	BRZC 22-4	Tanzania (captive specimen)	GU593478	I	ı	Röll et al. 2010
L. kimhowelli	1	TCU-Lk01	Tanzania (pet trade)	JX391873	I	I	Malonza et al. 2016
L. mombasicus	1	BRZC 09-3	Kenya—Mombasa Province, Mombasa	GU593447	I	I	Röll et al. 2010
L. mombasicus	ı	BRZC 09-2	Kenya—Kwale Province, Diani Beach	GU593446	GUS93571	ı	Röll et al. 2010
L. mombasicus	ı	BRZC 09-1	Kenya—Kwale Province, Diani Beach	GU593445	GUS93570	ı	Röll et al. 2010
L. picturatus	ı	BRZC 20-1	Kenya—Kwale Province, Diani Beach	GUS93472	GUS93S96	I	Röll et al. 2010
L. picturatus	ı	BRZC 20-2	Kenya—Kwale Province, Diani Beach	GU593473	GUS93S97	I	Röll et al. 2010
L. picturatus	1	TZ1	Tanzania—Dar es Salaam Region, Dar es Salaam	ı	I	I	Jesus et al. 2006
L. picturatus	1	TZ2	Tanzania—Dar es Salaam Region, Dar es Salaam	FJ829971	FJ830234	I	Rocha et al. 2009
L. picturatus	NMK-L3211/1	ı	Kenya—Taita-Taveta Province, Mount Kasigau	JX391874	JX399882	I	Malonza et al. 2016
L. picturatus	NMK-L3211/2	1	Kenya—Taita-Taveta Province, Mount Kasigau	JX391875	JX391875	ı	Malonza et al. 2016
L. picturatus	ı	LYG 4	Tanzania	HQ872462	ı	ı	Castiglia and Annesi 2011
L. williamsi	1	BRZC 01-1	Tanzania (captive specimen)	GUS93422	GUS93547	I	Röll et al. 2010
L. williamsi	I	BRZC 01-2	Tanzania (captive specimen)	GU593423	GU593548	ı	Röll et al. 2010
L. williamsi	1	TCU-Lw01	Tanzania (pet trade)	JX391877	I	ı	Malonza et al. 2016
L. wojnowskii	NMK-L3213/1	NMK-L3213/1	Kenya—Tharaka-Nithi Province, Chogoria Town, Mount Kenya	JX391872	I	I	Malonza et al. 2016
L. wojnowskii	I	LYG1	Kenya	HQ872459	1	ı	Castiglia and Annesi 2011
L. gutturalis	ı	BRZC 14-3	Guinea-Bissau	GU593460	GU593584	ı	Röll et al. 2010
L. gutturalis	ı	WME13	Guinea-Bissau	AY653251	I	I	Puente et al. 2009
L. gutturalis	ı	WME30	Guinea-Bissau	AY653252	I	I	Puente <i>et al.</i> 2009
L. gutturalis	IRD:TR 3843	TR3843	Guinea-Bissau—Gabú Region, Medina Boé	OR211690	OR220111	OR220067	This work
L. gutturalis	IRD:TR3850	TR3850	Guinea-Bissau—Gabú Region, Medina Boé	OR211691	OR220112	OR220068	
L. gutturalis	MNCN 51221	TR3840	Guinea-Bissau—Gabú Region, Medina Boé	OR211692	OR220113	OR220069	This work

Table 1. Continued

Species	Catalogue number	Field number	Locality	891	RAGI	C-mos	Source
			(arman)				
L. gutturalis	IRD:TR3845	TR3845	Guinea-Bissau—Gabú Region, Medina Boé	OR211693	OR220114	OR220070	This work
L. gutturalis	IRD:TR 3852	TR3852	Guinea-Bissau—Gabú Region, Medina Boé	OR211694	OR220115	OR220071	This work
L. gutturalis	MNCN 51228	TR3859	Guinea-Bissau—Gabú Region, Medina Boé	OR211695	OR220116	ı	This work
L. gutturalis	IRD:TR 3932	TR3932	Guinea-Bissau—Bafata Region, Sambatchur	OR211696	OR220117	OR220072	This work
L. gutturalis	MNCN 51227	TR3856	Guinea-Bissau—Gabú Region, Medina Boé	OR211697	OR220118	OR220073	This work
L. gutturalis	IRD:TR 3927	TR3927	Guinea-Bissau—Bafata Region, Sambatchur	OR211698	OR220119	OR220074	This work
L. gutturalis	MNCN 51223	TR3844	Guinea-Bissau—Gabú Region, Medina Boé	OR211699	OR220120	1	This work
L. gutturalis	IRD:TR 3841	TR3841	Guinea-Bissau—Gabú Region, Medina Boé	OR211700	OR220121	OR220075	This work
L. gutturalis	IRD:TR 3933	TR3933	Guinea-Bissau—Bafata Region, Sambatchur	OR211701	OR220122	OR220076	This work
L. gutturalis	IRD:TR 3930	TR G, M, B	Guinea-Bissau—Bafata Region, Sambatchur	OR211702	OR220123	1	This work
L. gutturalis	IRD:TR3855	TR3855	Guinea-Bissau—Gabú Region, Medina Boé	OR211703	OR220124	1	This work
L. gutturalis	IRD:TR3551	TR3551	Guinea-Bissau—Bolama Region, Bubaque	OR211704	OR220125	OR220077	This work
L. gutturalis	IRD:TR 3928	TR3928	Guinea-Bissau—Bafata Region, Sambatchur	OR211705	ı	ı	This work
L. gutturalis	MNCN 51219	TR3550	Guinea-Bissau—Bubaque	OR211706	OR220126	OR220078	This work
L. gutturalis	MNCN 51229	TR3913	Guinea-Bissau—Bafata Region, Bafata	OR211707	ı	I	This work
L. gutturalis	MNCN 51237	TR2450	Guinea—Kankan Region, Kalan-Kalan	OR211708	OR220127	OR220079	This work
L. gutturalis	MNCN 51238	TR2451	Guinea—Kankan Region, Kalan-Kalan	OR211709	OR220128	OR220080	This work
L. gutturalis	IRD:TR 2453	TR2453	Guinea—Kankan Region, Kalan-Kalan	OR211710	OR220129	OR220081	This work
L. gutturalis	IRD:TR 2449	TR2449	Guinea—Kankan Region, Kalan-Kalan	OR211711	1	OR220082	This work
L. gutturalis	IRD:TR 2541	TR2541	Guinea—Labe Region, Poré (Mamah)	OR211712	1	OR220083	This work
L. gutturalis	MNCN 51236	TR2975	Ghana—Sunyani Region, Nsonsomea	OR211713	OR220130	OR220084	This work
L. gutturalis	MNCN 51234	TR3289	Benin—Donga Department, Guiguisso	OR211714	OR220131	OR220085	This work
L. gutturalis	IRD:TR 3294	TR3294	Benin—Donga Department, Guiguisso	OR211715	ı	OR220086	This work
L. gutturalis	IRD:TR 3296	TR3296	Benin—Donga Department, Guiguisso	OR211716	ı	OR220088	This work
L. gutturalis	MNCN 51235	TR3299	Benin—Donga Department, Guiguisso	OR211717	1	OR220087	This work
L. gutturalis	MNCN 51247	TR3298	Benin—Donga Department, Guiguisso	OR211718	1	OR220089	This work
L. gutturalis	MNCN 51244	TR3290	Benin—Donga Department, Guiguisso	OR211719	1	1	This work
L. gutturalis	IRD:TR 3297	TR3297	Benin—Donga Department, Guiguisso	OR211720	OR220132	OR220090	This work
L. gutturalis	MNCN 51245	TR3291	Benin—Donga Department, Guiguisso	OR211721	OR220133	1	This work
L. gutturalis	MNCN 51246	TR3295	Benin—Donga Department, Guiguisso	OR211722	OR220134	OR220091	This work
L. gutturalis	IRD:TR 3293	TR3293	Benin—Donga Department, Guiguisso	OR211723	OR220135	1	This work
L. gutturalis	IRD:TR 938	TR938	Mali—Sikasso Region, Niakoni	OR211724	OR220136	1	This work
L. depressus	MNCN 50771	P1-305	Angola—Cuanza Sul Province, Barra do Cuanza	OR211725	OR220137	OR220092	This work
L. depressus	MNCN 50772	P1-306	Angola—Cuanza Sul Province, Barra do Cuanza	OR211726	OR220138	OR220093	This work
L. depressus	UTEP 22579	ELI 2128	DRC—Équateur Province, Npenda	OR211727	OR220139	OR220094	This work
L. depressus	UTEP 22578	ELI 1547	DRC—Équateur Province, Lake Tumba	OR211728	OR220140	OR220095	This work
L. depressus	UTEP 22595	ELI 3624	DRC—Maniema Province, Katopa	OR211729	OR220141	ı	This work

Table 1. Continued

Species	Catalogue number	Field number	Locality	168	RAGI	c-mos	Source
L. depressus	UTEP 22597	ELI 3585	DRC—Maniema Province, Katopa	OR211730	OR220142	OR220096	This work
Lygodactylus sp.	PEM R16817	ı	Tanzania—Arusha Province, Loliondo	I	MZ772297	ı	This work
L. kibera sp. nov.	UTEP 22571	ELI 1195	Burundi—Bubanza Province, Mpishi	OR211731	OR220143	OR220097	This work
L. kibera sp. nov.	UTEP 22566	ELI 1145	Burundi—Bubanza Province, Mpishi	OR211732	OR220144	OR220098	This work
L. kibera sp. nov.	1	20a	DRC—South Kivu Province, Lemera	OR211733	1	1	This work
L. kibera sp. nov.	1	20b	DRC—South Kivu Province, Lemera	OR211734	ı	I	This work
L. kibera sp. nov.	UTEP 22586	EBG 1556	DRC—South Kivu Province, N'Komo River	OR211735	OR220145	OR220099	This work
L. kibera sp. nov.	UTEP 22576	ELI 1071	Burundi—Bujumbura Mairie Province, Bujumbura	OR211736	OR220146	OR220100	This work
L. karamoja sp.	I	BRZC 14-1	Uganda	GU593458	GU593582	I	This work
							,
L. karamoja sp. nov.	I	BRZC 14-2	Uganda	GU593459	I	I	This work
L. karamoja sp. nov.	UTEP 22592	DFH 641	Uganda—Northern Region, Agoro Town, Imatong Foothills	OR211737	ı	ı	This work
L. karamoja sp. nov.	UTEP 22589	DFH 592	Uganda—Northern Region, Agoro Town, Imatong Foothills	OR211738	OR220147	OR220101	This work
L. karamoja sp. nov.	UTEP 22593	DFH 130	Uganda—Northern Region, Nakapiripirit, Mount Kadam	OR211739	OR220148	OR220102	This work
L. karamoja	I	NDU 718	DRC—Ituri Province, Lendu Plateu	OR211740	I	ı	This work
sp. nov.			CTATE OF THE PERSON OF THE PER				- F
L. karamoja sp. nov.	I	DFH 1140	Uganda—Western Region, Semuliki NP	OR211741	I	I	This work
L. mirabundus sp. nov.	UTEP 22585	CFS 1142w	DRC—Sankuru Province, Katako Kombe	OR211742	OR220149	OR220103 This work	This work
L. leopardinus sp. nov.	UTEP 22581	ELI 2330	DRC—Équateur Province, Balolombo	OR211743	OR220150	OR220104	This work
L. leopardinus sp. nov.	UTEP 22596	ELI 3584	DRC — Maniema Province, Katopa	OR211744	I	OR220105	This work
L. gamblei sp. nov. UTEP 22594	UTEP 22594	ELI 341	DRC—Tanganyika Province, Manono	OR211745	1	OR220106	This work
L. gamblei sp. nov. UTEP 22587	UTEP 22587	ELI 340	DRC—Tanganyika Province, Manono	OR211746	OR220151	OR220107	This work
L. gamblei sp. nov.	UTEP 22584	ELI 293	DRC—Haut-Lomami Province, Mulongo	OR211747	OR220152	OR220108	This work
Outgroups							
L. thomensis	1	BRZC 26-1	São Tomé and Principe—São Tomé Island	GU593485	GUS93606	1	Röll et al. 2010
L. wermuthi	I	719	São Tomé and Principe—Principe, Tvelho	OR211748	I	OR220109	Jesus et al. 2006
L. delicatus	1	644	Equatorial Guinea—Annobon	OR211749	1	OR220110	Jesus et al. 2006
L. conraui	ı	BRZC 06-1	Ghana—Greater Accra Region, Accra	GU593433	GU593558	ı	Röll et al. 2010

Molecular data

DNA was extracted using the EasySpin Genomic DNA Tissue Kit (Citomed, Portugal), following the manufacturer's protocols. The dataset consists of one partial mitochondrial ribosomal gene (16S) and two nuclear markers (RAG1 and c-mos). Primer details are provided in Supporting Information, Table S1. PCR amplifications were performed using the following concentrations: 5 µl QIAGEN PCR MasterMix, 0.4 µl of each primer, 3.2 µl H₂O, and 2 µl DNA (DNA elutions were adjusted to extraction results). PCR cycling reactions were carried out under the following conditions: initial denaturing step at 95 °C for 15 min, followed by five cycles of 95 °C for 30 s, 64 °C for 20 s, and 72 °C for 60 s (decreasing annealing temperature by -0.5 °C/ cycle), followed by 35 cycles of 95 °C for 30 s, 64 °C for 20 s, and 72 °C for 60 s, with a final extension at 60 °C for 10 min. The PCR products were purified and sequenced at the Centre for Molecular Analysis (CTM-CIBIO, Porto, Portugal).

The phylogenetic placement of the newly generated samples was determined by comparing them with previously published sequence data for the L. picturatus group generated by Puente et al. (2009), Röll et al. (2010), Castiglia and Annesi (2011), and Malonza et al. (2016). In addition to the ingroup taxa (eight of the 14 currently recognized species), the dataset was supplemented with sequences of two species (L. thomensis and L. conraui Tornier 1902) of the sister L. fischeri group (Gippner et al. 2021). All additional sequences were obtained from GenBank (https://www.ncbi.nlm.nih.gov/genbank/; Benson et al. 2013). All sequences were checked and edited using GENEIOUS Prime v.2021.1.1 (http://www.geneious.com/) and aligned using the MUSCLE plugin for GENEIOUS. For nuclear loci (RAG1 and c-mos), heterozygous individuals were identified based on the presence of two peaks of approximately equal height at a single nucleotide site with the PHASE algorithm (Stephens et al. 2001) in the software DNAsp v.6.12 with default settings, and not considering recombination, to resolve phased haplotypes (Rozas et al. 2017). Phased nuclear sequences were used for the network analyses and the unphased sequences for species-tree analyses. Sequence lengths were 594 bp for 16S, 399 bp for c-mos, and 639 bp for RAG1. All sequences have been deposited in GenBank (Table 1).

Phylogenetic analysis and network analysis

Maximum likelihood (ML) and Bayesian Inference (BI) were implemented using all 16S sequences available for the L. picturatus group, and outgroups included four species (L. thomensis, Lygodactylus delicatus Pasteur 1962, Lygodactylus wermuthi Pasteur, 1962, and L. conraui) of the sister L. fischeri group (Gippner et al. 2021). ML analysis was conducted using IQ-TREE v.2.1.2 (Nguyen et al. 2015), with a random starting tree, and the Ultrafast Bootstrap approximation (UFBoot) method (Hoang et al. 2018) with 1000 bootstrap replicates. The best substitution model of sequence evolution was selected using ModelFinder (Kalyaanamoorthy et al. 2017) in IQ-TREE v.2.1.2, with the Bayesian Information Criterion (BIC). Bootstrap values (BS) of 95% or higher were considered as strongly supported (Hoang et al. 2018). With the same alignment and substitution model, we ran BI (MrBayes v.3.2.7a; Ronquist et al. 2012) on the CIPRES Science Gateway XSEDE online resource

(http://www.phylo.org; Miller et al. 2010, Tamura et al. 2013) for 10×10^6 generations of the Metropolis-Coupled Markov Chain (MC3) Monte Carlo, sampling every 1000 generations. Convergence was assessed by examining the effective sample size (ESS) values with Tracer v.1.7 (Rambaut et al. 2018) with all parameter values having ESS values > 200, as recommended. Also, 25% of the obtained trees were discarded as burn-in to generate a 50% majority-rule consensus tree. Posterior probabilities (PP) were used to assess nodal support, and PP \geq 0.95 was considered strongly supported. Uncorrected pairwise sequence divergences (p-distance) were calculated for 16S sequences in MEGA v10.1.7 (Table 2). Median-joining haplotype networks were constructed for the phased nuclear alleles [two fragments of RAG1 (262 bp and 980 bp) and c-mos using Networks v.4.6.1.1 (Bandelt et al. 1999), applying default settings and with a parsimony cut-off of 95%.

Species trees and divergent times calibration

We constructed a time-calibrated species tree using StarBEAST as implemented in BEAST v.2.6.3 following the calibration points, partition scheme, and best-fitting model of Gippner et al. (2021). We used a pruned dataset in which sequences (16S, RAG1, and c-mos) of one representative specimen from each previously identified lineage was included in the supermatrix (10 141 bp). We also included sequences of Lygodactylus baptistai Marques, Ceriaco, Buehler, Bandeira, Janota & Bauer, 2020, L. delicatus, and L. wermuthi, which were not included in Gippner et al. (2021). A relaxed uncorrelated log-normal clock prior was selected for each gene (Carranza and Arnold 2012). As the tree prior, we employed a Birth-Death Process model with random starting trees. We used the calibration prior with a log-normal distribution and adjusted the mean and sigma parameters so that the distribution matched the 95% credible intervals from the primary study. Uninformative priors (gamma distribution, with parameters $\alpha = 0.1$ and $\beta = 10$) were set for the parameters of the molecular clock, which were then estimated during the analysis.

Morphology and morphometrics

For this study, we examined newly collected material of the L. gutturalis complex from Guinea-Bissau, Senegal, Mali, Ghana, Benin, DRC, Uganda, Burundi, Tanzania, and Angola, and historical material representing the L. gutturalis and L. angularis groups deposited at the Royal Museum of Central Africa (RMCA), Belgium, the Royal Belgian Institute of Natural Sciences (RBINS), Belgium, the Muséum d'histoire naturelle de la ville de Genève (MNGH), Switzerland, and the California Academy of Sciences (CAS), USA (see Supporting Information, Table S2). We examined 372 specimens of the *L. gutturalis* complex (Supporting Information, Table S2) and compared these to original descriptions and type material of nominal taxa within the L. gutturalis and L. angularis groups (Bocage 1873, Günther 1893, de Witte 1933, Laurent 1952, Bannikov and Darevsky 1969, Marques et al. 2020). The morphometric characters were: snout-vent length (SVL, from tip of snout to anterior margin of cloacal opening); trunk length (TRL, from posterior insertion of the forelimb to anterior insertion of the hind limb); crus or tibia length (CL, from base of heel to knee); tail length

(TL, from posterior margin of cloacal opening to tip of tail); head length (HL, from snout to the posterior point of the ear aperture); head width (HW, measured at the widest portion of the head); forelimb length (ForeL, from anterior insertion of the forelimb to base of the palm); forearm length (FL, from elbow to base of the palm); maximum horizontal orbital diameter (OD); maximum vertical aperture of ear (EarL); nares to eye distance (NE, distance between anteriormost point of eye and nostril); snout to eye distance (SE, distance between anteriormost point of eye and tip of snout); eye to ear distance (EE, distance from anterior edge of ear opening to posterior corner of eye); internarial distance (IN, shortest distance between nares); and interorbital distance (IO, shortest distance between left and right supraciliary scale rows). All measurements were taken in millimetres (mm) with a digital calliper (accuracy of 0.1 mm). The meristic data collected were: number of supralabials; number of infralabials; number of postmental scales; number of postpostmental scales; number of ventral scales across the venter at midbody; number of precloacal pores (in males; see Maderson 1968 for a discussion of the relationship between beta-glands and precloacal pores in Lygodactylus spp.) or enlarged precloacal plates (in females); subdigital lamellae of the fourth toe from the base of the digits to the claw, including divided lamellae under the most distal section of the toe and undivided lamellae under the medial and proximal section of the toe (No. lamellae on 4th toe); number of granular scales between the eyes; number of scansors on original tail tip; number of ventral enlarged scales on original tails; number, appearance and disposition of lines in the gular region; and dorsal coloration and ornamentation (ocelli, lines, etc.) of the head and body. Meristic data were taken using a dissection microscope and high-resolution macrophotography was accomplished with a Nikon D850 camera and Nikon 105mm f2.8 macro lens. For graphic visualization of the morphometric and meristic measurements see the Supporting Information (Fig. S1).

In order to identify osteological features between and within groups (the L. picturatus and L. angularis groups), we performed High Resolution X-ray Computed Tomography (HRCT) scans of 52 specimens, including 39 specimens of the L. gutturalis complex, nine of the 14 nominal taxa within the L. picturatus group [with the exception of Lygodactylus picturatus sudanensis Loveridge, 1935, Lygodactylus viscatus Vaillant 1873, Lygodactylus tsavoensis Malonza, Bauer, Granthon, Williams & Wojnowski, 2019, and Lygodactylus wojnowskii Malonza, Granthon & Williams, 2016); (Gippner et al. 2021)] and four of five nominal taxa within the L. angularis group (with the exception of Lygodactylus angularis grzimeki Bannikov & Darevsky, 1969). For scanning details see Supporting Information, Table S3. All 3D segmentation models were generated for the articulated skulls in Avizo Lite 2020.2 (Thermo Fisher Scientific). To facilitate visualization, individual bone units for skulls and jaws were coloured following the same colour palette as Lobón-Rovira and Bauer (2021). Annotations were made in Adobe Illustrator CC 22.0.1 (Adobe Systems Incorporated) following the anatomical terminology of Lobón-Rovira and Bauer (2021). We also recorded some other osteological information as follows: skull length (from the anterior most tip of premaxilla to the dorsomedial point of the foramen magnum), skull width

(widest skull distance, mainly between the most lateral points of the quadrate bones), jaw length (straight distance between the anterior most point of the dentary and the posterior most point of the compound bone or surangular), premaxilla tooth loci, maxillary tooth loci (right/left), dentary tooth loci (left), stage of the frontal bone (paired/semifused/fused), postorbitofrontal size (absent/small/medium/large), stage of compound bone + surangular (fused/semifused/unfused), jugal size (absent/small/medium), otostapes (perforate/unperforate). For a graphic visualization of the measurements see Supporting Information, Figure S1. Osteological measurements were taken in millimetres (mm) with a 3D measurement tool implemented in Avizo Lite 2020.2. Tomogram series for all scans are available on Morphosource.org.

Due to the high level of overlap in morphological characters found, we only included adult specimens in statistical morphometric analyses (here recognised as SVL ≥ 29 cm) that were either unequivocally identified genetically or were collected from localities that had been previously assigned to a specific lineage based on molecular data (N = 76; Supporting Information, Tables S4-S10). All continuous variables were log-transformed and SVL corrected before analyses. In order to undertake a preliminary examination of the overall morphometric variation in the L. gutturalis complex, we used Principal Components Analysis (PCA) and displayed the results using standard boxplots. Given the statistical limitations necessitated by the small sample sizes, we used permutational approaches. We tested the existence of differences between lineages (one by one) using permutational ANOVAs (in the case of SVL) and ANCOVAs (in the case of the other variables, using SVL as a covariate) with the R package RRPP (Collyer and Adams 2018). Homogeneity of regression slopes assumption was tested with an ANCOVA model including the interaction terms between the categorical factors and the covariate. Non-significant interaction terms meant that slopes were homogeneous, and as such, models were run again, this time excluding the interaction terms. Statistical analyses were performed with R v.3.6.2 (R Core Team).

Distribution mapping

To produce an up-to-date distribution map and better understanding of the spatial segregation of the L. gutturalis complex, we collected data from published datasets (Perret 1963, Dunger 1968, Chirio and Ineich 2006, Leaché et al. 2006, Chirio and LeBreton 2007, Largen and Spawls 2010, Segniagbeto et al. 2015, Spawls et al. 2018), museum databases, and new records provided in this work. Additionally, we collected information from online platforms [e.g. iNaturalist (http://www.inaturalist. org), VertNet (http://vertnet.org), GBIF (https://www.gbif. org), and Herpetology of Ethiopia and Eritrea (http://www. reptiles-of-ethiopia-and-eritrea.com)]. We only included records undoubtedly assigned to the L. gutturalis complex, based on gular and dorsal patterns. Distribution data were mapped in QGIS v.2.18 (http://qgis.org) and subsequently overlaid on a 1 arc-second coloured Shuttle Radar Topography Mission (SRTM) elevation map of Africa (NASA 2000) and Terrestrial Ecosystem Map of Africa (Sayre et al. 2013) in Adobe Illustrator CC 22.0.1 (Adobe Systems Incorporated).

Species assessment

The species delimitation followed in this work is based on an integrative approximation (Schlick-Steiner et al. 2010, Hillis 2019, Vences et al. 2022), where each taxon represents independent evolving lineages (de Queiroz 2007) that are well supported based on molecular, morphological, and biogeographic/ecological differences. Because of the high morphological conservativeness of *Lygodactylus*, we used 16S uncorrected p-distances and nuclear-encoded gene haplotypes to identify genetic units (Vences et al. 2022), followed by well-supported morphological evidence in those species found in sympatry. We chose type material from specimens that were either genetically identified or those from localities in which other specimens had been previously genetically identified. The remaining specimens for each nominal species have been listed as 'additional material'. Material from other regions where genetic material have not been recovered (e.g. Ethiopia or Sudan) are here referred to as L. cf. gutturalis until more information becomes available.

RESULTS

Phylogenetic reconstruction and network analyses

The topology of the phylogenetic reconstructions (BI and ML) was consistent with the results found by Röll et al. (2010) and Gippner et al. (2021), which retrieved an Afro-American clade (Clade C in Gippner et al. 2021), clustering the L. picturatus group as sister to the L. fischeri group. These results also agree with Röll et al. (2010) and Gippner et al. (2021), which recovered the same topology within the L. picturatus group, finding L. picturatus subgroup as basal, including L. chobiensis as the most basal branch in the *L. picturatus* group (PP: 1, BS: 96; Fig. 1). However, we found significant genetic diversity within *L*. gutturalis, regarding it as species complex, with seven genetically well-supported operational taxonomic units (OTUs) (Fig. 1) that show consistently large genetic 16S uncorrected p-distances (6.07-16.72%, Table 2). The results of the time tree date the split between the L. picturatus and L. gutturalis subgroups in the Mid-Miocene, about 15.0 Mya (95% confidence intervals, 19.9-11.0 Mya; Fig. 2A).

The phylogenetic reconstructions recovered a clade, here named A, that includes L. gutturalis s.s. from the sub-Saharan savannahs, and its sister species (here ascribed to L. depressus, see below) from the rainforest in the Congo Basin and the Angolan gallery forest, which differ by 9.04% (16S uncorrected p-distance, Table 2) from each other (PP: 0.99, BS: 87; Fig. 1). This clade diverged from the other members of the *L. gutturalis* subgroup by ~12.5 Mya (16.5–8.8 Mya, Fig. 2A). Sister to this group, the phylogenetic reconstructions recovered two more groups. A large clade (Clade B) that includes three new candidate species with 16S uncorrected p-distances of 6.07-9.82% between them (Table 2). This can be divided into two subclades (PP: 1, BS: 100, Fig. 1): first, a clade (B1) that includes two new candidate species that incorporates the genetically closest taxa (6.07%, 16S uncorrected p-distance between them, Table 2) from Burundi and Uganda, and one candidate species (B2) from DRC that differs by a minimum of 8.93% in p-distance from all previously mentioned OTUs. Finally, we recovered different topologies between the 16S tree and the time tree on the most basal clade of the *L. gutturalis* subgroup, Clade C; this clade is not monophyletic in our *16S* tree (Fig. 1). The time tree (Fig. 2A) recovered Clade C as sister to Clade B [which separated from each other by about 7.8 Mya (5–11 Mya, Fig. 2A)]. Clade C includes two distinctive candidate species (*16S* uncorrected p-distance 9.96%, PP: 1, BS: 96; Fig. 1) from non-forested habitats in south-eastern DRC.

The median-joining network for the 262 bp RAG1 nuclear marker (Fig. 2B), including all RAG1 sequences available within L. picturatus-fischeri, recovered a total of 33 alleles grouped as follows: three alleles in the *L. fischeri* group, 13 in the *L. picturatus* subgroup, and 17 in the *L. gutturalis* subgroup. Also, the medianjoining network for the 980 bp RAG1 nuclear marker for the L. gutturalis subgroup (excluding L. gutturalis s.s.) recovered a total of 24 largely consistent alleles (Fig. 2C). No allele sharing was detected between species within the *L. gutturalis* subgroup. However, we detected one case of allele sharing between L. mombasicus, L. keniensis, and L. kimhowelli (Fig. 2B), consistent with the phylogenetic results, and the low 16S mitochondrial genetic distance between them. Both analyses recovered eight well-differentiated taxa (Fig. 2B-C), including one taxon (Lygodactylus sp. in Fig. 2A) from Tanzania, not included in the mitochondrial phylogenetic analyses due to the lack of mitochondrial molecular data (Fig. 2).

Morphology

All tables with original measurements, character states, and counts are provided as Supporting Information (Tables S4–S10) and summarized in Table 3. All the individuals examined share the defining character states of the *L. gutturalis* subgroup as compared to other Lygodactylus, i.e. gular region with two or three dark ∩-shaped chevrons that converge anteriorly (with the exception of a separate clade from Balolombo, DRC, with a broken chevron pattern, and material from Kenya and Tanzania where ∩-shaped chevrons in males converge anteriorly, displaying a mostly uniform black gular pattern), mental scale undivided, enlarged subcaudal scales, 5-6 terminal scansors on the tail tip, and dull brown to grey dorsal coloration (Fig. 3). Morphological examination of the type series of *L. depressus*, in comparison to material from the entire Congo Basin south to Angola, including material from the type locality of L. depressus at Medje, Haut-Uele Province, DRC, tentatively ascribed to L. gutturalis, failed to recover any morphological differentiation, suggesting they are conspecific (see below). Morphometric and meristic analyses (pholidosis) of external morphology showed high intraspecific variation (i.e. two or four postmental scales, 1-3 internasal scales, or 5–8 precloacal pores), and extensive overlap between most of the clades identified here, with only a few significant differences between them (Supporting Information, Table S11, Figs S3–S6; Fig. 4). Our PCA analysis showed that PC1 (26.1% of variation) and PC2 (14.4% of variation) exhibited a high level of overlap among the different mitochondrial clades previously identified (Fig. 4A). However, the univariate morphometric analysis between different OTUs revealed minor differences between lineages (see Supporting Information, Table S11).

The osteological Computered Tomographies (CT-reconstructions) showed that all individuals examined in the *L. gutturalis* subgroup (Supporting Information, Fig. S8), as well as other representatives of the *L. picturatus* group (Table

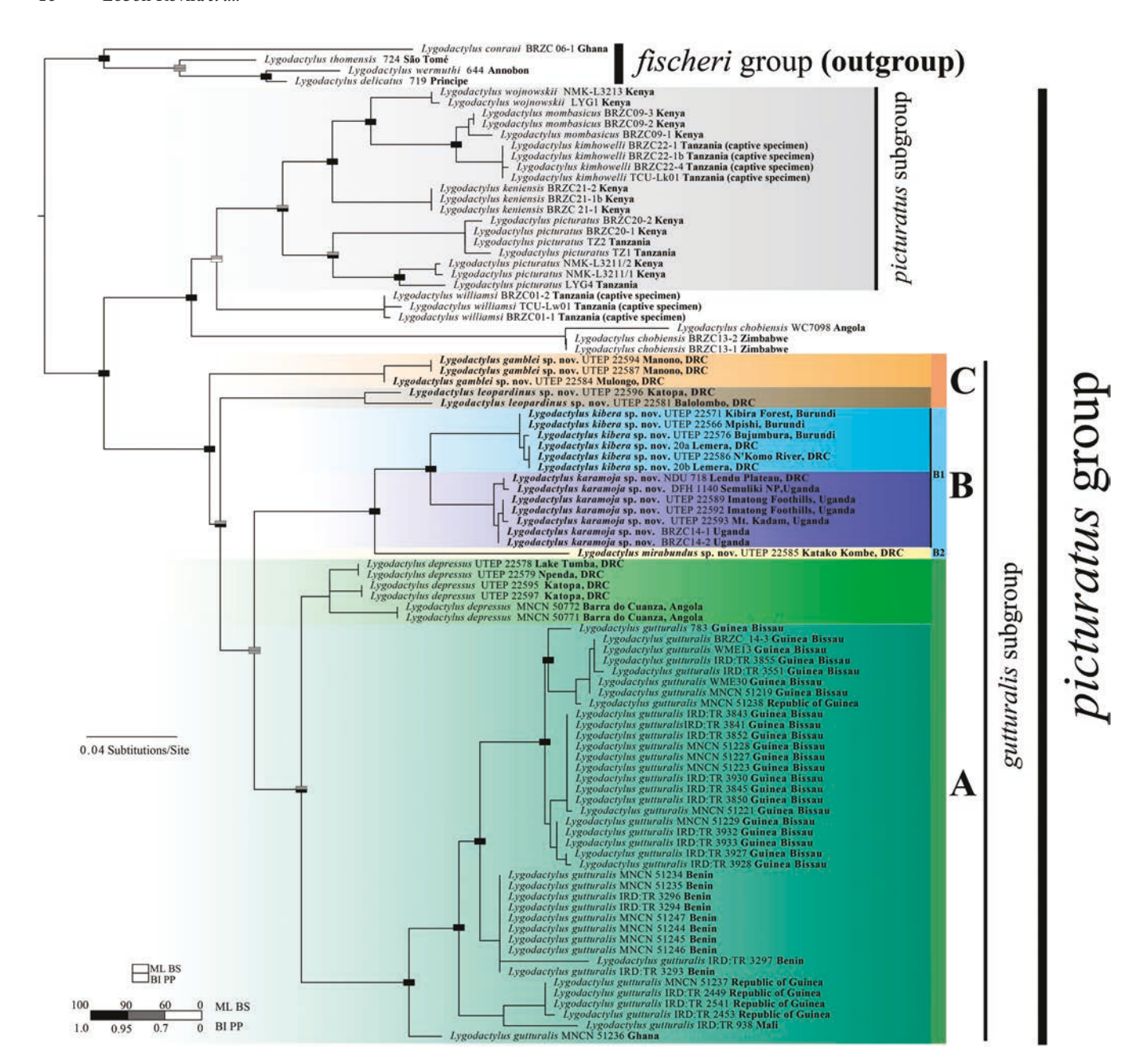


Figure 1. Maximum likelihood analysis based on 532 bp of the mitochondrial 16S rRNA gene, for all available samples of the Afro-American *Lygodactylus* Clade (Clade C of Gippner *et al.* 2021). Support values (ML BS = Maximum Likelihood bootstrap values; BI PP = Bayesian Inference posterior probabilities) are shown graphically at the nodes according to the colours shown in the inset key.

3; Supporting Information, Fig. S9), share the defining characters observed in *L. picturatus* (Lobón-Rovira and Bauer 2021), i.e. reduced postorbitofrontal bone and reduced or lost jugal bone. However, the comparisons did not recover osteological differences within and between species of the *L. picturatus* group (Supporting Information, Fig. S9) or the *L. gutturalis* subgroup (Supporting Information, Fig. S8) as defined above. On the other hand, despite the extremely conservative skull structure, the osteological comparison between the *L. picturatus* and *L. angularis* groups has revealed an unequivocal osteological diagnostic character that could be used to differentiate these two groups: reduced or absent postorbitofrontal bone in the *L. picturatus* group vs. large postorbitofrontal (about three times

larger than in the *L. picturatus* group, when present) tapering anteriorly and posteriorly around the frontoparietal suture in the *L. angularis* group (Fig. 5). These results have allowed us to confirm that *L. paurospilus* belongs to the *L. angularis* group and *L. dysmicus* to the *L. gutturalis* group as previously suggested by Laurent (1952) and Kluge (1991), respectively. More details about morphological characteristics of each group are addressed in the species account section.

Geographic distribution (Fig. 6)

We analysed a total of 324 records that can undoubtedly be assigned to the *L. gutturalis* complex, covering its entire geographic distribution. Clade A contains two lowland species that include

1.31 4 Fable 2. 16S mitochondrial divergences (uncorrected pairwise distances) between and within members of the L. picturatus group. Bold numbers represent mean divergence within species. 10.72 3.85 13 10.10 96.6 12 13.69 12.49 12.36 10.45 12.70 11.41 8.93 9.82 9.83 13.62 12.49 12.54 9.04 15.63 14.65 13.55 13.87 13.28 13.48 12.24 14.19 14.35 15.09 13.15 14.09 14.03 14.44 14.84 11.03 15.60 10.25 13.55 13.27 13.57 13.86 12.13 10.73 8.03 14.80 10.89 13.56 13.73 14.14 15.27 15.98 15.59 16.42 16.72 13.50 11.83 14.57 15.25 7.93 90.6 11. Lygodactylus mirabundus sp. nov. 3. Lygodactylus leopardinus sp. nov. 10. Lygodactylus karamoja sp. nov. 14. Lygodactylus gamblei sp. nov. 9. Lygodactylus kibera sp. nov. 8. Lygodactylus gutturalis s.s. 2. Lygodactylus mombasicus 3. Lygodactylus wojnowskii 12. Lygodactylus depressus 1. Lygodactylus kimhowelli 5. Lygodactylus picturatus 7. Lygodactylus chobiensis 6. Lygodactylus williamsi 4. Lygodactylus keniensis L. picturatus subgroup L. gutturalis subgroup

L. gutturalis s.s., widely distributed across the sub-Saharan savannahs from Senegal to the Central African Republic, spanning an elevational range from sea level to ~700 m a.s.l., and L. depressus, also widely distributed in the rainforest of the Congo Basin, and gallery forest and mangroves to the Angolan mangroves, with a maximum elevational range ~500 m a.s.l. (Fig. 6; Supporting Information, Table S2). Clade B is the most diverse subgroup and can be subdivided into one sub-subgroup, mostly from the Albertine Rift region (sub-subgroup B1) that includes two new candidate species, and another sub-subgroup from Katako Kombe, Sankuru Province, DRC (sub-subgroup B2), in a transition zone between the Congo Basin Rainforest and the southern Congolian Miombo Forest. Members of the B1 clade include one candidate species from non-forested habitats of the Lendu Plateau (DRC), Semuliki National Park, and several montane areas of Uganda, and a second candidate species from the Albertine Rift of Burundi and adjacent DRC. Clade C has two new candidate species from DRC, present in two welldifferentiated biomes. Although one is known from Balolombo and Katopa, on the north-western and south-eastern corners of the Congo Basin rainforest in DRC, its sister taxon is found only in Miombo Woodland, south-eastern DRC, mainly in the area near Upemba National Park (Fig. 6). Finally, an additional taxon identified in the median-joining nuclear network (Lygodactylus sp. in Fig. 2B-C), and morphologically well differentiated from other members of the *L. gutturalis* group (Fig. 3), is distributed to the east of the Albertine Rift and south of Lake Victoria within the arid savannah of Kenya and Tanzania.

Additionally, *L. dysmicus* was not included in the phylogenetic analysis, but can be distinguished morphologically from other nominal and candidate species within the *L. gutturalis* subgroup (see species accounts). It is only known from two localities along the northern rim of the Congo Basin of Cameroon, west of the Ubangi River, at elevations above 600 m a.s.l.

SYSTEMATICS

Lygodactylus angularis group

The taxonomic status of all nominal taxa within the *L. angularis* group remains controversial. Whereas *L. a. heeneni* has previously been included in a phylogenetic framework (Gippner et al. 2021), *L. a. dysmicus, L. a. grzimeki*, and *L. a. paurospilus* have been subject to frequent misidentifications, and thus need further validation. The results of our osteological comparisons confirms that *L. a. heeneni* and *L. a. paurospilus* belong to the *L. angularis* group, sharing the same osteological features (see above) as *L. angularis* and *L. baptistai* (Fig. 5). On the other hand, *L. a. dysmicus* shares the same cranial features with all members of the *L. picturatus* group (Fig. 5).

Based on a detailed external examination of the type material of *L. a. heeneni* (Fig. 7; Supporting Information, Fig. S2), and 27 specimens deposited at RMCA and RBINS, we confirm the morphological variation in pholidosis and morphometrics of *L. a. heeneni* recorded by de Witte (1953) and Pasteur, 1965(1964). However, despite the meristic overlap and skull similarities, we did not observe any intergradation in throat pattern with *L. angularis s.s.*, as recorded by Broadley and Cotterill (2004). Thus, we revalidate *L. heeneni* as a full species as proposed by de

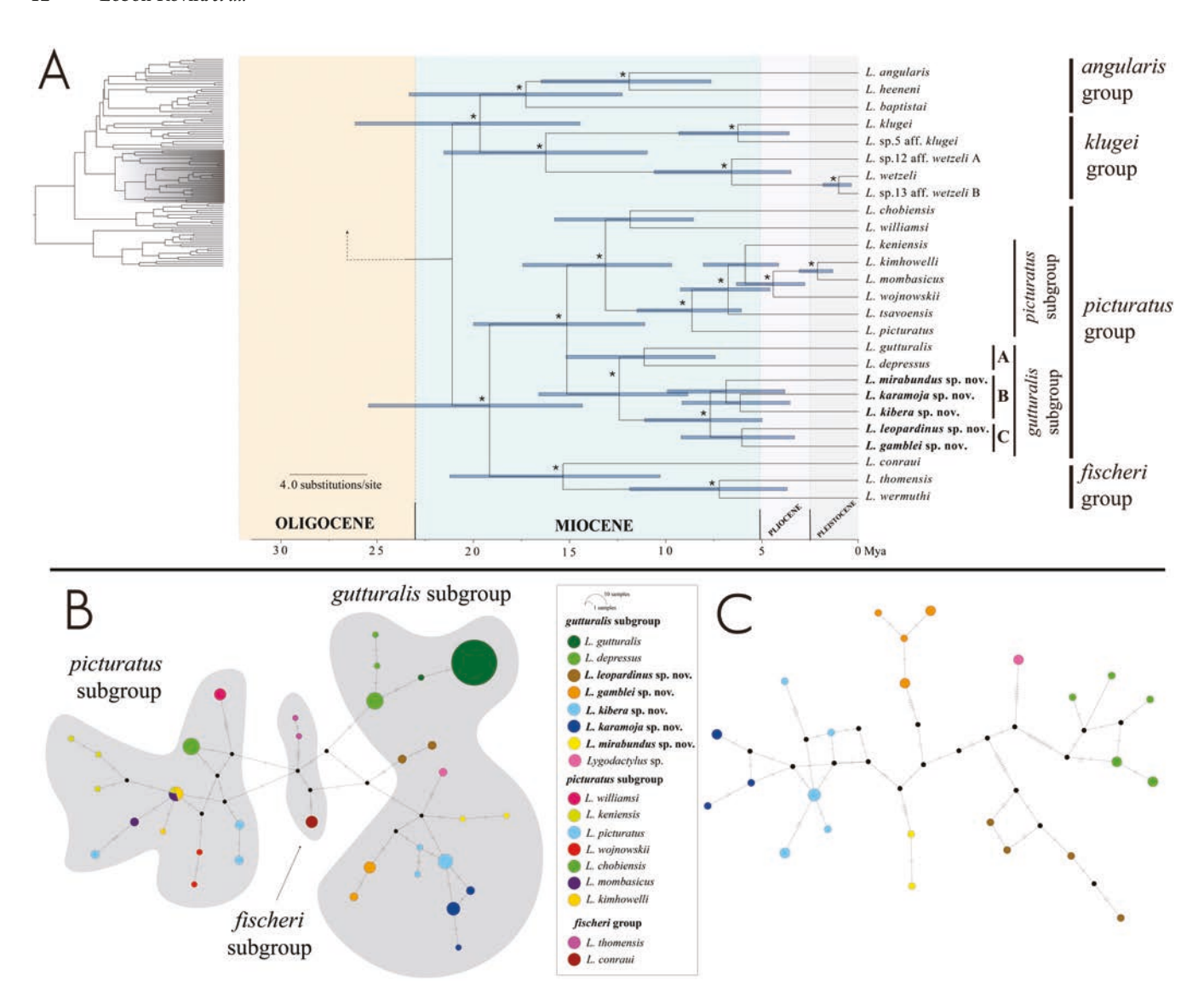


Figure 2. A, Multilocus species tree and Bayesian chronogram of divergences among Afro-American *Lygodactylus* clade (Clade C of Gippner *et al.* 2021), based on an alignment of 13 concatenated markers (including eight nuclear-encoded genes, four protein-coding mitochondrial genes, and the *16S* mitochondrial rRNA gene, see Gippner *et al.* 2021). Branches with posterior probability > 0.9 are denoted by asterisks (*) at relevant nodes. Blue bars depict 95% High Probability Density (HPD) intervals of estimated divergence dates. B, Median-joining nuclear allele network showing the relationships between the *L. picturatus-fischeri* groups, inferred from the *RAG1* nuclear gene (262 bp including all available *RAG1* sequences of the *L. picturatus-fischeri* groups). C, Median-joining nuclear allele network of the *RAG1* nuclear gene (980 bp) showing the relationships within the *L. gutturalis* subgroup, excluding *L. gutturalis s.s.* In all networks, circle frequency of alleles and small lines represent mutational steps.

Witte (1933), in contradiction to Loveridge (1947). This result agrees with the high genetic p-distance in 16S (11.3%) and ND2 (21.5%) between L. angularis (PEM R16821) and L. heeneni (PW133) by Gippner et al. (2021). This is markedly above the 5.5% 16S and > 20% ND2 p-distance noted for Lygodactylus species in the latter study. It is noteworthy that the specimens of L. angularis (PEM R16821) used by Gippner et al. (2021) were collected from Mbeya, southern Tanzania, ~700 km north of the type locality of L. angularis, and it differs in dorsal pattern from topotypic material of L. angularis (Supporting Information, Fig. S3). Also, it differs by ~15% ND2 p-distance from material of L. angularis from Lichinga, Nyassa Province, Mozambique (MVZ 2662139), ~140 km from the origin of the type material, as reported by Travers et al. (2014). This may suggest additional

cryptic species within *L. angularis* and probably greater genetic distance between topotypic material of *L. angularis* and *L. heeneni*, which needs further investigation.

External morphological comparisons between *L. a.* paurospilus and *L. heeneni* revealed a few subtle morphological differences in contradiction to Pasteur, 1965 (1964). These morphological differences may, however, overlap when larger series of *L. a.* paurospilus are analysed, due to the high level of morphological conservatism of this group. Also, the distributions of these two taxa, which do not overlap and occur in highly distinctive habitats, suggest the need for taxonomic recognition of *L. a.* paurospilus. Therefore, in light of the results we consider *L. paurospilus* as a valid species, which should be confirmed with molecular data in future studies.

Downloaded from https://academic.oup.com/zoolinnean/advance-article/doi/10.1093/zoolinnean/zlad123/7281514 by guest on 03 October 2023

Table 3. Summary of external and osteological morphological data of all members within the *L. gutturalis* complex. Measurements are shown in mm (average and SD). For abbreviations see Material and methods section.

N (N=27) (N=1) Elevation (m a.s.l.) 10−761 665 State of postnasal scale 81.5% not in contact In broad contact Gular lines pattering 2-3 2 Aaximum SVL 36.2 (N=61) 27.6 SVL 33.3 ± 1.8 27.6 TL 33.6 ± 2.3 27.6 TL 33.6 ± 2.3 25.5 TL 3.0 ± 0.6 6.2 OD 2.3 ± 0.2 2.1 HW 6.2 ± 0.6 6.2 OD 2.3 ± 0.2 2.1 EarL 0.7 ± 0.1 0.7 CL 5.8 ± 0.5 8.3 NE 5.2 ± 0.5 (N = 24) 4.7 NB 3.1 ± 0.3 3.1 NB 1.8 ± 0.2 2.4 IN 1.8 ± 0.2 2.4 No. postmental scales 2.4 4 No. post-postmental 4.6 4 No. post-postmental 4.0 4 No. infralabial scales 6.7/6-8 6	(N = 8) $7-331$ 2 38.0 38.6 ± 1.4 25.3 ± 0.0 16.2 ± 1.8 9.2 ± 0.4 6.6 ± 0.2 2.1 ± 0.3 0.8 ± 0.1 5.6 ± 0.6 5.0 ± 0.5 8.5 ± 2.5 3.5 ± 0.3 4.5 ± 0.3 1.6 ± 0.3	(N = 12) 811-1705 In contact 3 37.7 34.7 ± 2.5 37.5 ± 3.1 14.9 ± 1.5 9.4 ± 0.8 6.7 ± 0.6 6.7 ± 0.6 6.7 ± 0.6 6.7 ± 0.6 7.3 ± 0.2 1.0 ± 0.1 5.7 ± 0.5 4.7 ± 0.4 9.5 ± 0.6 3.4 ± 0.3 4.6 ± 0.4	(N = 6) 1193-1730 70% not in contact 3 37.7 34.4 ± 2.9 35.0 ± 2.8 14.5 ± 2.6 9.4 ± 0.7 6.9 ± 0.6 2.1 ± 0.3 0.9 ± 0.2 5.2 ± 0.6 5.0 ± 0.3 8.8 ± 0.4 4.5 ± 0.3 4.5 ± 0.3	(N = 1) 551 Not in contact 21/2 34.8 34.8 - 15.4 8.9 7.4 1.8 1.1 6.1	(N = 4) 305 In contact Broken pattern 34.7 33.6 ± 1.3 32.7 ± 1.7 15.0 ± 1.2 9.2 ± 0.5 6.4 ± 0.3 2.2 ± 0.3 0.7 ± 0.1 5.5 ± 0.2 4.9 ± 0.6 9.4 ± 0.6 3.3 ± 0.3	$(N = 16)$ $634-875$ 15% not in contact $2.1/2$ or 3 39.8 36.1 ± 2.1 36.8 ± 2.6 16.2 ± 1.3 10.1 ± 0.8 7.2 ± 0.6 2.4 ± 0.2 0.8 ± 1.0 6.2 ± 0.8 5.4 ± 0.3 $(N = 10)$ 10.2 ± 0.9 3.6 ± 0.3
ion (m a.s.l.) 10–761 lines pattering 2–3 num SVL 36.2 (N = 61) 33.3 ± 1.8 33.6 ± 2.3 15.3 ± 1.3 9.0 ± 0.6 6.2 ± 0.6 6.2 ± 0.6 7.2 ± 0.1 8.8 ± 0.2 0.7 ± 0.1 8.8 ± 0.5 8.2 ± 0.5 8.2 ± 0.5 1.8 ± 0.2 3.1 ± 0.3 3.0 ± 0.5 1.8 ± 0.2 3.7 ± 0.3 3.7 ± 0.3 3.7 ± 0.3 3.7 ± 0.3 4.3 ± 0.3 3.7 ± 0.3 4.4 ← 6 set pralabial scales 2–4 set-postmental 4–6 set ht/left) fralabial scales 6–7/6–8 ht/left) fralabial scales 1–3 strassl scales 1–3 strassl scales 1–3		811–1705 In contact 3 37.7 34.7 ± 2.5 37.5 ± 3.1 14.9 ± 1.5 9.4 ± 0.8 6.7 ± 0.6 6.7 ± 0.6 2.3 ± 0.2 1.0 ± 0.1 5.7 ± 0.4 4.7 ± 0.4 4.5 ± 0.4 4.6 ± 0.4	1193–1730 70% not in contact 3 37.7 34.4 ± 2.9 35.0 ± 2.8 14.5 ± 2.6 9.4 ± 0.7 6.9 ± 0.7 6.9 ± 0.2 2.1 ± 0.3 0.9 ± 0.2 5.2 ± 0.6 5.0 ± 0.3 8.8 ± 0.4 3.4 ± 0.3 4.5 ± 0.3	551 Not in contact 2 1/2 34.8 34.8 - 15.4 8.9 7.4 1.8 1.1 6.1	305 In contact Broken pattern 34.7 33.6 ± 1.3 32.7 ± 1.7 15.0 ± 1.2 9.2 ± 0.5 6.4 ± 0.3 2.2 ± 0.3 0.7 ± 0.1 5.5 ± 0.2 4.9 ± 0.2 9.4 ± 0.6	634–875 15% not in contact 2 1/2 or 3 39.8 36.1 ± 2.1 36.8 ± 2.6 16.2 ± 1.3 10.1 ± 0.8 7.2 ± 0.6 2.4 ± 0.2 0.8 ± 1.0 6.2 ± 0.8 5.4 ± 0.3 (N = 10) 10.2 ± 0.9 3.6 ± 0.3 3.6 ± 0.3 3.6 ± 0.3 3.7 ± 0.6 3.8 ± 0.0 3.8 ±
Innes pattering 2–3 aum SVL 36.2 (N = 61) 33.3 ± 1.8 33.6 ± 2.3 15.3 ± 1.3 9.0 ± 0.6 6.2 ± 0.6 2.3 ± 0.2 0.7 ± 0.1 5.8 ± 0.5 5.2 ± 0.5 (N = 24) 9.5 ± 0.8 3.1 ± 0.3 4.3 ± 0.3 3.0 ± 0.5 1.8 ± 0.2 3.7 ± 0.3 3.7 ± 0.3 3.7 ± 0.3 4.4 ± 0.5 best postmental scales 2–4 set matal scales 2–4 br/left) fralabial scales 6–7/6–8 ht/left) fernasal scales 1–3 strassal scales 1–3 strassal scales 1–3		In contact 3 37.7 34.7 ± 2.5 34.7 ± 2.5 37.5 ± 3.1 14.9 ± 1.5 94 ± 0.8 6.7 ± 0.6 6.7 ± 0.6 2.3 ± 0.2 1.0 ± 0.1 5.7 ± 0.4 4.7 ± 0.4 9.5 ± 0.6 3.4 ± 0.3 4.6 ± 0.4	70% not in contact 3 37.7 34.4 ± 2.9 35.0 ± 2.8 114.5 ± 2.6 9.4 ± 0.7 6.9 ± 0.7 6.9 ± 0.2 2.1 ± 0.3 0.9 ± 0.2 5.2 ± 0.6 5.0 ± 0.3 8.8 ± 0.4 3.4 ± 0.3 4.5 ± 0.3	Not in contact 2 1/2 34.8 34.8 15.4 8.9 7.4 1.1 6.1 5.0	In contact Broken pattern 34.7 33.6 ± 1.3 32.7 ± 1.7 15.0 ± 1.2 9.2 ± 0.5 6.4 ± 0.3 0.7 ± 0.1 5.5 ± 0.2 4.9 ± 0.2 9.4 ± 0.6	15% not in contact 2 1/2 or 3 39.8 36.1 ± 2.1 36.8 ± 2.6 16.2 ± 1.3 10.1 ± 0.8 7.2 ± 0.6 2.4 ± 0.2 0.8 ± 1.0 6.2 ± 0.8 5.4 ± 0.3 (N = 10) 10.2 ± 0.9 3.6 ± 0.3
lines pattering 2–3 aum SVL 36.2 (N = 61) 33.3 ± 1.8 33.6 ± 2.3 15.3 ± 1.3 9.0 ± 0.6 6.2 ± 0.6 2.3 ± 0.2 0.7 ± 0.1 5.8 ± 0.5 5.2 ± 0.5 (N = 24) 9.5 ± 0.8 3.1 ± 0.3 3.0 ± 0.3 3.0 ± 0.5 1.8 ± 0.2 3.7 ± 0.3 3.7 ± 0.3 3.7 ± 0.3 4.4 ± 0.3 4.5 ± 0.8 5.4 ± 0.5 5.5 ± 0.6 8.6 ± 0.6 8.7 ± 0.9 9.7 ± 0.1 9.6 ± 0.6 8.7 ± 0.3 9.7 ± 0.3	2 38.0 35.6 ± 1.4 25.3 ± 0.0 16.2 ± 1.8 9.2 ± 0.4 6.6 ± 0.2 2.1 ± 0.3 0.8 ± 0.1 5.6 ± 0.6 5.0 ± 0.5 8.5 ± 2.5 8.5 ± 2.5 3.5 ± 0.3 4.5 ± 0.3 1.6 ± 0.3 1.7 ± 0.3	3 37.7 34.7 ± 2.5 37.5 ± 3.1 14.9 ± 1.5 9.4 ± 0.8 6.7 ± 0.6 6.7 ± 0.6 2.3 ± 0.2 1.0 ± 0.1 5.7 ± 0.5 4.7 ± 0.4 9.5 ± 0.6 3.4 ± 0.3 4.6 ± 0.4	3 37.7 34.4 ± 2.9 35.0 ± 2.8 14.5 ± 2.6 9.4 ± 0.7 6.9 ± 0.6 2.1 ± 0.3 0.9 ± 0.2 5.2 ± 0.6 5.0 ± 0.3 8.8 ± 0.4 3.4 ± 0.3 4.5 ± 0.3	21/2 34.8 34.8 15.4 15.4 8.9 7.4 1.1 6.1 5.0	Broken pattern 34.7 33.6 ± 1.3 32.7 ± 1.7 15.0 ± 1.2 9.2 ± 0.5 6.4 ± 0.3 2.2 ± 0.3 0.7 ± 0.1 5.5 ± 0.2 4.9 ± 0.2 9.4 ± 0.6	21/2 or 3 39.8 36.1 ± 2.1 36.8 ± 2.6 16.2 ± 1.3 10.1 ± 0.8 7.2 ± 0.6 2.4 ± 0.2 0.8 ± 1.0 6.2 ± 0.8 5.4 ± 0.3 ($N = 10$) 10.2 ± 0.9 3.6 ± 0.3
36.2 (N = 61) 33.3 ± 1.8 33.6 ± 2.3 15.3 ± 1.3 9.0 ± 0.6 6.2 ± 0.6 6.2 ± 0.6 2.3 ± 0.2 0.7 ± 0.1 5.8 ± 0.5 5.2 ± 0.5 (N = 24) 9.5 ± 0.8 3.1 ± 0.3 4.3 ± 0.3 3.0 ± 0.5 1.8 ± 0.2 3.7 ± 0.3 3.0 ± 0.5 1.8 ± 0.2 3.7 ± 0.3 3.7 ± 0.3 4.3 ± 0.3 4.4 ± 0.2 3.7 ± 0.3 4.4 ± 0.2 3.7 ± 0.3 4.4 ± 0.2 4.4 ± 0.2 5.6 4.6 4.6 4.6 4.6 4.6 4.6 4.6 4.6 4.6 4	38.0 35.6 ± 1.4 25.3 ± 0.0 16.2 ± 1.8 9.2 ± 0.4 6.6 ± 0.2 2.1 ± 0.3 0.8 ± 0.1 5.6 ± 0.6 5.0 ± 0.5 8.5 ± 2.5 3.5 ± 0.3 4.5 ± 0.3 1.6 ± 0.3 1.6 ± 0.3	37.7 34.7 ± 2.5 37.5 ± 3.1 14.9 ± 1.5 9.4 ± 0.8 6.7 ± 0.6 2.3 ± 0.2 1.0 ± 0.1 5.7 ± 0.5 4.7 ± 0.4 9.5 ± 0.6 3.4 ± 0.3 4.6 ± 0.4	37.7 34.4 ± 2.9 35.0 ± 2.8 14.5 ± 2.6 9.4 ± 0.7 6.9 ± 0.6 2.1 ± 0.3 0.9 ± 0.2 5.2 ± 0.6 5.0 ± 0.3 8.8 ± 0.4 3.4 ± 0.3 4.5 ± 0.3	34.8 34.8 15.4 8.9 7.4 1.1 6.1 5.0	34.7 33.6 ± 1.3 32.7 ± 1.7 15.0 ± 1.2 9.2 ± 0.5 6.4 ± 0.3 2.2 ± 0.3 0.7 ± 0.1 5.5 ± 0.2 4.9 ± 0.2 9.4 ± 0.6	39.8 36.1 ± 2.1 36.8 ± 2.6 16.2 ± 1.3 10.1 ± 0.8 7.2 ± 0.6 2.4 ± 0.2 0.8 ± 1.0 6.2 ± 0.8 5.4 ± 0.3 (N = 10) 10.2 ± 0.9 3.6 ± 0.3
33.3 ± 1.8 33.6 ± 2.3 15.3 ± 1.3 9.0 ± 0.6 6.2 ± 0.6 6.2 ± 0.6 6.2 ± 0.6 0.7 ± 0.1 5.8 ± 0.5 9.5 ± 0.8 3.1 ± 0.3 3.1 ± 0.3 3.1 ± 0.3 3.1 ± 0.3 3.1 ± 0.3 3.1 ± 0.3 3.1 ± 0.2 3.7 ± 0.1 8 ± 0.2 3.7 ± 0.3 9.5 ± 0.8 9.5 ± 0.8 3.1 ± 0.3 3.1 ± 0.3 4.3 ± 0.3 3.1 ± 0.3 4.3 ± 0.3 5.2 ± 0.5 6.5 ± 0.8 3.1 ± 0.3 3.1 ± 0.3 5.2 ± 0.5 6.5 ± 0.8 5.5 ± 0.8 5.6 ± 0.8 5.7 ± 0.3 5.7 ±	35.6 ± 1.4 25.3 ± 0.0 16.2 ± 1.8 9.2 ± 0.4 6.6 ± 0.2 2.1 ± 0.3 0.8 ± 0.1 5.6 ± 0.6 5.0 ± 0.5 8.5 ± 2.5 3.5 ± 0.3 4.5 ± 0.3 1.6 ± 0.3	34.7 ± 2.5 37.5 ± 3.1 14.9 ± 1.5 9.4 ± 0.8 6.7 ± 0.6 2.3 ± 0.2 1.0 ± 0.1 5.7 ± 0.5 4.7 ± 0.4 9.5 ± 0.6 3.4 ± 0.3 4.6 ± 0.4	34.4 ± 2.9 35.0 ± 2.8 14.5 ± 2.6 9.4 ± 0.7 6.9 ± 0.6 2.1 ± 0.3 0.9 ± 0.2 5.2 ± 0.6 5.0 ± 0.3 8.8 ± 0.4 3.4 ± 0.3 4.5 ± 0.3	34.8 - 15.4 8.9 7.4 1.8 1.1 6.1 5.0	33.6 ± 1.3 32.7 ± 1.7 15.0 ± 1.2 9.2 ± 0.5 6.4 ± 0.3 2.2 ± 0.3 0.7 ± 0.1 5.5 ± 0.2 4.9 ± 0.2 9.4 ± 0.6	36.1 ± 2.1 36.8 ± 2.6 16.2 ± 1.3 10.1 ± 0.8 7.2 ± 0.6 2.4 ± 0.2 0.8 ± 1.0 6.2 ± 0.8 5.4 ± 0.3 ($N = 10$) 10.2 ± 0.9 3.6 ± 0.3
33.6 ± 2.3 15.3 ± 1.3 9.0 ± 0.6 6.2 ± 0.6 2.3 ± 0.2 0.7 ± 0.1 5.8 ± 0.5 5.2 ± 0.5 (N = 24) 9.5 ± 0.8 3.1 ± 0.3 3.1 ± 0.3 3.0 ± 0.5 1.8 ± 0.2 3.7 ± 0.3 3.7 ± 0.3 3.7 ± 0.3 3.7 ± 0.3 4.3 ± 0.3 5.4 6.5 6.6 6.7 6.8 pralabial scales 6.7/6-8 ht/left) fralabial scales 6.7/6-8 ht/left) fralabial scales 1.3 strassl scales 1.3 strassl scales 1.3	25.3 ± 0.0 16.2 ± 1.8 9.2 ± 0.4 6.6 ± 0.2 2.1 ± 0.3 0.8 ± 0.1 5.6 ± 0.6 5.0 ± 0.5 8.5 ± 2.5 3.5 ± 0.3 4.5 ± 0.3 1.6 ± 0.2	37.5 ± 3.1 14.9 ± 1.5 9.4 ± 0.8 6.7 ± 0.6 2.3 ± 0.2 1.0 ± 0.1 5.7 ± 0.4 9.5 ± 0.6 3.4 ± 0.3 4.6 ± 0.4	35.0 ± 2.8 14.5 ± 2.6 9.4 ± 0.7 6.9 ± 0.6 2.1 ± 0.3 0.9 ± 0.2 5.2 ± 0.6 5.0 ± 0.3 8.8 ± 0.4 3.4 ± 0.3 4.5 ± 0.3	- 15.4 8.9 7.4 1.8 1.1 6.1	32.7 ± 1.7 15.0 ± 1.2 9.2 ± 0.5 6.4 ± 0.3 2.2 ± 0.3 0.7 ± 0.1 5.5 ± 0.2 4.9 ± 0.2 9.4 ± 0.6	36.8 ± 2.6 16.2 ± 1.3 10.1 ± 0.8 7.2 ± 0.6 2.4 ± 0.2 0.8 ± 1.0 6.2 ± 0.8 5.4 ± 0.3 $(N = 10)$ 10.2 ± 0.9 3.6 ± 0.3
15.3 ± 1.3 9.0 ± 0.6 6.2 ± 0.6 6.2 ± 0.6 2.3 ± 0.2 0.7 ± 0.1 5.8 ± 0.5 5.2 ± 0.5 (N = 24) 9.5 ± 0.8 3.1 ± 0.3 3.0 ± 0.5 1.8 ± 0.2 3.7 ± 0.3 3.7 ± 0.3 3.7 ± 0.3 3.7 ± 0.3 4.3 ± 0.3 5.4 5.5 ± 0.8 5.6 5.6 5.7 ± 0.8 5.7 ± 0.8 5.8 ± 0.8 5.9	16.2 ± 1.8 9.2 ± 0.4 6.6 ± 0.2 2.1 ± 0.3 0.8 ± 0.1 5.6 ± 0.6 5.0 ± 0.5 8.5 ± 2.5 8.5 ± 2.5 3.5 ± 0.3 4.5 ± 0.3 1.6 ± 0.3 1.6 ± 0.2	14.9 ± 1.5 9.4 ± 0.8 6.7 ± 0.6 2.3 ± 0.2 1.0 ± 0.1 5.7 ± 0.5 4.7 ± 0.4 9.5 ± 0.6 3.4 ± 0.3 4.6 ± 0.4	14.5 ± 2.6 9.4 ± 0.7 6.9 ± 0.6 2.1 ± 0.3 0.9 ± 0.2 5.2 ± 0.6 5.0 ± 0.3 8.8 ± 0.4 3.4 ± 0.3 4.5 ± 0.3	15.4 8.9 7.4 1.8 1.1 6.1 5.0	15.0 ± 1.2 9.2 ± 0.5 6.4 ± 0.3 2.2 ± 0.3 0.7 ± 0.1 5.5 ± 0.2 4.9 ± 0.2 9.4 ± 0.6	16.2 ± 1.3 10.1 ± 0.8 7.2 ± 0.6 2.4 ± 0.2 0.8 ± 1.0 6.2 ± 0.8 $5.4 \pm 0.3 (N = 10)$ 10.2 ± 0.9 3.6 ± 0.3
9.0 ± 0.6 6.2 ± 0.6 6.2 ± 0.6 2.3 ± 0.2 0.7 ± 0.1 5.8 ± 0.5 5.2 ± 0.5 (N = 24) 9.5 ± 0.8 3.1 ± 0.3 4.3 ± 0.3 3.0 ± 0.5 1.8 ± 0.2 3.7 ± 0.3 3.7 ± 0.3 3.7 ± 0.3 3.7 ± 0.3 4.4 + 6 es pralabial scales 6-7/6-8 ht/left) fralabial scales 6-7/6-8 ht/left) fralabial scales 1-3 strassi scales 1-3	9.2 ± 0.4 6.6 ± 0.2 2.1 ± 0.3 0.8 ± 0.1 5.6 ± 0.6 5.0 ± 0.5 8.5 ± 2.5 8.5 ± 2.5 3.5 ± 0.3 4.5 ± 0.3 1.6 ± 0.2	94 ± 0.8 6.7 ± 0.6 2.3 ± 0.2 1.0 ± 0.1 5.7 ± 0.5 4.7 ± 0.4 9.5 ± 0.6 3.4 ± 0.3 4.6 ± 0.4	9.4 ± 0.7 6.9 ± 0.6 2.1 ± 0.3 0.9 ± 0.2 5.2 ± 0.6 5.0 ± 0.3 8.8 ± 0.4 3.4 ± 0.3 4.5 ± 0.3	8.9 7.4 1.1 6.1 5.0	9.2 ± 0.5 6.4 ± 0.3 2.2 ± 0.3 0.7 ± 0.1 5.5 ± 0.2 4.9 ± 0.2 9.4 ± 0.6	10.1 \pm 0.8 7.2 \pm 0.6 2.4 \pm 0.2 0.8 \pm 1.0 6.2 \pm 0.8 5.4 \pm 0.3 (N = 10) 10.2 \pm 0.9 3.6 \pm 0.3
6.2 ± 0.6 2.3 ± 0.2 0.7 ± 0.1 5.8 ± 0.5 5.2 ± 0.5 (N = 24) 9.5 ± 0.8 3.1 ± 0.3 4.3 ± 0.3 3.0 ± 0.5 1.8 ± 0.2 3.7 ± 0.3 3.7 ± 0.3 3.7 ± 0.3 3.7 ± 0.3 4.4 ± 0.2 3.7 ± 0.4 5.6 5.6 5.7 ± 0.8 6.7 ± 0.8	6.6 ± 0.2 2.1 ± 0.3 0.8 ± 0.1 5.6 ± 0.6 5.0 ± 0.5 8.5 ± 2.5 3.5 ± 0.3 4.5 ± 0.3 2.9 ± 0.3 1.6 ± 0.2	6.7 ± 0.6 2.3 ± 0.2 1.0 ± 0.1 5.7 ± 0.5 4.7 ± 0.4 9.5 ± 0.6 3.4 ± 0.3 4.6 ± 0.4	6.9 ± 0.6 2.1 ± 0.3 0.9 ± 0.2 5.2 ± 0.6 5.0 ± 0.3 8.8 ± 0.4 4.5 ± 0.3	7.4 1.8 1.1 6.1 5.0	6.4 ± 0.3 2.2 ± 0.3 0.7 ± 0.1 5.5 ± 0.2 4.9 ± 0.2 9.4 ± 0.6	7.2 ± 0.6 2.4 ± 0.2 0.8 ± 1.0 6.2 ± 0.8 $5.4 \pm 0.3 (N = 10)$ 10.2 ± 0.9 3.6 ± 0.3
2.3 ± 0.2 0.7 ± 0.1 5.8 ± 0.5 8.2 ± 0.5 8.2 ± 0.5 9.5 ± 0.8 3.1 ± 0.3 4.3 ± 0.3 3.0 ± 0.5 1.8 ± 0.2 3.0 ± 0.5 1.8 ± 0.2 3.7 ± 0.3 3.7 ± 0.3 3.7 ± 0.3 4.3 ± 0.3 4.4 ± 0.2 3.7 ± 0.4 5.6 5.6 6.7 6.8 6.7 6.7 6.8 6.7 6.7 6.8 6.7 6.7 6.7 6.7 6.7 6.7 6.7 6.7 6.7 6.7	2.1 ± 0.3 0.8 ± 0.1 5.6 ± 0.6 5.0 ± 0.5 8.5 ± 2.5 3.5 ± 0.3 4.5 ± 0.3 2.9 ± 0.3 1.6 ± 0.2	2.3 ± 0.2 1.0 ± 0.1 5.7 ± 0.5 4.7 ± 0.4 9.5 ± 0.6 3.4 ± 0.3 4.6 ± 0.4	2.1 ± 0.3 0.9 ± 0.2 5.2 ± 0.6 5.0 ± 0.3 8.8 ± 0.4 3.4 ± 0.3 4.5 ± 0.3	1.8 1.1 5.0	2.2 ± 0.3 0.7 ± 0.1 5.5 ± 0.2 4.9 ± 0.2 9.4 ± 0.6	2.4 ± 0.2 0.8 ± 1.0 6.2 ± 0.8 $5.4 \pm 0.3 (N = 10)$ 10.2 ± 0.9 3.6 ± 0.3
0.7 ± 0.1 5.8 ± 0.5 5.2 ± 0.5 5.2 ± 0.5 ($N = 24$) 9.5 ± 0.8 3.1 ± 0.3 4.3 ± 0.3 3.0 ± 0.5 1.8 ± 0.2 3.7 ± 0.3 $3.7 \pm$	0.8 ± 0.1 5.6 ± 0.6 5.0 ± 0.5 8.5 ± 2.5 3.5 ± 0.3 4.5 ± 0.3 2.9 ± 0.3 1.6 ± 0.2	1.0 ± 0.1 5.7 ± 0.5 4.7 ± 0.4 9.5 ± 0.6 3.4 ± 0.3 4.6 ± 0.4 3.2 ± 0.4	0.9 ± 0.2 5.2 ± 0.6 5.0 ± 0.3 8.8 ± 0.4 3.4 ± 0.3 4.5 ± 0.3	1.1 6.1 5.0	0.7 ± 0.1 5.5 ± 0.2 4.9 ± 0.2 9.4 ± 0.6	0.8 ± 1.0 6.2 ± 0.8 $5.4 \pm 0.3 (N = 10)$ 10.2 ± 0.9 3.6 ± 0.3
$\begin{array}{c} 8.8 \pm 0.5 \\ 5.2 \pm 0.5 \ (N = 24) \\ 9.5 \pm 0.8 \\ 3.1 \pm 0.3 \\ 3.1 \pm 0.3 \\ 4.3 \pm 0.3 \\ 3.0 \pm 0.5 \\ 1.8 \pm 0.2 \\ 3.7 \pm 0.3 \\ 3.7 \pm 0.3 \\ 3.7 \pm 0.3 \\ 3.7 \pm 0.3 \\ 3.7 \pm 0.4 \\ 8struental scales 2-4 \\ 8strpostmental 4-6 \\ es \\ pralabial scales 6-7/6-8 \\ ht/left) \\ fralabial scales 6-7/6-8 \\ ht/left) \\ ternasal scales 1-3 \\ stransal scales 1 \\ 1 \\ stransal scales 1 \\ transal scales 1 \\ transal scales 1 \\ transal scales 1 \\ transal scales $	5.6 ± 0.6 5.0 ± 0.5 8.5 ± 2.5 3.5 ± 0.3 4.5 ± 0.3 2.9 ± 0.3 1.6 ± 0.2	5.7 ± 0.5 4.7 ± 0.4 9.5 ± 0.6 3.4 ± 0.3 4.6 ± 0.4 3.2 ± 0.4	5.2 ± 0.6 5.0 ± 0.3 8.8 ± 0.4 3.4 ± 0.3 4.5 ± 0.3	6.1 5.0	5.5 ± 0.2 4.9 ± 0.2 9.4 ± 0.6	6.2 ± 0.8 $5.4 \pm 0.3 (N = 10)$ 10.2 ± 0.9 3.6 ± 0.3
$5.2 \pm 0.5 \ (N = 24)$ 9.5 ± 0.8 3.1 ± 0.3 4.3 ± 0.3 3.0 ± 0.5 3.0 ± 0.5 3.0 ± 0.5 3.0 ± 0.2 3.7 ± 0.3 3.7 ± 0.3 3.7 ± 0.3 3.7 ± 0.3 3.7 ± 0.3 4.4 to set the constraint of the	5.0 ± 0.5 8.5 ± 2.5 3.5 ± 0.3 4.5 ± 0.3 2.9 ± 0.3 1.6 ± 0.2	4.7 ± 0.4 9.5 ± 0.6 3.4 ± 0.3 4.6 ± 0.4 3.2 ± 0.4	5.0 ± 0.3 8.8 ± 0.4 3.4 ± 0.3 4.5 ± 0.3	5.0	4.9 ± 0.2 9.4 ± 0.6	$5.4 \pm 0.3 \ (N = 10)$ 10.2 ± 0.9 3.6 ± 0.3
9.5 ± 0.8 3.1 ± 0.3 4.3 ± 0.3 4.3 ± 0.3 3.0 ± 0.5 1.8 ± 0.2 3.7 ± 0.3 3.7 ± 0.3 3.7 ± 0.3 3.7 ± 0.4 set the control of the con	8.5 ± 2.5 3.5 ± 0.3 4.5 ± 0.3 2.9 ± 0.3 1.6 ± 0.2	9.5 ± 0.6 3.4 ± 0.3 4.6 ± 0.4 3.2 ± 0.4	8.8 ± 0.4 3.4 ± 0.3 4.5 ± 0.3		9.4 ± 0.6	10.2 ± 0.9 3.6 ± 0.3
3.1 ± 0.3 4.3 ± 0.3 3.0 ± 0.5 1.8 ± 0.2 3.7 ± 0.3 5-6 8	3.5 ± 0.3 4.5 ± 0.3 2.9 ± 0.3 1.6 ± 0.2	3.4 ± 0.3 4.6 ± 0.4 3.2 ± 0.4	3.4 ± 0.3 4.5 ± 0.3	9.6	22+02	3.6 ± 0.3
4.3 ± 0.3 3.0 ± 0.5 1.8 ± 0.2 3.7 ± 0.3 5.6 es 2.4 1 4.6 s 6-7/6-8 i 1-3	4.5 ± 0.3 2.9 ± 0.3 1.6 ± 0.2	4.6 ± 0.4 3.2 ± 0.4	4.5 ± 0.3	3.8	5.5 ± U.5	
3.0 \pm 0.5 1.8 \pm 0.2 3.7 \pm 0.3 5-6 8 2-4 1 4-6 8 6-7/6-8 6 1-3	2.9 ± 0.3 1.6 ± 0.2	3.2 ± 0.4		4.5	4.2 ± 0.2	4.0 ± 0.4
1.8 ± 0.2 3.7 ± 0.3 5-6 5-6 1 4-6 5 6-7/6-8 5 1-3 1 1-3	1.6 ± 0.2		3.3 ± 0.4	3.6	3.1 ± 0.2	3.2 ± 0.2
3.7 ± 0.3 5-6 1 4-6 ss 6-7/6-8 s 1-3		1.6 ± 0.1	1.7 ± 0.3	1.8	1.6 ± 0.1	1.4 ± 0.1
5-6 1 4-6 1s 6-7/6-8 5 6-7/6-8 1 1-3	4.0 ± 0.4	4.1 ± 0.4	3.9 ± 0.3	3.8	4.4 ± 0.5	4.1 ± 0.3
es 2-4 1 4-6 1s 6-7/6-8 s 6-7/6-8 i 1-3 1	S	2	5	\$	\$	5
ss 6-7/6-8 6-7/6-8 1-3	2	2–3	2–3	3	2	3
ss 6-7/6-8 s 6-7/6-8 i 1-3	4-5	2-6	4-7	5	4-5	5-6
ss 6-7/6-8 s 6-7/6-8 i 1-3						
s 6-7/6-8 1 1-3	6-2/6-2	6-2/6-2	8-2/7-8	8/7	7-8/8	6-9/6-9
-	2-9/2-9	2-2//9-2	6-7/5-7	9/9	2-9/2-9	2-9/2-9
No. postnasal scales 1 1	1–2	1-2	1-2	1	2–3	1-2
	1	1	1	1	1	1
No. ventral scales 15-20 21	16–19	16–18	16-18	21	14-15	15-19
No. scales between 17-24 25	22–29	19–28	19–22	19	30–36	20-25
eyes						
No. dorsal scales – – –	ı	ı	ı	ı	1	1
No. preanal pores $5-8 (\bar{x}=6.73)$ 9	7	7-8 (x=7.17)	∞	10	7	$7-9 (\bar{x}=7.5)$
Lamellae tail tip 5–6 6	-	5–6	9	1	9	5-6

Table 3. Continued

Species	L. gutturalis s.s.	L. dysmicus	L. depressus	L. kibera sp. nov.	L. karamoja sp. nov.	L. mirabundus sp. nov.	L. leopardinus sp. nov. L. gamblei sp. nov.	L. gamblei sp. nov.
OSTEOLOGICAL FEATURES (N)	(N=7)	(N = 1)	(N=7)	(N=11)	(N=6)	(N=1)	(N=1)	(N=2)
Skull length	9.2 ± 0.6	8.2	9.5 ± 0.5	9.9 ± 0.5	9.1 ± 0.5	9.4	9.6	9.0 ± 0.8
Skull width	4.6 ± 0.4	5.0	5.5 ± 0.2	5.9 ± 0.3	5.6 ± 0.5	0.9	5.5	5.2 ± 0.3
Jawlength	8.1 ± 0.5	7.2	8.3 ± 0.4	8.6 ± 0.5	8.0 ± 0.8	7.9	8.3	7.2 ± 0.9
Premaxillary tooth loci 11	11	111	9-11	9-11	9-11	11	11	11
Maxillary tooth loci (right)	16–20	16	16–18	16–19	16-18	15	18	18
Maxillary tooth loci (left)	16–20	16	16–18	16–19	16-18	15	18	17–18
Dentary tooth loci (left)	20	20	18–21	20–24	20-22	19	21	20–22
Frontal	Fused/semifused	Paired	Fused/ semifused	Fused/semifused	Fused	Semifused	Fused	Semifused
Parietal	Paired	Paired	Paired	Paired	Paired	Paired	Paired	Paired
Postorbitofrontal	Small/absent	Small	Small/medium	Small/medium	Small/ medium	Small	Medium	Small/ medium
Braincase	Fused/semifused	Unfused	Fused/ semifused	Fused/unfused/ semifused	Fused/ unfused/ semifused	Unfused	Semifused	Unfused
Compound bone + surangular	Fused/semifused	Unfused	Fused/unfused	Fused/ unfused/ semifused	Fused/ unfused	Unfused	Fused	Semifused
Jugal	Small	Small	Absent/small/medium	Small/absent	Small	Small	Absent	Absent

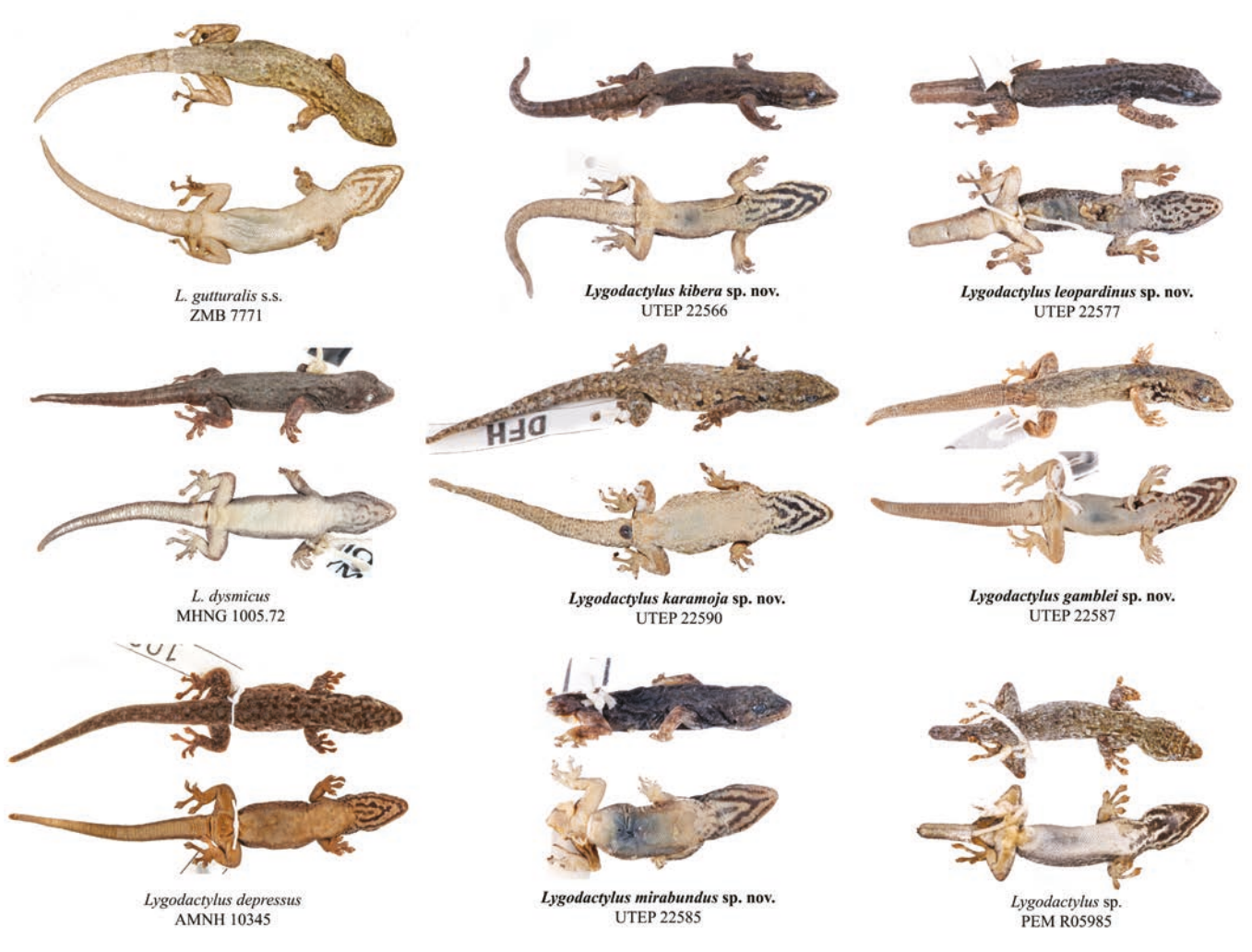


Figure 3. Comparative figure including dorsal (or dorsolateral) and ventral views of preserved holotypes (with exception of *Lygodactylus gutturalis* that is represented by a paratype) of all species within the *L. gutturalis* subgroup used in the current study.

Additionally, based on three factors [1] external morphological variation observed in one individual of *L. angularis*, also from Mbeya, Tanzania (not collected; Supporting Information, Figs S3E–F), ~700 km away from the type localities of *L. angularis* and *L. a. grzimeki*, respectively, which has intermediate morphological states between *L. angularis* and *L. a. grzimeki*, 2) the current lack of access to type material of *L. a. grzimeki*, and 3) the potential habitat overlap between *L. a. grzimeki* and *L. angularis s.s.*], we prefer to not make any taxonomic action regarding *L. a. grzimeki*, and continue to treat this taxon as a subspecies, until molecular information becomes available.

Finally, we elevate *L. dysmicus* to a full species, as part of the *L. gutturalis* group instead of the *L. angularis* group, as proposed by Kluge (1991) (see the *L. gutturalis* group accounts for more information). Based on the poor description of *L. paurospilus* provided by Laurent (1952), and to ensure clarity and facilitate future taxonomic action, we provide a detailed redescription of the taxon below.

LYGODACTYLUS PAUROSPILUS Laurent, 1952 (Fig. 8; Supporting Information, Fig. S4; Table S4)

Lygodactylus angularis paurospilus: Laurent 1952; Wermuth (1965); Greenbaum and Kusamba (2012).

Lygodactylus gutturalis paurospilus: Kluge (1991, 1993, 2001); Röll (2005); de Lisle et al. (2013, 2016).

Lygodactylus (Lygodactylus) gutturalis paurospilus: Rösler (2000).

Lygodactylus angularis heeneni: Pasteur, 1965 (1964).

Material examined: Holotype, RMCA (=MRAC) R.27408 (Supporting Information, Fig. S4), adult female, collected at Haute Lubitshako, between 1900–2000 m a.s.l., South Kivu Province, DRC between 26–30 October 1950 by Raymond Laurent. Paratype, RMCA (=MRAC) R.27409 (Fig. 8), adult male, with same collection information as the holotype.

Original description (Laurent 1952): 'Race differing from the typical form in the gular patterns, which instead of being chevrons, exhibits irregular spots or lines that are less marked in the male (paratype) than in the female (holotype). There are three postsymphisials as in heeneni de Witte, but the preanal pores are

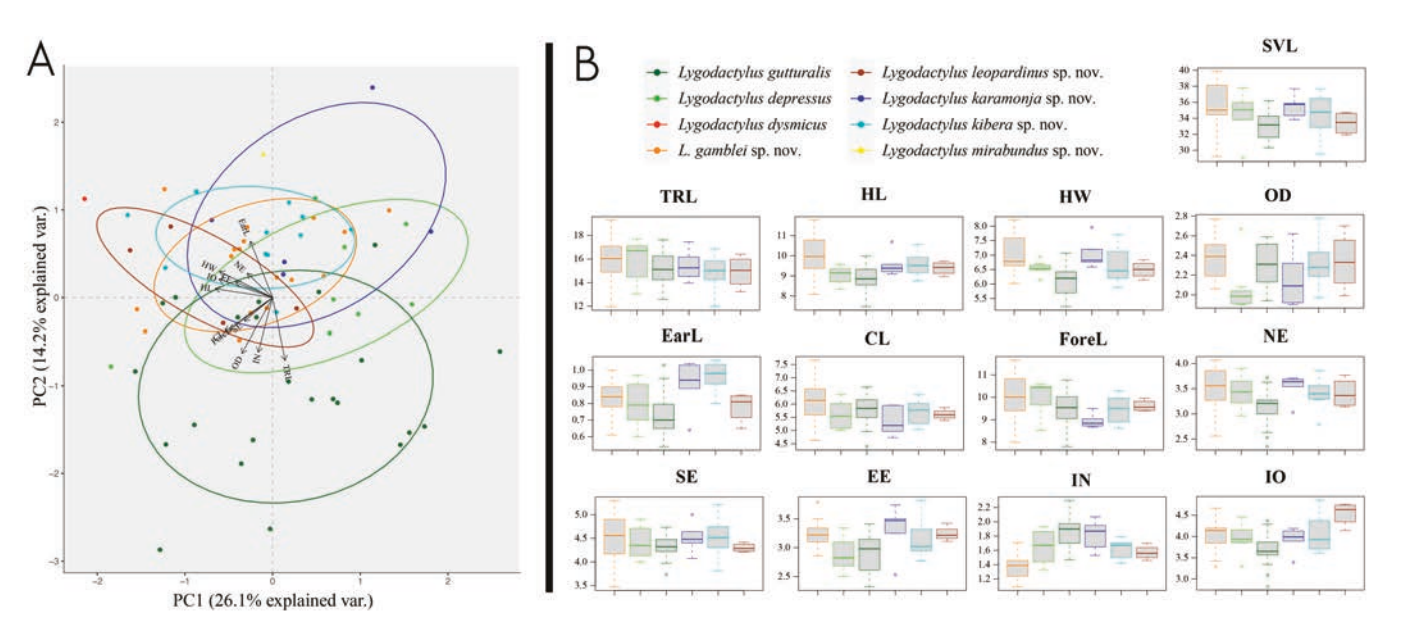


Figure 4. A, PCA plots of the first principal component (PC1) vs. the second principal component (PC2). Species are represented by different colours included in the legend. B, Boxplots (top whisker–maximum value; lower whisker–minimum value; dark horizontal line–median) of the body size (SVL) and linear measurements analysed in this study. Values in all the variables with the exception of SVL, are represented using the Least-squares means interaction plot (function Lsmip, package lsmeans). For abbreviations and further details see Material and methods section.

only seven as in *angularis* Günther (5 to 8)' (translated from the original French).

Diagnosis: Medium-sized Lygodactylus with maximum snoutvent length (SVL) of 38.2 mm. Body slender, nape moderately distinct. Head as broad as body, and moderate head length (HW/ HL 0.73). Canthus rostralis not prominent. Circular pupil. Ear to eye distance slightly larger than orbit diameter. Snout rounded and slightly pointed. Granular scales of frontal larger than occipital scales. Dorsal scales granular from rostral to tail. Rostral undivided, in contact with 1st supralabial, prenasals, and one large internasal scale. Seven supralabials and six infralabials. Prenasal scale present but not contacting the 1st supralabial. Nostril circular, surrounded by rostral, 1st supralabial, prenasal, one supranasal, and one postnasal. Mental large, triangular, and rounded posteriorly, with two or three large rounded postmental scales. Five post-postmental scales. Male with seven precloacal pores. Gular scales granular, rounded, and slightly smaller than ventral scales. Ventral scales larger than gulars, imbricate, with 19 scale rows across the venter. Terminal scansors on tail tip absent. Digits elongated and unwebbed with 5-6 terminal scansors. Thumb rudimentary with a small claw.

Lygodactylus paurospilus can be distinguished from *L. angularis* based on its gular pattern which consists of several irregular lines [vs. three or four lines in a V-shaped chevron in *L. angularis* (Supporting Information, Fig. S3)]. It can be differentiated from *L. heeneni* by having a lower number of supralabials (seven vs. nine in *L. heeneni*). Also, the two types of *L. paurospilus* seem to lack the white-cream vertebral ocelli (Fig. 8; Supporting Information, Fig. S4) present in all specimens of *L. heeneni* examined in this work (Supporting Information, Fig. S2). However, we are aware that this could be the consequence of preservation history and we only tentatively regard this as diagnostic until fresh specimens of *L. paurospilus* can be examined.

Variation: Measurements and meristic characters of the holotype and paratype are presented in Supporting Information, Table S4.

Habitat and distribution: Known from Haute Lubitshako (modern-day Kabobo Plateau), South Kivu Province, DRC, between 1900–2000 m a.s.l. This area is in a transition zone between montane forest and highland savannah, so we cannot provide an accurate habitat description for this species.

Natural history: Nothing is known about the natural history of this species.

Lygodactylus gutturalis complex

Herein, the L. gutturalis complex is resolved into nine distinctive taxa, from which seven consistently show large genetic 16S p-distances (6.07-16.72%, Table 2). The morphological analyses retrieved few diagnostic characters that support recognition of these nominal and candidate species. Therefore, following Struck and Cerca De Oliveira (2019), Davis et al. (2020), and Lobón-Rovira et al. (2022) we consider this group as a cryptic species complex. Despite the morphological overlap found among all nominal and new candidate species, the genetic results are also supported by biogeographic patterns (see above). Because of the difficulty of accessing material from South Sudan, Ethiopia, and Somalia, the cryptic character of the group, and the complex biogeography of East Africa, we refer all records from these regions to L. cf. gutturalis until new specimens or more molecular and morphological information becomes available.

The median-joining network recovered a well-differentiated taxon within the *L. gutturalis* subgroup from Tanzania, which was not included in the mitochondrial phylogenetic analyses

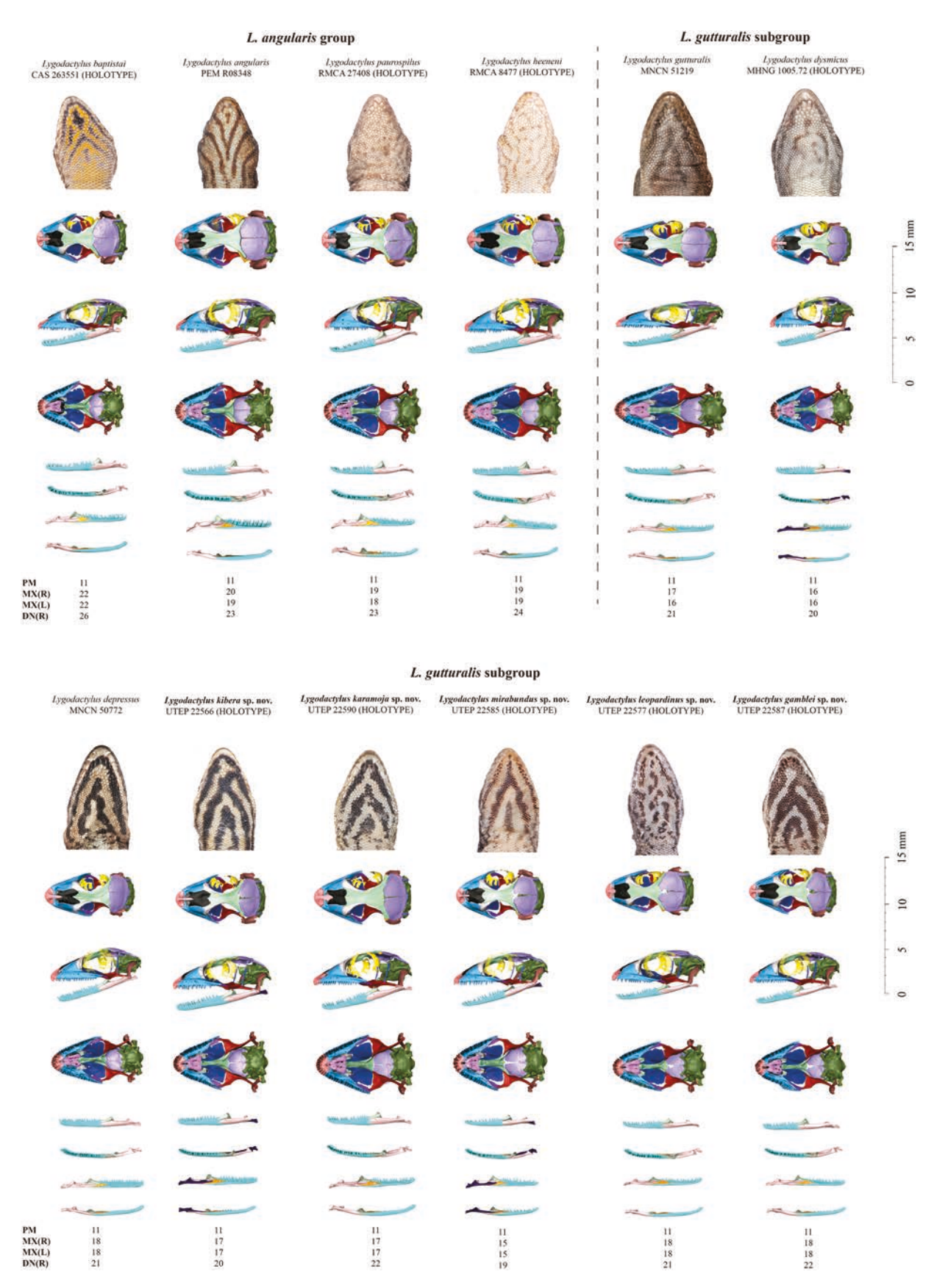


Figure 5. Gular and skull osteology comparisons between holotype material or representative material of all members of the *L. gutturalis* subgroup and the *L. angularis* group mentioned in this work. From top to bottom, ventral view gular section; dorsal, lateral, and ventral view of the skull; lateral, dorsal, medial, and ventral view of jaw; and number of tooth loci. PM = PRM = PR

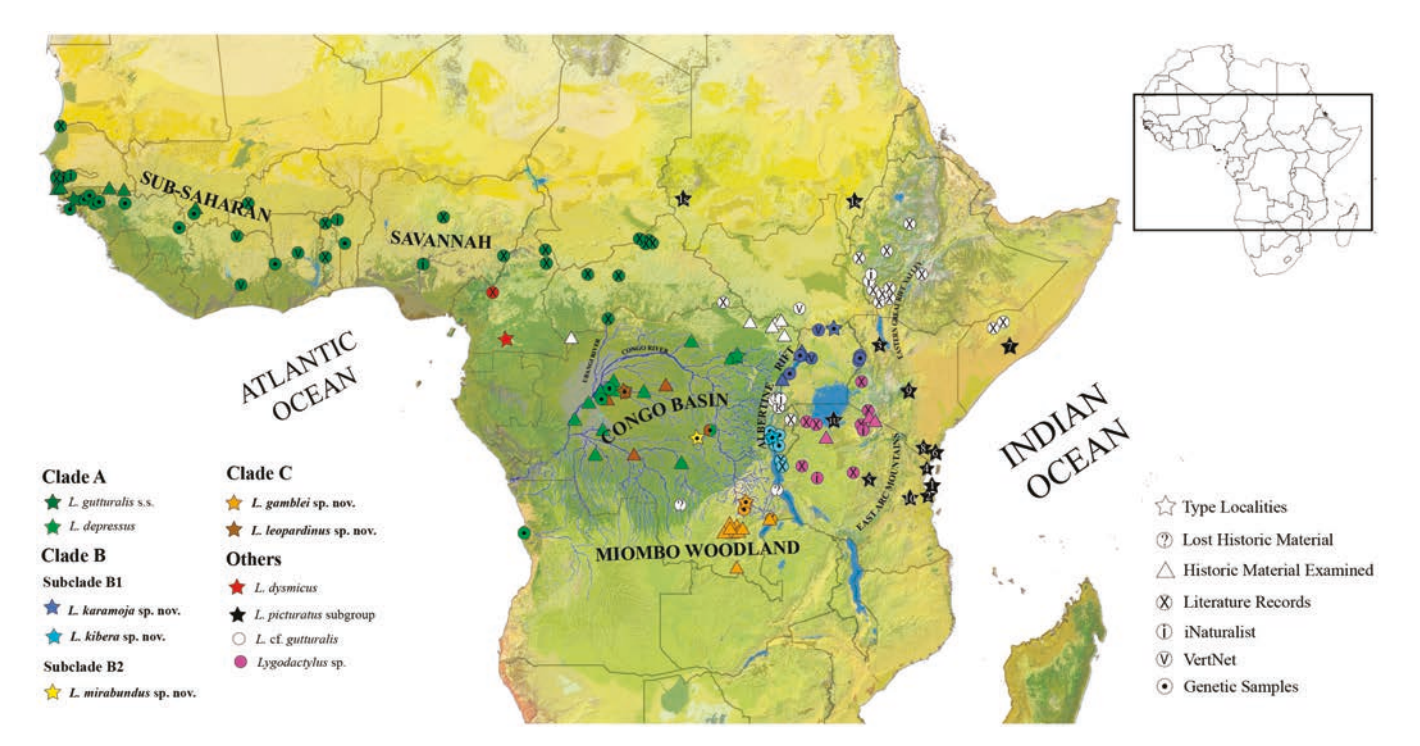


Figure 6. Geographical distribution of the *L. gutturalis* complex in Africa, on a hybrid map of the major vegetation divisions (Sayre *et al.* 2013) and 1 arc-second elevation map across tropical Africa (NASA 2000). Different colours depict records of different species within the *L. gutturalis* subgroup; see inset for explanations of symbols. White circles denote records of *L. cf. gutturalis* that cannot be assigned to any of the nominate taxa. Black stars represent the type localities of each nominate taxon within the *L. picturatus* subgroup (1–*L. picturatus*, 1S–*L. picturatus sudanensis*, 1U–*L. picturatus ukerewensis*, 2–*L. inexpectatus*, 3–*L. keniensis*, 4–*L. kimhowelli*, 5–*L. manni*, 6–*L. mombasicus*, 7–*L. scorteccii*, 8–*L. tsavoensis*, 9–*L. wojnowskii*, 10–*L. williamsi*).

(Figs 2B-C). Detailed examination of that specimen and additional photographed individuals and preserved specimens from Kenya and Tanzania (Supporting Information, Table S2) showed clear morphological differentiation (based on gular patterning) from related taxa within the L. gutturalis subgroup. However, this material partially agrees with the original descriptions of two taxa (Lygodactylus picturatus ukerewensis Loveridge, 1935 and Lygodactylus manni Loveridge, 1928), both lacking molecular data or explicit phylogenetic hypotheses. Lygodactylus manni was described to recognize geckos exhibiting a variant of the gular pattern of L. picturatus picturatus (Loveridge 1928). Lygodactylus picturatus ukerewensis was described by Loveridge (1935: 200) from Ukerewe Island in Kenya as follows '... no yellow colouring ... throat black, posteriorly with four indentations of white from the breast; rest of under surface white except for a dusky line along the underside of tail ...', two characters that are absent in the type series of *L*. manni. However, L. manni was synonymized with L. picturatus picturatus by Loveridge (1960), and Pasteur, 1965(1964) subsequently synonymised L. p. ukerewensis with L. manni. Our material of Lygodactylus sp. from Kenya and Tanzania exhibit the same gular patterning as L. p. ukerewensis and L. manni, and they have a well-developed line along the underside of the tail. Due to morphological overlap of these characters, the taxonomic confusion surrounding these names, and the lack of phylogenetic context for the latter two taxa, we refer to the material from Kenya and Tanzania as Lygodactylus sp. pending further revision.

LYGODACTYLUS GUTTURALIS S.S. (Bocage, 1873)
(Figs 9–11, Table 3; Supporting Information, Fig. S5; Table S5)

Hemidactylus gutturalis: Bocage (1873).

Lygodactylus gutturalis: Boulenger (1885); Kluge (1991, 1993, 2001); Broadley and Cotterill (2004) [part]; Chirio and LeBreton (2007); Trape et al. (2012); Spawls et al. (2018) [part].

Lygodactylus picturatus gutturalis: Schmidt (1919) [part]; Loveridge (1947); de Witte (1953) [part]; Pasteur, 1965 (1964) [part]; Wermuth (1965) [part]; Bauer and Günther (1991).

Lygodactylus (Lygodactylus) gutturalis gutturalis: Rösler (2000).

Lygodactylus gutturalis gutturalis: Röll (2005) [part]; de Lisle et al. (2013, 2016).

Lygodactylus gutturalis was described by Bocage (1873) based on a type series collected from Bissao (Bissau), Portuguese Guinea (now Guinea-Bissau), but he did not make any reference to the number of specimens used for his description. Nevertheless, three traceable specimens are known from the type series: a specimen from MBL destroyed in the Lisbon Museum fire in 1978, ZMB 7771 (Bauer and Günther 1991), and BMNH 1875.4.26.8 (now Boulenger 1885, NHMUK 1900386). Bauer and Günther (1991) referred to the ZMB specimen as a paratype, and Boulenger (1885) noted in his catalogue: 'one of the types'.

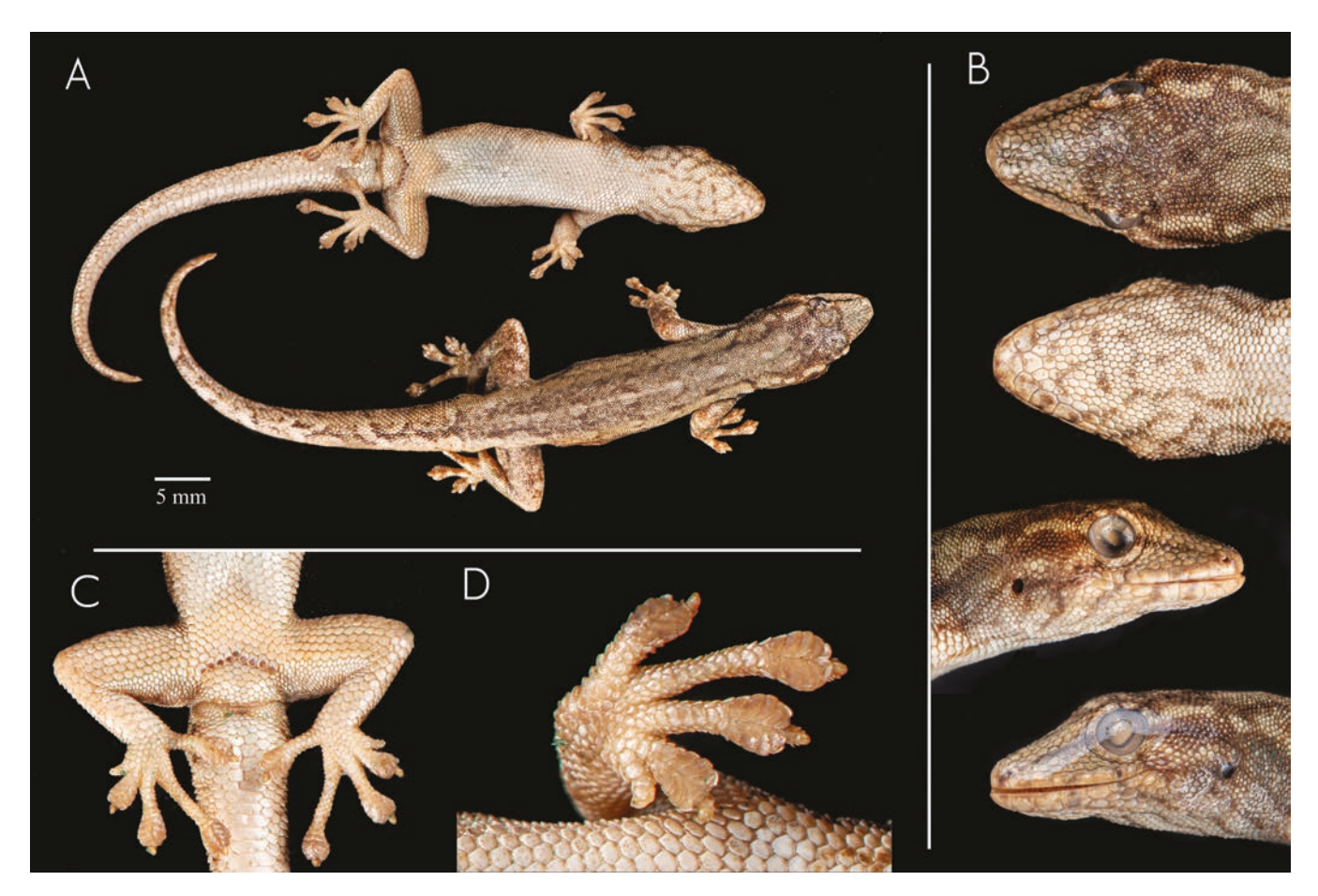


Figure 7. Holotype of *L. heeneni* [RMCA (= MRAC) R.8477] from Kapiri, Lualaba Province, DRC. A, Ventral and dorsal view of body. B, Details of head in dorsal, ventral, and lateral views (from top to bottom). Photos by J.L.R.

However, we believe that all three specimens are most appropriately considered as syntypes. Given that there are multiple morphologically similar species within the *L. gutturalis* complex, stability would be threatened if the nominate form could not be unambiguously defined. As none of these syntypes has explicitly been designated as a lectotype, we take this opportunity to select a lectotype from among the surviving syntypes to avoid this eventuality. The specimen in Berlin was not only sent by Bocage, but it is recorded in the ZMB register as having been collected from the type locality by the same collector as the destroyed Lisbon specimen (Bauer and Günther 1991). The NHMUK register verifies that the London specimen came from Bocage, but does not provide information about the collector (Boulenger 1885). Based on this, we here designate ZMB 7771 as the lectotype and BMNH 1875.4.26.8 becomes a paralectotype.

Our phylogenetic analyses revealed that *L. gutturalis s.s.* represents a widespread taxon in the sub-Saharan savannah, from West Africa to the Central African Republic, with low intraspecific genetic variation across its range (< 4.50% 16S uncorrected p-distance over a distance of approximately 2000 km). Our results support *L. gutturalis* as sister to *L. depressus* from the Congo Basin, and they are well-differentiated genetically by 9.04% (16S uncorrected p-distance).

All of the topotypic L. gutturalis material examined for this work agree with the detailed description provided by Bocage (1873) and the lectotype (ZMB 7771), which was examined by us. Moreover,

L. gutturalis is the only Lygodactylus species reported from Guinea-Bissau (Trape et al. 2012). Therefore, based on morphological distinctiveness and its exclusive biogeographic distribution in West Africa, we can reliably assign the type specimens (Fig. 9) to the molecular lineage identified from our own genotyped samples (Fig. 1). However, L. gutturalis has been frequently misidentified, with several authors assigning material from regions of Africa far from the type locality to L. gutturalis (Chirio and LeBreton 2007, Spawls et al. 2018). As a result, morphological characters not found in the typical form have been erroneously ascribed to this taxon. The large amount of material examined in this work has allowed us to identify some intraspecific morphological variation within L. gutturalis s.s. that was not reported before. Therefore, we provide an updated, detailed description and diagnosis of L. gutturalis to facilitate its identification and comparison to the new candidate species described below.

Lectotype: ZMB 7771 (Fig. 9, designated here), adult male, collected from Bissau, Bissau Region, Guinea-Bissau by Mr Sá Nogueira.

Paralectotypes: MBL (destroyed in the 1978 fire) collected from Bissau, Bissau Region, Guinea-Bissau by Mr Sá Nogueira in 1870. NHMUK 1900386 (formerly BMNH 1875.4.26.8), male, collected from Bissau, Bissau Region, Guinea-Bissau, without precise information of date or collector.

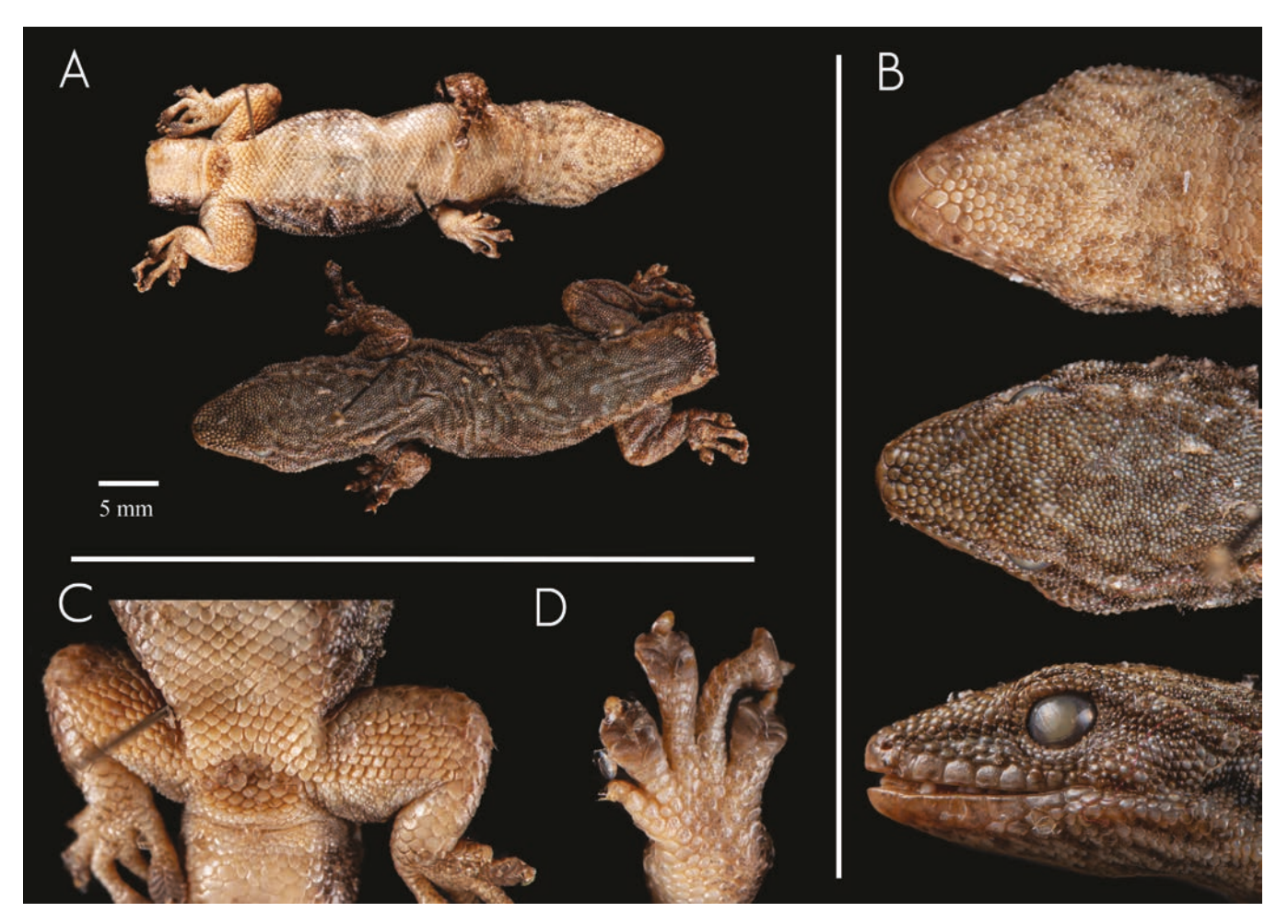


Figure 8. Paratype of *L. paurospilus* [RMCA (=MRAC) R.27409] from Haute Lubitshako, South Kivu Province, DRC. A, Ventral and dorsal views of body. B, Details of head in ventral, dorsal, and lateral views (from top to bottom). C, Details of cloacal region. D, Details of right manus. Photos by J.L.R.

Other material examined (85 specimens): • Guinea Bissau (38 specimens collected in 2010/2011 by Jean-François Trape and one specimen collected in 2014 by T. Cabuy): MNCN51220-8, IRD:TR 3836-37/39/41/43/45/47/49-52/54-55/57-58, from Medina Boe, Gabu Region; MNCN51229, from Bafata, Bafata Region; IRD:TR 3802/3924/26-30/33, MNCN51230-31, from Sambatchur, Bafata Region; MNCN51219, TR3551, from Bubaque, Bolama Region; RMCA 2014.015.R.0004, from Beli, Gabu Region. • Senegal (20 specimens collected in 2000-2003 by Jean-François Trape): IRD:B1457/59, MNCN51239-40, IRD:B1462/65, from Ibel, Kedougou Region; IRD:B1697, from Kagnut, Ziguinchor Region; MNCN51232-3/41-43, IRD:B148, IRD:B150, IRD:B255, IRD:B1492, IRD:B1512/14, IRD:B1534, IRD:B1667, from Mlomp, Ziguinchor Region. • Benin (12 specimens collected in 2010 by Jean-François Trape): IRD:TR3288, MNCN51234, MNCN51244-47, IRD:TR3292-94, IRD:TR3296-97, from Guiguisso, Donga Department. • Ghana (two specimens collected in 2010 by Jean-François Trape): IRD:TR2974, MNCN 51236, from Nsonsomea, Bono Region. • Republic of Guinea (10 specimens collected between 2004-2008 by Jean-François Trape): IRD:TR2974, MNCN51237-38, IRD:TR2452-56, from Kalan-Kalan, Kankan Region; IRD:TR2541, from Poré (Mamah),

Labe Region; MNCN 51248, from Samballo, Boke Region. • *Mali* (two specimens collected in 2004 by Jean-François Trape): IRD:TR938, from Niakoni, Sikaso Region; MNCN51249, from near Niariako, Sikaso Region. See Supporting Information, Table S2 for details.

Diagnosis: A large-sized species within the genus Lygodactylus (max. SVL 36.2 mm). The species is covered by uniform granular scales dorsally, and by small, rounded, and imbricate scales ventrally (Fig. 9). Ventral scales frequently serrated posteriorly with three or four denticulations (Fig. 10F). Original tail as long as SVL (Table 3; Supporting Information, Table S5), with enlarged series of scutes ventrally and tail tip thickened bearing five or six terminal lamellae (Fig. 10G). Head longer than wide. Six to eight supralabials and 6-8 infralabials. Usually, two symmetrical postmental scales; however, some specimens have one additional smaller medial postmental, and one specimen (IRD:TR3932) had four asymmetric postmental scales (Supporting Information, Fig. S5). Head with 1-3 internasal scales and 17-24 scales between the eyes (Supporting Information, Fig. S5; Table 3). Four to six post-postmentals. Nostril surrounded by a large prenasal scale, one supranasal, one supralabial, and occasionally, in contact with one postnasal scale (Fig. 10E). Rostral not in contact

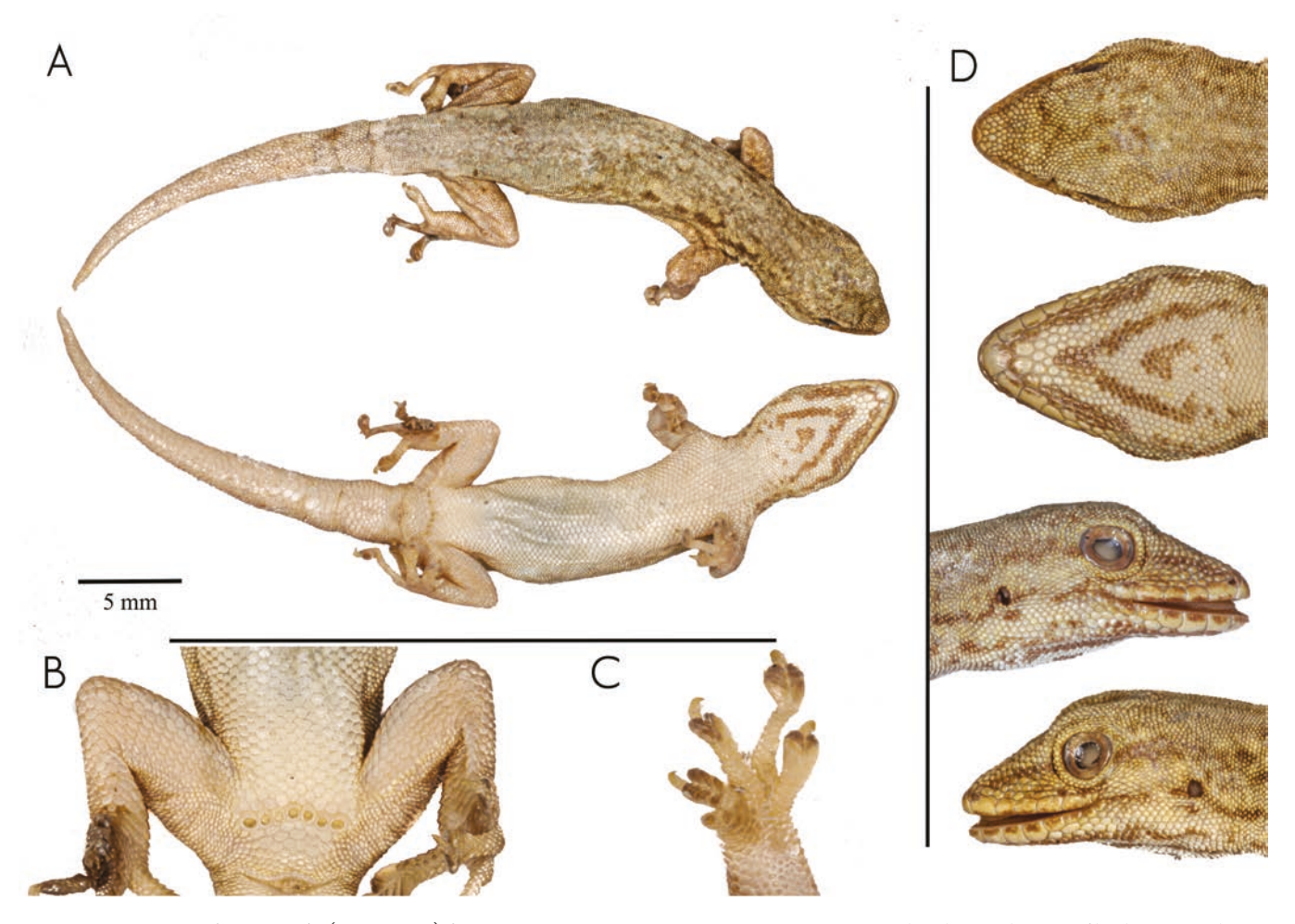


Figure 9. Lectotype of *L. gutturalis* (ZMB 7771) from Bissau, Bissau Region, Guinea-Bissau. A, Dorsal and ventral views of body. B, Details of cloacal region. C, Details of left manus. D, Detailed views of head in dorsal, ventral, and both lateral views (from top to bottom). Photos by Frank Tillack: Museum für Naturkunde, Berlin (ZMB).

with the nostril. Males with 5-8 precloacal pores and females usually with 6-7 enlarged plates that may have undeveloped pores.

Generally, brownish above, with two series of black-bordered russet ocelli or lines dorsally (Figs 10A–D), followed by a series of five or six light brown or cream ocelli dorsally (Figs 11A, D). One black line on each side, from nostril to eye, that usually meet anterior to the nostril. Black W-shaped mask between the eyes. The gular region bears two black gular ∩-shaped chevrons, with some individuals having a small black spot or an additional small chevron (giving the appearance of a 3rd chevron) between the branches of the inner chevron; markings more intense in males than females (Supporting Information, Fig. S5). Chevrons extend from mental scale to posterior part of mandibular region, but never reaching the chest. *In life*, chevron also more prominent in males than females, interspersed with orange, yellow, or whitish coloration (Fig. 11B−C, E).

Fore- and hind limbs moderately short, stout; forearm medium sized (FL/SVL 0.14–0.18); tibia short (CL/SVL 0.18). Digits elongated with 5–6 terminal scansors. Thumb rudimentary with a small terminal claw (Fig. 10F). Relative length of digits: I < II = V < III < IV (manus); I < II < V < III < IV (pes).

Lygodactylus gutturalis can be easily distinguished from the L. angularis group by the following characters: two black gular ∩-shaped chevrons that converge anteriorly vs. two gular V-shaped or broken pattern (in L. heeneni and L. paurospilus) of chevrons that converge posteriorly except for L. baptistai, which has a singular gular pattern that consists of an inverted Y-shaped chevron, with two incomplete broken lines laterally and parallel to the chevron, and an additional medial line posterior to the chevron (Fig. 5); nostril never in contact with the rostral vs. extensive contact with the rostral in the L. angularis group (Supporting Information, Figs S2-S3); reduced, almost vestigial postorbitofrontal vs. well-developed postorbitofrontal bone in the L. angularis group. It differs from the L. picturatus subgroup based on dorsal and gular colour patterns, lacking light blueish and yellowish dorsal coloration. It further differs from L. chobiensis by ∩-shaped gular chevrons vs. inverted Y-shaped chevrons interceded by a medial line posteriorly and by having fewer precloacal pores than *L. chobiensis* (5–8 vs. 10). Diagnostic characters from the newly named or re-evaluated taxa are presented in each respective diagnosis below.

Habitat and distribution (Figs 6, 11): Lygodactylus gutturalis is widely distributed in the sub-Saharan savannahs from northern

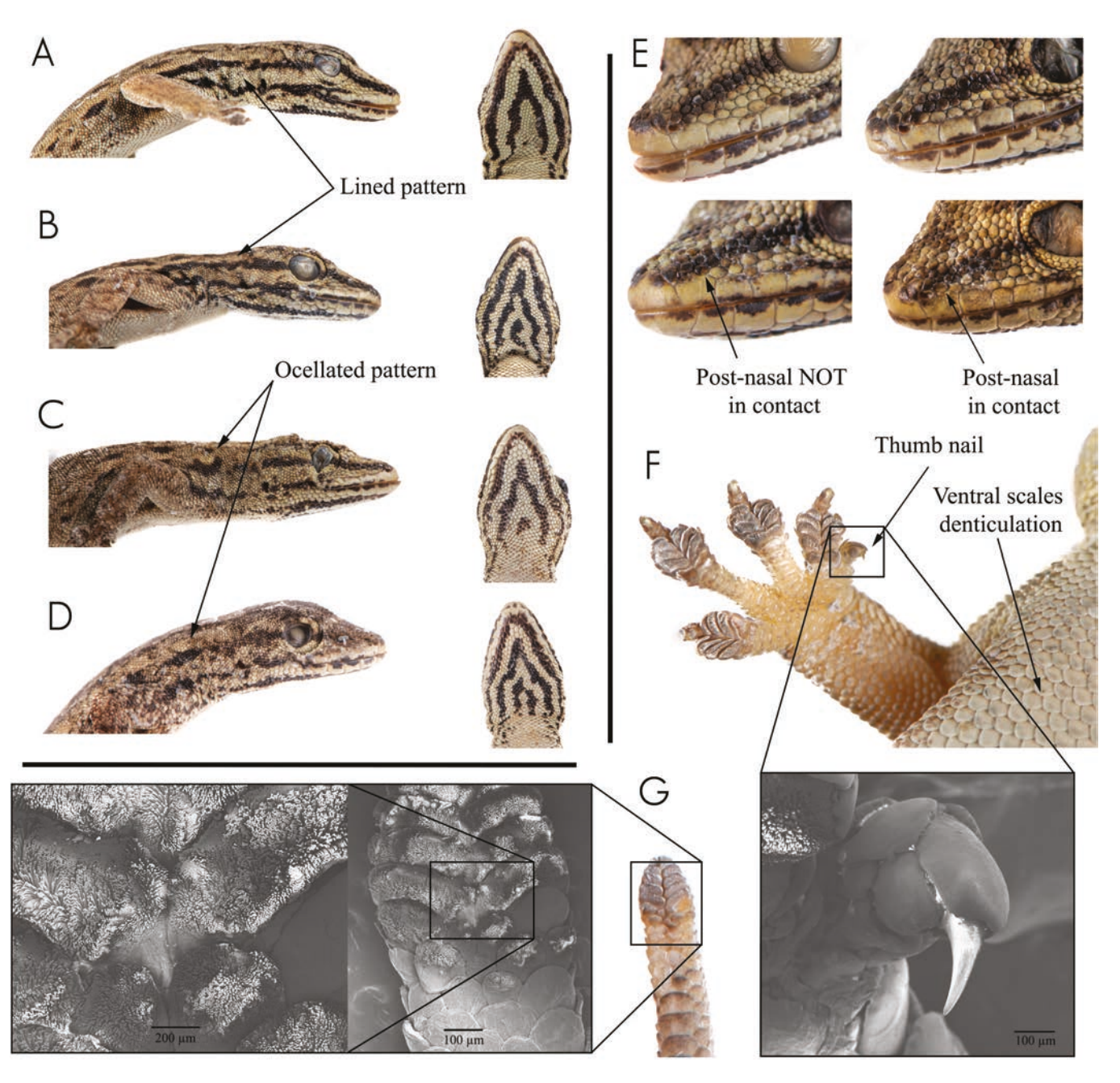


Figure 10. A–D, Lateral view and gular detail of four representatives of *L. gutturalis* that present four different combinations of dorsolateral + gular pattern (between lined or ocellated dorsolateral pattern, and two or three gular chevrons). E, Details of nostril, showing intraspecific variation in *L. gutturalis*. F, Detailed view of the right manus with a visible thumb claw in *L. gutturalis*, and SEM image of isolated claw. G, Detailed view of the tail tip in *L. gutturalis*, and two different SEM images of terminal tail scansors.

Senegal to the Central African Republic and Chad (including Gambia, Guinea-Bissau, Republic of Guinea, Benin, Togo, Burkina Faso, Ghana, Togo, Ivory Coast, Nigeria, and Cameroon). The species has been recorded from sea level to 761 m a.s.l.

Natural history (Fig. 11): An arboreal species always found on trunks or branches of trees in savannah. Some specimens have been observed at night sleeping on thin branches. They can be found next to villages, on riparian banks, or in open savannah.

LYGODACTYLUS DYSMICUS Perret, 1963 (Fig. 12; Table 3)

Lygodactylus angularis dysmicus: Perret (1963).

Lygodactylus gutturalis dysmicus: Pasteur (1964); Kluge (1991, 1993, 2001); Schätti and Perret (1997); LeBreton (1999); Schätti et al. (2002); Röll (2005); de Lisle et al. (2013, 2016).

Lygodactylus (Lygodactylus) gutturalis dysmicus: Rösler (2000).

Lygodactylus dysmicus: Chirio and LeBreton (2007).

Lygodactylus picturatus dysmicus: Thys van den den Audenaerde (1967).

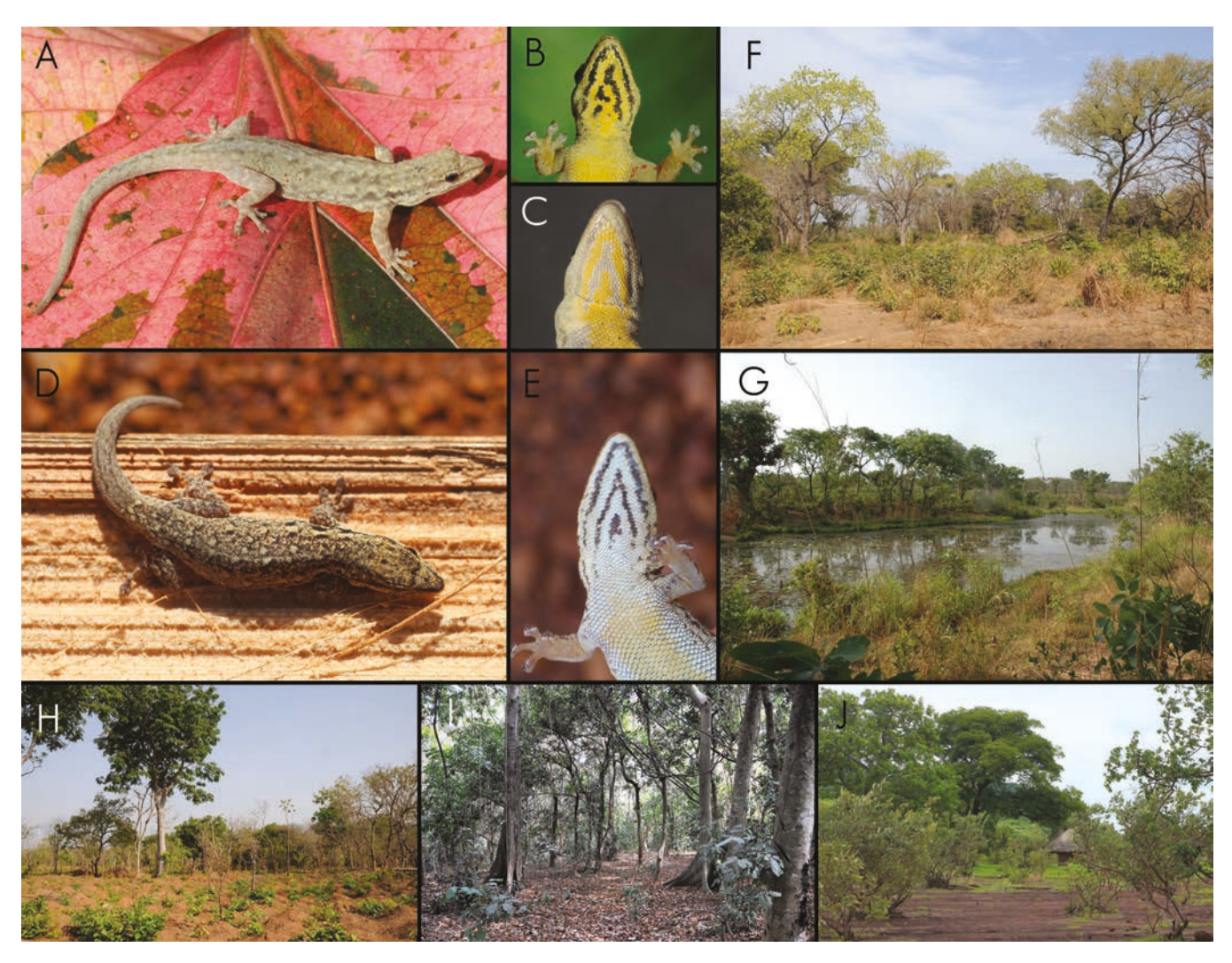


Figure 11. Specimens of *L. gutturalis* in life from (A–C) Guinea Bissau and (D–E) Senegal. Photos of habitat at (F) Sambatchur, Bafata Region, Guinea Bissau, (G) Kalan Kalan, Kankan Region, Guinea, (H) Guiguisso, Donga Department, Benin, (I) Nsonsomea, Sunyani Region, Ghana, and (J) Mlomp, Zinguinchor Region, Senegal. Photographs by J.F.T. (A–C and F–J) and Alberto Sanchez-Vialas (D–E).

Perret (1963) described L. a. dysmicus from Foulassi, South Region, Cameroon, as the western race of L. angularis that differs from the nominotypical form by its gular ornamentation. However, Perret never compared this species to L. gutturalis in neighbouring areas. In 1991, Kluge considered L. a. dysmicus as a subspecies of *L. gutturalis*, although he did not provide any justification. This taxonomic change was followed by other authors until Chirio and LeBreton (2007) considered L. dysmicus as a full species in their 'Atlas des reptiles du Cameroun' again without justification. Until then, the only known record of this species was the holotype; however, Chirio and LeBreton (2007) added a new photographic record from Nglochifen, West Region, Cameroon, in their book. Herein, based on the osteological evidence mentioned above, and the presence of terminal scansors on the tail tip, which are absent in the L. angularis group, we regard L. dysmicus to be part of the L. gutturalis subgroup. Despite the lack of molecular data, distinctive morphology supports the validation of L. dysmicus as a full species, as suggested by Chirio and LeBreton (2007) and Kluge (1991). Based on the detailed description provided by Perret (1963), we provide

only a diagnosis and comparison with L. $gutturalis\ s.s.$ and the L. $angularis\ group.$

Holotype: MHNG 1005.72, adult male, collected from forest at Foulassi, South Region, Cameroon (~665 m a.s.l.), at the north-west limit of the Congo Basin. Specimen fixed in formalin, now preserved in ethanol.

Diagnosis (Fig. 12): As noted by Perret (1963), the species differs from the *L. angularis* group mainly by the gular ornamentation, which consists of two ∩-shaped chevrons, one within the other, and a central mark vs. two *V*-shaped marks or broken pattern (in *L. heeneni* and *L. paurospilus*) chevrons that converge posteriorly. It also differs from the *angularis* group by having a reduced, almost vestigial postorbitofrontal vs. a well-developed postorbitofrontal bone in the *angularis* group. *Lygodactylus dysmicus* can be differentiated from *L. gutturalis* by having more precloacal pores (9 vs. 5–8); nostril in narrow contact with rostral scales vs. never in contact in *L. gutturalis*. We have also recorded some minor differences as follows: fewer

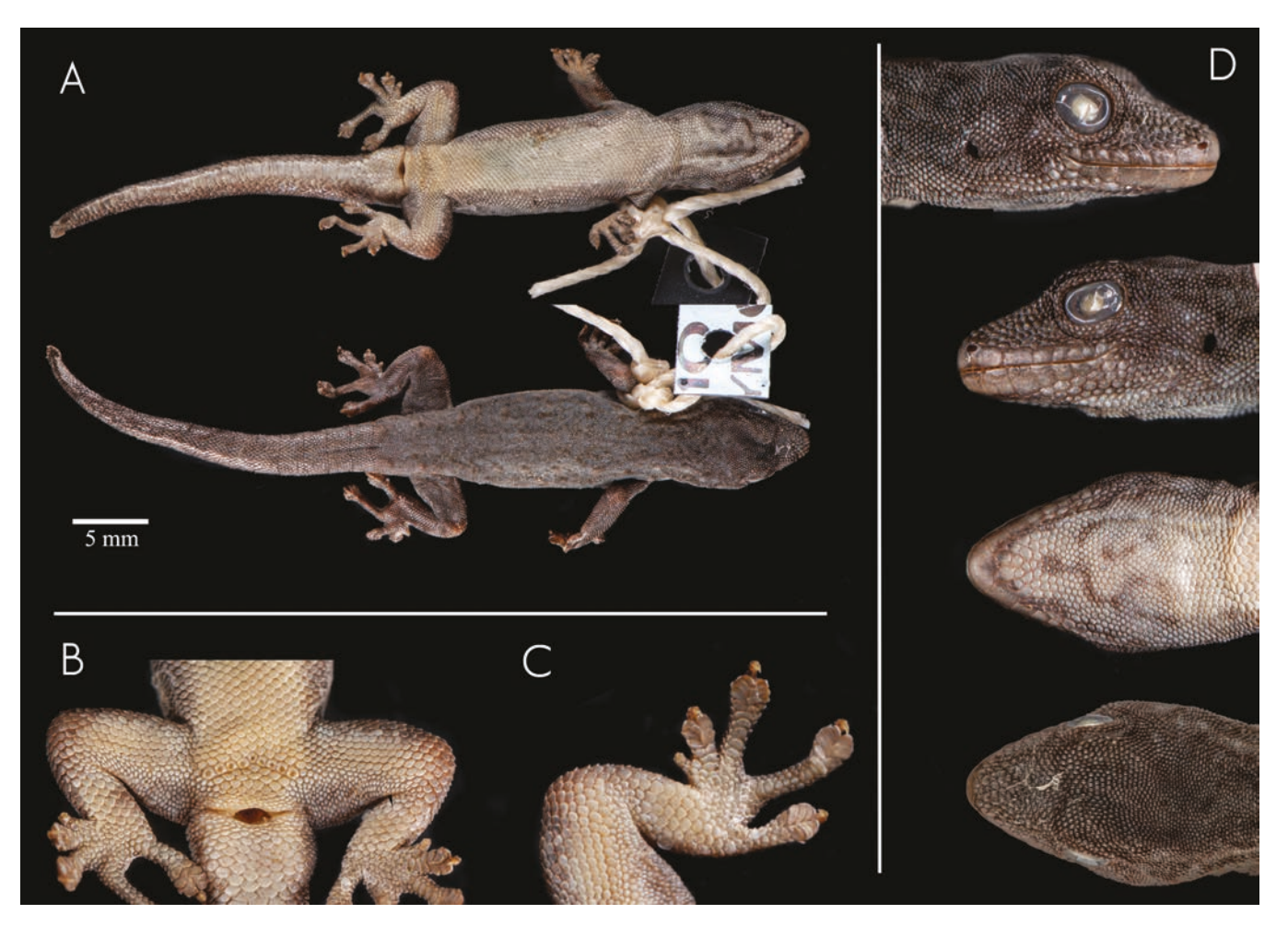


Figure 12. Holotype of *L. dysmicus* (MHNG 1005.72) from Foulassi, South Region, Cameroon. A, Ventral and dorsal view of body. B, Details of cloacal region. C, Details of left pes. D, Detailed view of head in both lateral views and ventral and dorsal views (from top to bottom). Photos by J.L.R.

lamellae under fourth toe (4 vs. 5–6); a greater number of ventral scales across the body (21 vs. 15–20); and a greater number of scales between the eyes (25 vs. 17–24). It is noteworthy that L. dysmicus is small [SVL 27.6 mm vs. 33.3 \pm 1.8 mm (mean) in L. gutturalis], with a paedomorphic skull that has an unfused frontal bone, braincase, and compound bone + surangular (Fig. 5). However, the well-developed state of the precloacal pores suggest sexual maturity of this specimen (Rhen $et\ al.\ 2005$; Fig. 12B). Finally, L. dysmicus can be differentiated from L. gutturalis based on its distribution in lowland Congolian rainforest vs. the sub-Saharan savannah (Fig. 6).

Habitat and distribution (Fig. 6): Lygodactylus dysmicus is only known from the type locality in Foulassi, South Region, Cameroon, and an additional photographic record (unconfirmed) from Nglochifen, West Region, Cameroon. Lygodactylus dysmicus is considered a rainforest species distributed near the northern limit of the Congolian Rainforest.

Natural history: Diurnal gecko that lives on trees in dense semi-deciduous forests (Chirio and LeBreton 2007).

LYGODACTYLUS DEPRESSUS Schmidt, 1919 (Figs 13–16, Table 3; Supporting Information, Table S6)

Lygodactylus picturatus depressus: Loveridge (1947), Wermuth (1965).

Lygodactylus depressus: Pasteur, 1965 (1964); Kluge (1991, 1993, 2001); Rösler (2000); Chirio and LeBreton (2007); Röll et al. (2010); de Lisle et al. (2013, 2016)

Lygodactylus depressus was described from Medje, Haut-Uele Province, DRC, by Schmidt, who described the species as an intermediate form between L. picturatus and L. gutturalis: '... The relation of this species with *L. picturatus picturatus* (Peters) appears to be close; its coloration is in some respects similar but does not seem to fall within the wide variation ... chevrons of the throat equally distinct in the female (only two V's in three of the paratypes) narrower than in gutturalis ... Venter and enlarged subcaudals immaculate yellow in life—an apparently constant distinction from Lygodactylus picturatus gutturalis' (Schmidt 1919: 466). However, Loveridge (1947: 227), relegated this taxon to a subspecies of L. picturatus, stating: '... a somewhat doubtful race, differing from gutturalis only in gular and subcaudal markings This taxonomic action was ignored by Pasteur, 1965 (1964), but followed by Wermuth (1965), both authors without justification. Kluge (1993) included L. depressus as a full species, in his checklist again without any justification of his taxonomic decision.

Since then this species has been collected in different regions of the Congo Basin. However, this material was overlooked in many publications that revisited the L. picturatus group (Röll et al. 2010, Malonza et al. 2016, 2019). We recovered a genetic clade that is sister to L. gutturalis, from the rainforest of the Congo Basin (Figs 1, 6) that differs by c. 9.04% (16S uncorrected p-distance; Table 2) from its sister taxon. Among this material, we included specimens from Lake Tumba, where historical material of L. depressus was previously collected. Consequently, we revised historical material collected from the Congo Basin, tentatively attributed to L. gutturalis and L. depressus (Supporting Information, Table S2). After morphological examination and comparison of preserved specimens (faded), we observed a complete overlap between specimens ascribed to these two taxa, failing to identify any morphological differences based on pholidosis or gular ornamentation. In his description of L. depressus, Schmidt (1919: 466) remarked: '... coloration dark blueish grey, irregularly mottled with black, more heavily anteriorly ...' However, he also made reference to colour variation recorded by Herbert O. Lang (collector): '... one specimen was entirely black when caught, turning blueish grey when injected' We observed that two specimens allocated to L. depressus and collected at Lotende (a river at Mabali, the site of a colonial-era research station at Lake Tumba; Marlier 1958), Lake Tumba (RMCA 1981.065.R.005) by Laurent, exhibit both colour morphs described for *L. depressus* (mottled and uniform). In contrast, two specimens (RMCA R.8575/A and RMCA R.8575/B) collected from Flandria, Équateur Province, DRC (~110 km north-east from the previous locality) and identified by de Witte in 1923 (RMCA unpublished data) as L. gutturalis, show the same two dorsal patterns as the previous specimens mentioned above (Fig. 13). Two additional specimens (RMCA 1038/B and 1038/C) were collected from the Ituri Forest (without a precise locality within this region, but in the same region as the type locality of L. depressus) and tentatively assigned to L. gutturalis by de Witte in 1923 (RMCA unpublished data). However, these specimens have morphological characters that are intermediate between these two taxa. Thus, material from DRC and

Angola (previously attributed to *L. gutturalis*), shows substantial morphological overlap with topotypic material of *L. depressus*, making it impossible to differentiate them from the type series (Figs 15, 16). The specimen collected from Angola (MNCN 50772) has a dark blueish coloration *in life* (Fig. 15G), as described in *L. depressus*. Consequently, due to the high morphological and geographic overlap, we consider that this clade, sister to *L. gutturalis s.s.* (Fig. 1), represents *L. depressus*. Nevertheless, we recommend caution until topotypic material can be included in a phylogenetic context, because the possibility of further cryptic diversification within this group cannot be excluded.

A photographic record from Molondou, East Region, Cameroon, reported by Chirio and LeBreton (2007), and attributed to *L. depressus*, does not agree with the diagnostic dark blueish coloration mentioned by Schmidt (1919). Therefore, because of the highly diverse character of the *picturatus* subgroup, records from Cameroon and other localities west and north of the Ubangi and Congo rivers might belong to an undescribed taxon.

Holotype (Fig. 14): AMNH 10345, adult male with original tail, collected at Medje, Ituri Forest, Haut-Uele Province, DRC, on 5 July 1914 by Herbert O. Lang.

Additional material examined (12 specimens): • DRC (10 specimens): RMCA R.3216 (formerly AMNH 10346) and MCZ R45987 (formerly AMNH 10344), males (paratypes), with same collection data as the holotype; UTEP 22579/UTEP 22582 (ELI 2128/ ELI 2152), males, and UTEP 22580–81/ UTEP 22583 (ELI 2129–30/ ELI 2153), females, collected at Npenda Village, north-east of Lake Tumba, Équateur Province, S00.7465, E18.2243, 311 m a.s.l. on 6 July 2013 by locals and brought to Eli Greenbaum; UTEP 22578 (ELI 1547), female, collected at Lake Tumba, Équateur Province, c. S00.80, E18.15, 300 m a.s.l. on 13 February 2010 by Chifundera Kusamba; UTEP 22595 (ELI 3624), female, collected at Katopa, Maniema Province, S02.75128, E25.10403, 455 m a.s.l. on 4 July 2015 by locals and brought to Eli Greenbaum; UTEP 22597 (ELI



Figure 13. Dorsolateral and ventral variation of two male specimens [RMCA R.8575/A (left) and RMCA R.8575/B (right)] of *L. depressus*, collected in sympatry at Flandria, Équateur Province, DRC.

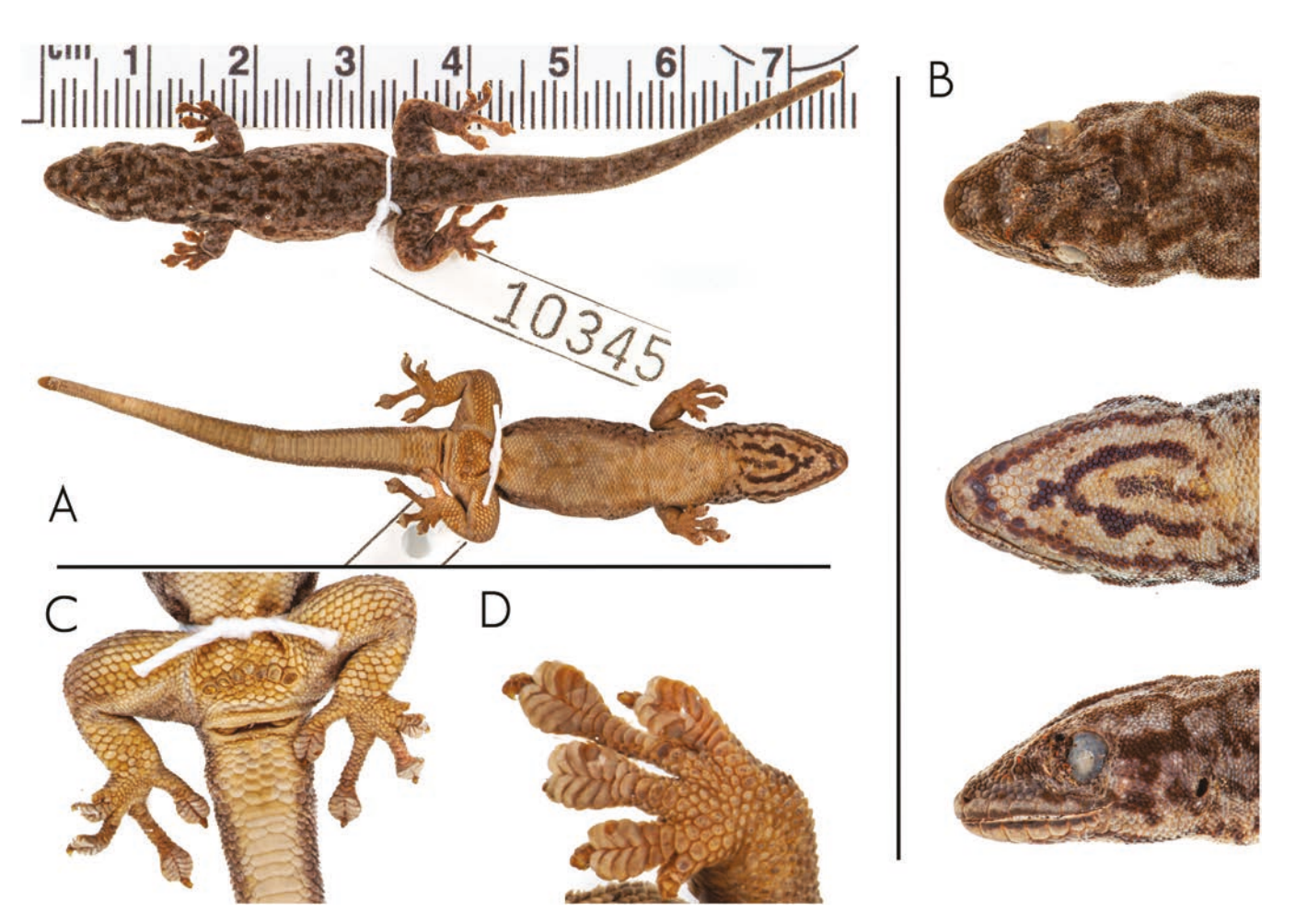


Figure 14. Holotype of *L. depressus* (AMNH 10345) from Medje, Ituri Forest, Haut-Uele Province, DRC. A, Dorsal and ventral view of body. B, Detailed view of head in dorsal, ventral, and lateral views (from top to bottom). C, Details of cloacal region. D, Details of left manus. Photos provided by Lauren Vonnahme: American Museum of Natural History, New York City (AMNH).

3585), male collected from Katopa, ICCN Camp, Maniema Province, S02.74769, E25.10323, 450 m a.s.l. on 2 July 2015 by Eli Greenbaum. • *Angola* (two specimens): MNCN 50771–72 (P1-307 and P1-306), males, collected at Barra do Cuanza, Luanda Province, S09.19518, E13.20327, 7 m a.s.l. on 10 September 2021 by Pedro Vaz Pinto and Timoteo Julio.

Diagnosis: Lygodactylus depressus is a large-sized Lygodactylus with a maximum SVL 37.8 mm (mean 35.6 ± 1.4 mm) that has the typical gular pattern of the gutturalis group. Seven to nine supralabials and 6-7 infralabials. Dorsal pholidosis with granular scales that become flattened, larger, and imbricate in original tails. Large triangular mental followed by 2-3 symmetric postmental scales (Fig. 16). Males with 7-8 precloacal pores. Ventral pholidosis with large, flattened, and imbricate scales. Ventral scales usually with small denticulation posteriorly. Digits elongated with five terminal scansors on the fourth toe (Supporting Information, Table 86).

Like other members of the *L. gutturalis* subgroup, this species can be easily differentiated from *L. angularis* group members and from other members of the *picturatus* subgroup by the gular pattern and dorsal colour pattern (Fig. 5). It should be noted that *L. depressus* has a dark blueish grey dorsum *in life*, unlike the light blueish dorsal coloration in the *picturatus* subgroup.

Lygodactylus depressus can be differentiated from other species within the gutturalis subgroup by having a dark blueish grey coloration of the dorsum, with some specimens having a mottled pattern on the dorsum, vs. brownish or light grey without a mottled pattern in L. gutturalis. However, blackish specimens can only be differentiated by subtle morphometric and meristic data, being almost impossible to differentiate in the field. Lygodactylus depressus can be partially differentiated from L. gutturalis as follows: eye proportionally smaller in L. depressus $(OD/HL \le 0.25 \text{ vs. } 0.26-0.31 \text{ in } L. \text{ gutturalis})$; and narrower snout (IN/HW \leq 0.29 vs. 0.30–0.34 in *L. gutturalis*). It also differs by a minimum of c. 9.04% uncorrected p-distance for 16S (Table 2), lacks any nuclear haplotype sharing with L. gutturalis in RAG1 (Fig. 2), and habitat (rainforest for L. depressus and sub-Saharan savannah for L. gutturalis). It can also be differentiated from L. dysmicus by having fewer precloacal pores (7-8 vs. 9 in L. dysmicus) and nostril never in contact with rostral scale vs. nostril contacting the rostral in *L. dysmicus*. For a distinction from other species not included above, described herein, see the respective diagnoses below.

Coloration: In life (Fig.15), dorsal colour is highly variable; predominantly dark grey, with lighter grey blotches surrounded by black dots on the flanks, which can form a diffuse dorsolateral

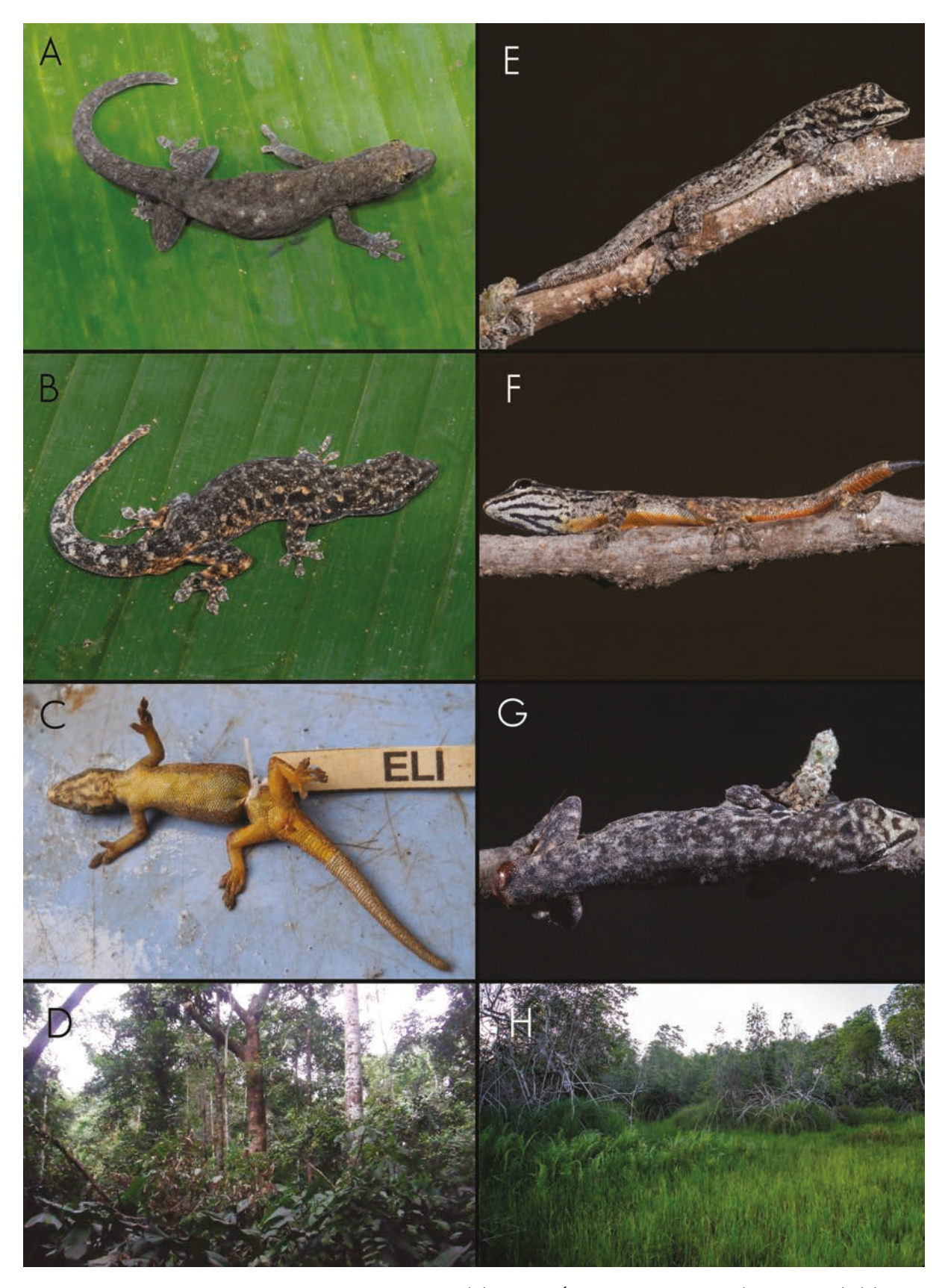


Figure 15. Specimens of *L. depressus* in life or freshly euthanized from (A) Npenda, Équateur Province, DRC (UTEP 22580), (B) Katopa, Maniema Province, DRC (UTEP 22597), (C) Lake Tumba, Équateur Province, DRC (UTEP 22578), and (E–G) Barra do Cuanza, Cuanza Sul Province, Angola (MNCN 50772). Photo of habitat at (D) Lake Tumba, Équateur Province, DRC and (H) Barra do Cuanza, Cuanza Sul Province, Angola. Photographs by E.G. (A–C), C.K. (D), P.V.P. (E–G), and J.L.R. (H).



Figure 16. Dorsal and ventral views of head showing gular ornamentation and pholidosis variation in *L. depressus*. Red points denote males and blue points denote females.

band; dark *V*-shaped line between the eyes (absent in darker specimens), and black line from snout to anterior insertion of the forelimb; tail with diffuse bars of lighter grey; throat usually with white background and black chevrons; venter vivid yellow, orange, or cream from tail tip to posterior part of the gular region. *In preservative* (holotype; Fig. 14), dorsum grey with dark brown dots from head to midbody; venter uniform light cream to yellow with whitish colouration on all digits.

Variation: Meristic and morphometric data are summarized and depicted in the Supporting Information (Table S6) and Figures 15–16. Lygodactylus depressus is the most variable taxon within the L. gutturalis group with respect to coloration, particularly the gular pattern (Fig. 16). Some specimens lose the dorsal pattern, resulting in a uniform dorsal coloration. However, other specimens have a mottled dorsal pattern (Fig. 13).

Habitat and distribution (Figs 6, 15): This species is widely distributed within the Congo Basin, from the Ituri Forest in the north-east, through the heart of the Congo River at Npenda and Lake Tumba, south to Angola at the southernmost extreme of its range. The material from Angola was collected from mangroves growing at the mouth of the Cuanza River. However, all material from DRC was collected in dense Congolian rainforest.

Natural history: Individuals in Angola were observed actively moving and hunting between the branches and trunk of trees during the day, but due to the difficult access to the mangroves, specimens were collected at night while sleeping on thin branches. Specimens from Lotende, DRC, were collected in the canopy, as recorded by Laurent in his field notes.

LYGODACTYLUS KIBERA SP. NOV.

(Figs 17–18, Table 3; Supporting Information, Fig. S6; Table S7)

Zoobank registration: https://zoobank.org/26F76FD8-043A-4226-BDD5-E971235D474C

Lygodactylus picturatus gutturalis: Schmidt (1919) [part]; de Witte (1953) [part]; Pasteur, 1965(1964) [part]; Wermuth (1965) [part].

Lygodactylus gutturalis: Röll (2005) [part]; Spawls et al. (2018) [part].

Lygodactylus kibera sp. nov. belongs to a distinctive clade (B1), from the Albertine Rift of Burundi and eastern DRC, which clusters as sister to another candidate new species from the northern Albertine Rift in the Lendu Plateau of DRC and several highlands of Uganda, but differs from it by c. 6.07% in 16S uncorrected p-distance (Table 2), and a lack of nuclear haplotype sharing in RAG1 (Fig. 2B–C).

Holotype: UTEP 22566 (ELI 1145), a male with a ventral incision, collected in a village near montane forest at Mpishi, near Kibira National Park, Bubanza Province, Burundi, S03.06974, E29.48445, 1660 m a.s.l. on 20 December 2011 by locals and brought to Eli Greenbaum.

Paratypes (11 specimens): • Burundi (10 specimens): UTEP 22567–69 (ELI 1146–48), females, and UTEP 22570 (ELI 1149), male with the same collection data as the holotype; UTEP 22571–73 (ELI 1195–97), males, and UTEP 22574–75 (ELI 1199–98), a male and a female, respectively, collected in a banana

field at Mpishi, near Kibira National Park, Bubanza Province, S03.06749, E29.48560, 1705 m a.s.l. on 21 December 2011 by Wandege M. Muninga and Eli Greenbaum; UTEP 22576 (ELI 1071), female, collected at Bujumbura City, Bujumbura Mairie Province, S03.38236, E29.36419, 811 m a.s.l. on 16 December 2011 by Wandege M. Muninga and Eli Greenbaum. • DRC (one specimen): UTEP 22586 (EBG 1556), male, collected in a gallery forest at N'Komo River, road. Bukavu-Uvira, South Kivu Province, S02.71471, E28.94641, 1260 m a.s.l. on 15 June 2008 by Maurice Luhumyo, Chifundera Kusamba, Mwenebatu M. Aristote, Wandege M. Muninga, John Akuku, Felix Akuku, Asukulu M'Mema, and Eli Greenbaum.

Diagnosis: A large Lygodactylus [maximum SVL 37.7 mm (mean 34.7 ± 2.5 mm)], that shares a similar distinctive gular chevron ornamentation with the *L. gutturalis* subgroup. It has 7–9 supralabials and 5–7 infralabials. Dorsal pholidosis with granular scales that become flattened, larger, and imbricate on original tails. Large triangular mental followed by usually three (occasionally two) symmetrical postmental scales (Supporting Information, Fig. S6). Nostril never in contact with rostral. Ventral pholidosis with large, flattened, imbricate scales. Five to six terminal scansors on the tail tip. Digits elongated with five terminal scansors on the fourth toe (Supporting Information, Table S7).

This species may be easily differentiated from the L. angularis group by the characteristic \cap -shaped gular pattern as L. gutturalis (see L. gutturalis diagnosis). It can be differentiated from L. paurospilus, found in the same region, on the basis of three \cap -shaped thick chevrons reaching the chest vs. two V-shaped broken gular chevrons in paurospilus; and by having a reduced, almost vestigial postorbitofrontal bone vs. well-developed postorbitofrontal in L. paurospilus. It can also be differentiated from other members of the L. picturatus group based on dorsal coloration and gular pattern (see L. gutturalis account).

Lygodactylus kibera sp. nov. can be differentiated from other species within the L. gutturalis subgroup by subtle morphometric and meristic features. This species is best regarded as cryptic, but we provide some characters that are diagnostically useful. Lygodactylus kibera sp. nov. differs from L. dysmicus by its larger size (maximum SVL 37.7 mm vs. 27.6 mm); gular patterning always with three ∩-shaped thick chevrons reaching the chest (vs. two thinner ∩-shaped chevrons, that never extend beyond the posterior part of the lower jaw); fewer precloacal pores (7–8 vs. 9); usually three symmetrical postmental scales vs. two; nostril never in contact with rostral scale (vs. nostril contacting rostral); and lower number of ventral scales across the body (16–18 vs. 21 in L. dysmicus). It can be distinguished from L. gutturalis s.s. by its slightly larger size [maximum SVL 37.7 mm (mean 34.7 \pm 2.5 mm) vs. 36.2 mm (mean 33.3 \pm 1.8 mm)]; snout proportionally narrower (IN/HW 0.20-0.27 vs. 0.29–0.34) with usually one large internasal scale vs. two smaller internasal scales (this character has shown to be variable in both species). It also differs from L. gutturalis and L. depressus based on gular pattern always having three thick ∩-shaped chevrons reaching the chest [vs. two or three (in L. gutturalis), or one or two (in *L. depressus*) thinner ∩-shaped chevrons that never extend beyond the posterior part of the lower jaw]; proportionally

more elongated head (HL/SVL 0.27–0.30 vs. 0.24–0.26) with larger eyes (OD/HL 0.24–0.27 vs. 0.20–0.23) than *L. depressus* (Fig. 4; Table 3). The new species occurs in mid-elevation moist forest, agricultural fields, and human habitations, vs. lowland dry sub-Saharan savannah (*L. gutturalis*) and lowland rainforest of the Congo Basin (*L. dysmicus*; see Fig. 6). For a distinction with other species described below, see their respective diagnoses.

Etymology: The name 'kibera' derives from the word 'kibira' or 'kibera' in Kinubi—a Sudanese Arabic-based creole language spoken in some regions of Burundi, Kenya, and Uganda—that means 'forest', the main habitat type associated with the species.

Description of the holotype (Fig. 17): Measurements and meristic characters of the holotype are presented in Supporting Information, Table S7. Adult male, with a snout-vent length (SVL) of 36.9 mm and a slightly larger original tail length (TL = 40.6 mm). Body slender, nape moderately distinct. Head as broad as body, and moderate head length (HW/HL 0.70). Canthus rostralis not prominent. Eye diameter 2.5 mm, with circular pupil. Ear to eye distance slightly larger than orbit diameter (3.7 mm). Snout rounded and slightly pointed. Frontal granular scales larger than occipital scales. Dorsal scales granular from rostral to tail. Rostral undivided, in contact with 1st supralabial, prenasals, and one large internasal scale. Eight to nine supralabials and six infralabials. Prenasal scale in contact with 1st supralabial. Nostril circular, bordered by 1st supralabial, prenasal, one supranasal, and one postnasal. Four rows of scales between supralabials and the orbit. Mental large, triangular, and rounded posteriorly, with two large rounded postmental scales separated by one small rounded postmental scale. Five post-postmental scales. Gular scales granular, rounded, and slightly smaller than ventral scales. Ventral scales large, imbricate, with 17 scales rows across the venter. Body relatively robust and slightly elongated (TRL/SVL 0.43). Tail with 51 enlarged transverse scales and six pairs of terminal scansors on the tip. Seven precloacal pores. Fore- and hind limbs moderately short, stout; forearm medium-sized (FL/SVL 0.14); tibia short (CL/SVL 0.16). Digits elongated and unwebbed with 5-6 terminal scansors. Thumb rudimentary with a small claw. Relative length of digits: I < II = V < III < IV (manus); I < II < V < III < IV (pes).

Coloration: In life (Fig. 18), dorsal coloration brownish grey with light cream-beige lines from nape to tail on each side of the dorsum interspersed by five or six lighter cream dots surrounded by black flanks. Black line from nostril to the anterior insertion of the forelimb. Gular region with white coloration and three black ∩-shaped chevrons. First and second chevrons in contact. Venter uniform orange from second chevrons to anterior portion of the tail and extending onto the hind limbs. Ventral surface of tail tip and digits whitish. *In preservative* (holotype; Fig. 17) dorsum dark brown and venter with uniform light cream coloration.

Variation: The meristic characters of the head and body of this species are variable (see Supporting Information, Table S7). Coloration of this species seems to be consistent, with the gular coloration slightly lighter in females. First and second gular chevrons may be in contact or not (Supporting Information, Fig. S6).

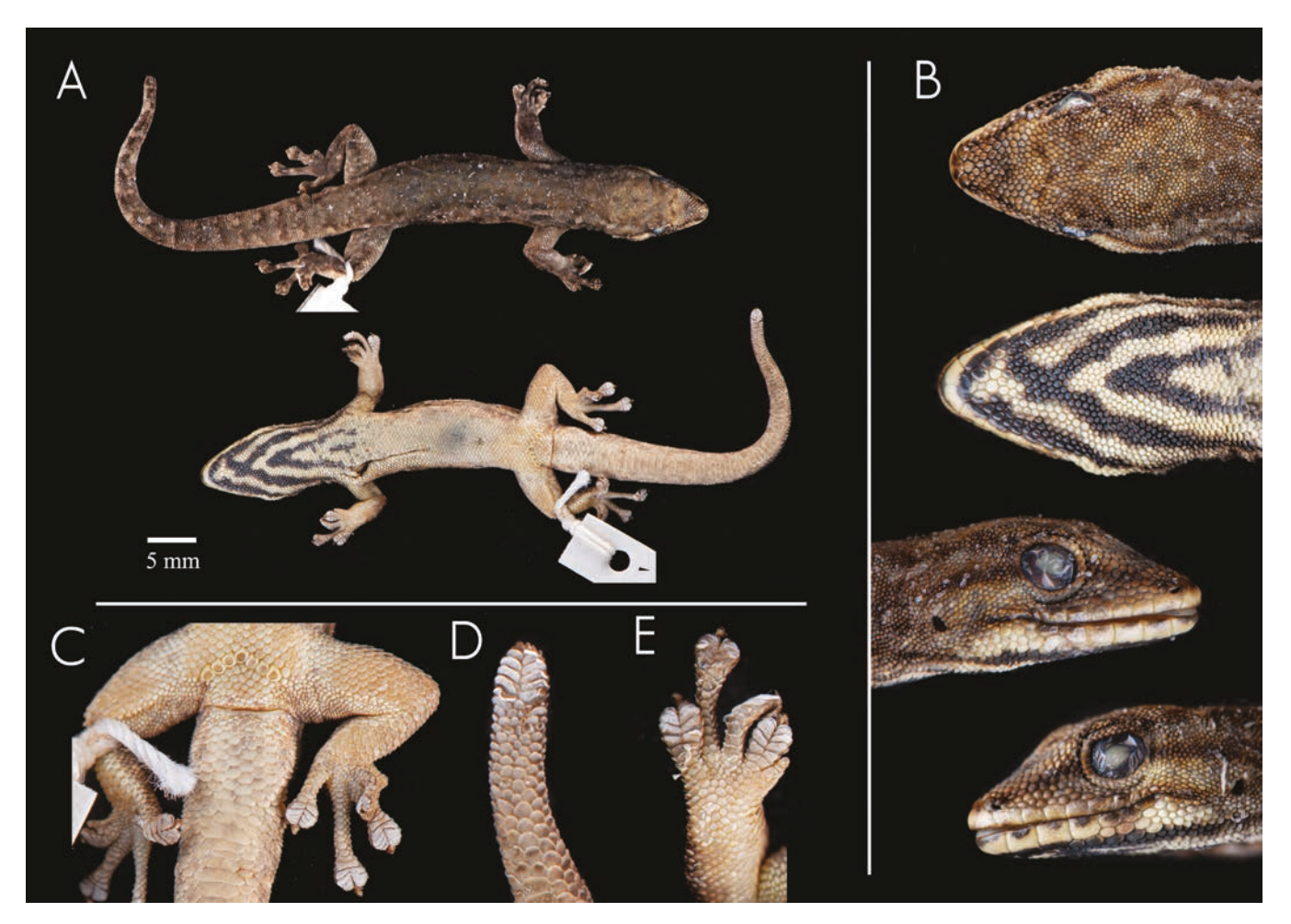


Figure 17. Holotype of *Lygodactylus kibera* sp. nov. (UTEP 22566) from Mpishi, near Kibira National Park, Bubanza Province, Burundi. A, Dorsal and ventral view of body. B, Detailed view of head in dorsal, ventral, and lateral views (from top to bottom). Details of cloacal region (C), (D) tail tip, and (E) left manus.

Habitat and distribution (Figs 6, 18): Lygodactylus kibera sp. nov. is known from the Albertine Rift adjacent to Lake Tanganyika in Burundi and DRC. Specimens from Mpishi, Burundi, were collected near montane forest in banana fields. The specimen from Bujumbura, Burundi, was collected inside a hotel in the middle of the city. The specimen from N'Komo River, DRC, was found on a tree near a small river between secondary gallery forest and grassland.

Natural history: An arboreal species with diurnal habits frequently found on the trunk or branches of trees, and also around anthropogenically altered areas such as buildings and plantations.

LYGODACTYLUS KARAMOJA SP. NOV.

(Figs 19–20, Table 3; Supporting Information, Fig. S7; Table S8)

Zoobank registration: https://zoobank.org/F64BBDF9-A337-4130-A65D-B3E2481112D4

Lygodactylus picturatus gutturalis: Schmidt (1919) [part]; Pasteur (1964) [part]; Wermuth (1965) [part].

Lygodactylus gutturalis: Röll (2005) [part]; Spawls et al. (2018) [part]; Behangana et al. (2020)

Lygodactylus karamoja sp. nov. is known from the northern Albertine Rift in the Lendu Plateau of DRC and several highlands of Uganda, and it is the sister taxon to **L. kibera sp. nov.** in clade (B1), from which it differs by *c*. 6.07% for the 16S mitochondrial gene (Table 2) and a lack of nuclear haplotype sharing in RAG1 (Fig. 2B–C). The new species differs from *L. gutturalis* and *L. depressus* by *c*. 12.49% and 10.45%, respectively, for the 16S (uncorrected p-distance) mitochondrial gene (Table 2) and a lack of nuclear haplotype sharing in RAG1 (Fig. 2B–C).

Holotype: UTEP 22590 (DFH 593), male with original tail, collected on a large tree at the edge of a village at Agoro Town, Imatong Foothills, Northern Region, Uganda, N03.83156, E33.01974, 1193 m a.s.l. on 5 July 2015 by Daniel F. Hughes, Wilber Lukwago, and Mathias Behangana.

Paratypes (six specimens): UTEP 22588–89 (DFH 591–92) and UTEP 22591 (DFH 594), males, with same collection data as the holotype; UTEP 22592 (DFH 641), female, collected at Agoro Town, Imatong Foothills, Northern Region, Uganda,

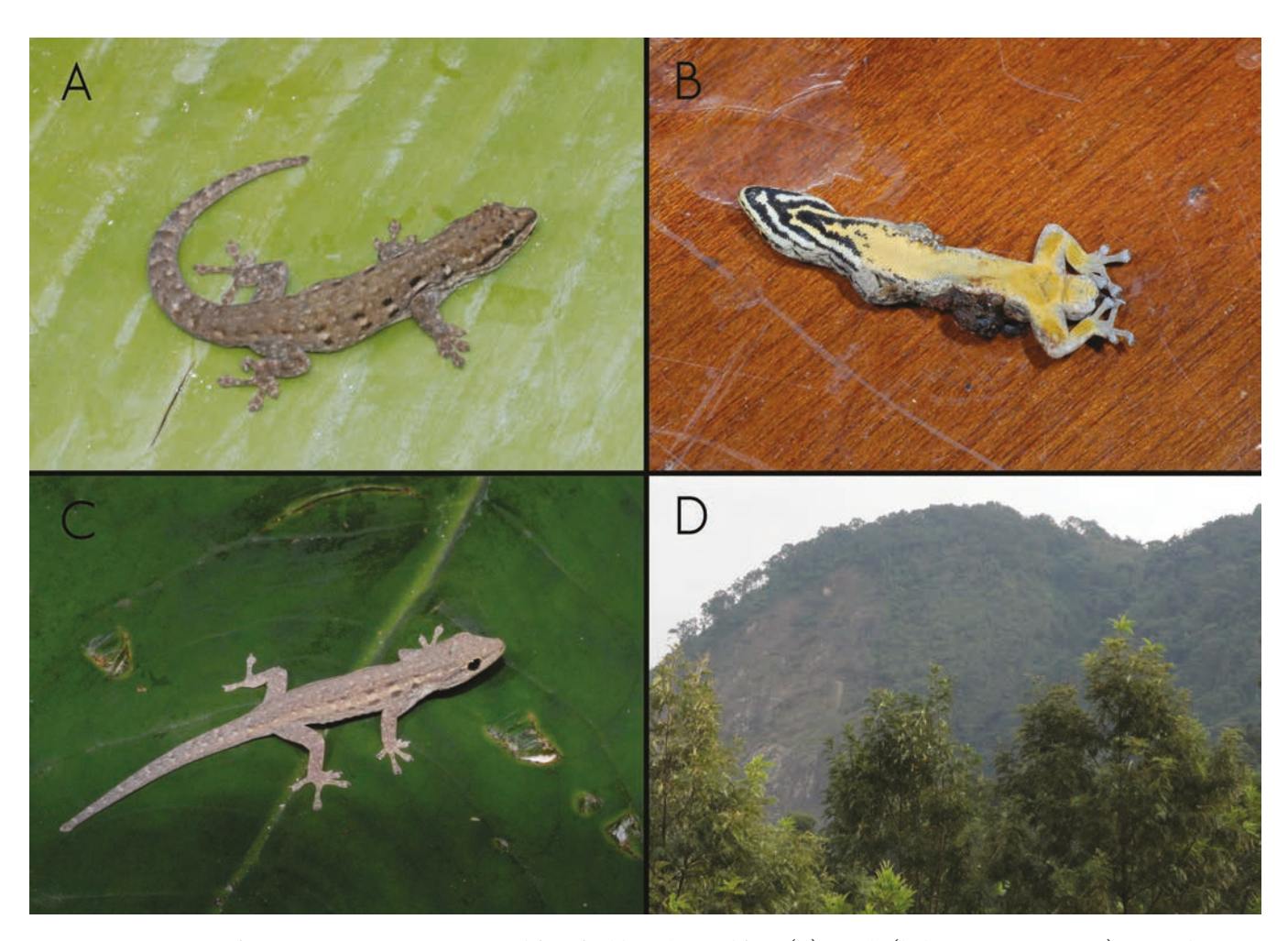


Figure 18. Specimens of *Lygodactylus kibera* sp. nov. in life or freshly euthanized from (A) Mpishi (holotype: UTEP 22566), near Kibira National Park, Bubanza Province, Burundi, (B) N'Komo River (UTEP 22586), South Kivu Province, DRC, and (C) Bujumbura city, Bujumbura Mairie Province (UTEP 22576), Burundi. Photo of habitat at (D) Mpishi, Bubanza Province, Burundi. Photographs by E.G. (A–C) and C.K. (D).

N03.80548, E32.98836, 1153 m a.s.l. on 5 July 2015 by Daniel F. Hughes, Wilber Lukwago, and Mathias Behangana; UTEP 22593 (DFH 130), juvenile, and UTEP 22594 (DFH 131), female, collected at Nakapiripirit, Mount Kadam, Northern Region, Uganda, N01.82270, E34.74603, 1730 m a.s.l. on 31 May 2015 by Daniel F. Hughes and Mathias Behangana.

Diagnosis: Lygodactylus karamoja sp. nov. is the sister taxon of L. kibera sp. nov. that is also a large-sized Lygodactylus [maximum SVL 37.7 mm (mean 34.4 ± 2.9 mm)] and shares the gular patterning of the L. gutturalis subgroup. Seven to eight supralabials and 5–7 infralabials. Dorsal pholidosis with granular scales that become flattened, larger, and imbricate on original tails. Large triangular mental followed by usually two (or occasionally three) symmetric postmental scales (Supporting Information, Fig. S7). Ventral pholidosis with large, flattened, and imbricate scales. Ventral scales usually denticulated posteriorly. Six terminal scansors on the tail tip. Digits elongated with five terminal scansors on the fourth toe (Table 3).

Like other *Lygodactylus* within the *gutturalis* group, this species can be easily differentiated from members of the L. angularis group by its characteristic \cap -shaped gular chevrons (vs.

V-shaped gular chevrons in *L. angularis* group), and from other members of the *L. picturatus* group based on dorsal coloration (light brown with five or six laterodorsal cream ocelli vs. usually blueish dorsum with yellow to white head in *L. picturatus* group).

Lygodactylus karamoja sp. nov. can be differentiated from other species within the gutturalis subgroup by only minor morphometric and meristic data, reflecting its cryptic nature. However, we provide some characters that are putatively diagnostic. Lygodactylus karamoja sp. nov. differs from L. dysmicus by its larger size (maximum SVL 37.7 mm vs. 27.6 mm); fewer precloacal pores (8 vs. 9); nostril not in contact with rostral scale (vs. nostril contacting rostral); and lower number of ventral scales across the body (16-18 vs. 21 in L. dysmicus). It can be easily distinguished from L. kibera sp. nov. by the gular pattern that comprises two or three thinner ∩-shaped chevrons that never extend beyond the posterior part of the lower jaw vs. three thick ∩-shaped chevrons reaching the chest; there are usually two symmetrical postmental scales vs. usually three smaller postmental scales; and a proportionally smaller orbital diameter (OD/HL 0.19-0.23 vs. 0.22-0.26 in *L. kibera* sp. nov.). Also, L. karamoja sp. nov. can be differentiated in the same way as L. gutturalis from L. depressus, based on gular patterning (always

two or three ∩-shaped chevrons vs. one ∩-shaped followed by one posterior central mark).

Etymology: The name 'karamoja' is a noun in apposition and refers to the Karamoja region in north-eastern Uganda where many individuals of this species have been found. The species is named in honour of this arid region, which is occupied by the Karamojong people who are mostly nomadic pastoralists related to the Maasai in Kenya.

Description of the holotype (Fig. 19): Measurements and meristic characters of the holotype are presented in Supporting Information, Table S8. Adult male, with a snout-vent length (SVL) of 34.3 mm and an original tail length slightly larger (TL = 36.1 mm). Body slender, nape moderately distinct. Head as broad as body and moderate head length (HW/HL 0.72). Canthus rostralis not prominent. Eye diameter 1.9 mm with circular pupil. Ear to eye distance twice the orbital diameter (3.2 mm). Snout rounded and slightly pointed. Granular scales on frontal area larger than occipital scales, with 22 small granular scales between the eyes. Dorsal scales granular from rostral to tail. Rostral undivided, in contact with 1st supralabial, prenasals, and one large internasal scale. Eight supralabials

and 5-6 infralabials. Prenasal scale present and in contact with 1st supralabial. Nostril circular, bordered by 1st supralabial, prenasal, and one supranasal. Postnasal not contacting nostril, separated by 1st supralabial, which it contacts posteriorly. Four rows of scales between supralabials and orbit. Mental large, triangular, and rounded, bordered posteriorly by two large rounded symmetric postmental scales. Six asymmetrical post-postmental scales. Gular scales granular, rounded, and slightly smaller than ventral scales. Ventral scales imbricate, rounded, and larger than dorsal scales, with 16 scales rows across the venter. Body relatively robust and slightly elongated (TRL/SVL 0.42). Tail with 34 enlarged transverse scales and six pairs of terminal scansors at the tip. Eight precloacal pores. Fore- and hind limbs moderately short, stout; forearm medium-sized (FL/SVL 0.16); tibia short (CL/SVL 0.17). Digits elongated and unwebbed with 5-6 terminal scansors. Thumb rudimentary with a small terminal claw. Relative length of digits: I < II = V < III < IV (manus); I < II < V < III < IV (pes).

Coloration: In life (Fig. 20), dorsal coloration from light to dark brown to greyish or almost black (Fig. 20D), with lighter cream-beige lines with five or six lighter cream dots surrounded by black flanks. Some specimens have lighter cream-beige dots

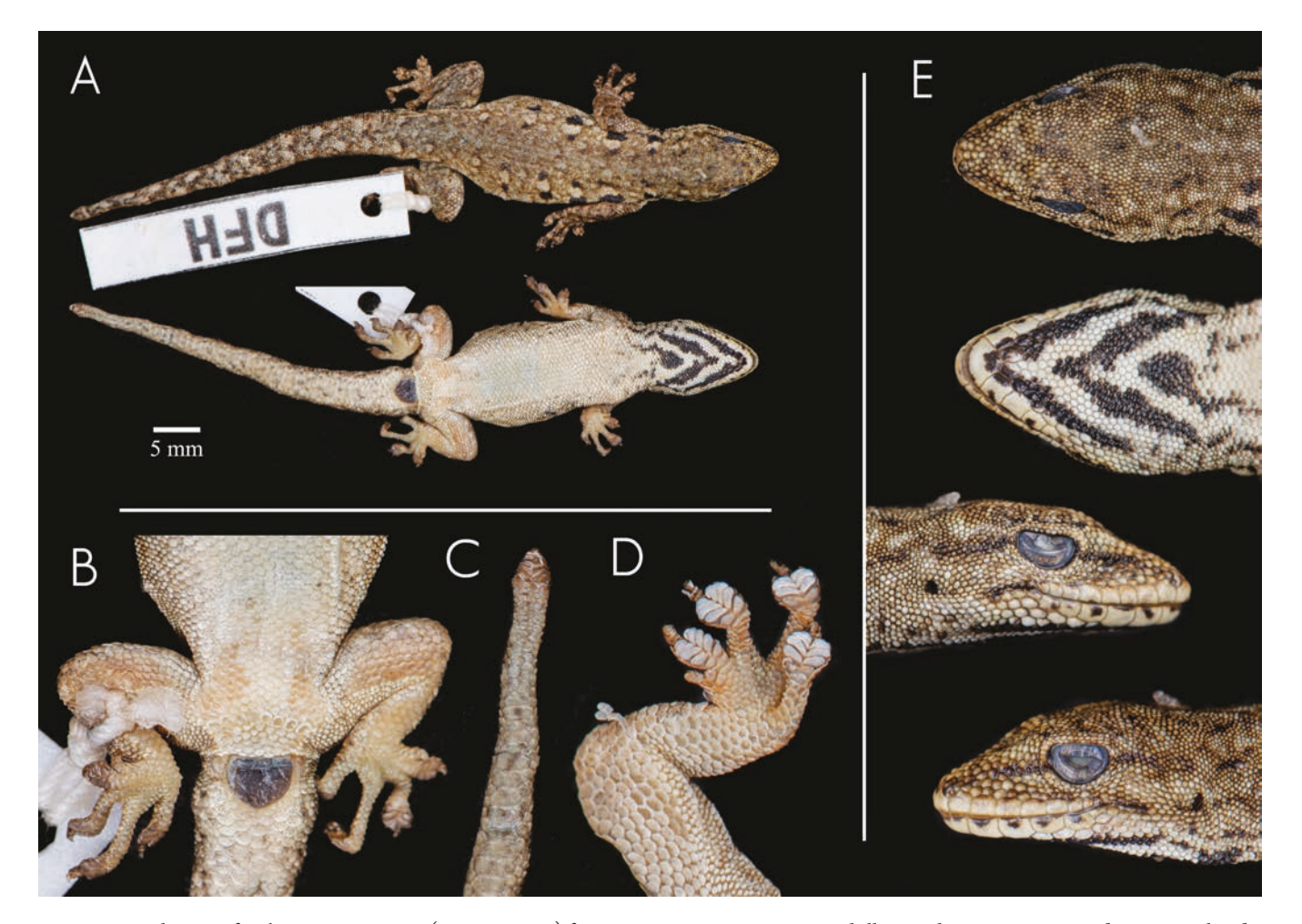


Figure 19. Holotype of L. karamoja sp. nov. (UTEP 22590) from Agoro Town, Imatong Foothills, Northern Region, Uganda. A, Dorsal and ventral view of body, (B) details of cloacal section, (C) regenerated tail tip, and (D) left pes. E, Detailed view of head in dorsal, ventral, and lateral views (from top to bottom). Photos by J.L.R.

along the vertebral line, giving them a granitic appearance (Fig. 20A). Black line from nostril to the anterior insertion of the forelimb. Gular region white and two or three black, ∩-shaped chevrons. Venter uniformly orange or white. Tip of tail and digits dark brown. *In preservative* (holotype; Fig. 19): dorsum dark brown and venter with uniform light cream coloration.

Variation: The meristic and morphometric data are summarized in Supporting Information, Table S8. Coloration of this species

seems to be consistent, with gular coloration slightly lighter in females. Number and shape of postmentals and internasals vary between specimens (Supporting Information, Fig. S7).

Habitat and distribution (Figs 6, 20): Lygodactylus karamoja sp. nov. has been recorded from mid-elevation savannahs of the northern Albertine Rift to the Karamoja Region, eastern Uganda, an arid area characterized by mostly woodland savannah habitat with several isolated mountain ranges. This suggests that

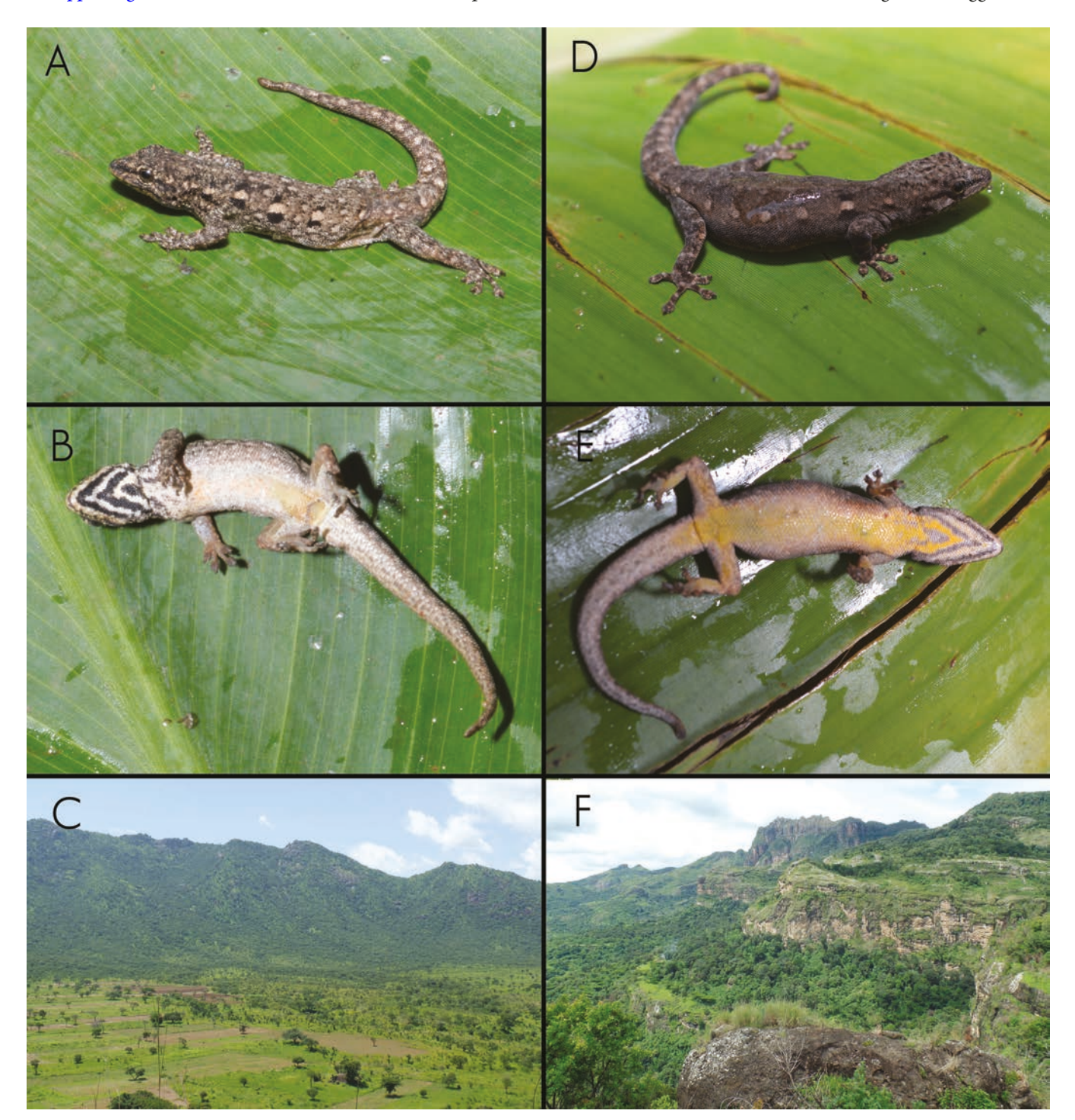


Figure 20. Specimens of *L. karamoja* sp. nov. in life from (A–B) Agoro Town (holotype: UTEP 22590), Imatong Foothills and (D–E) Nakapiripirit (UTEP 22594), Mount Kadam, Northern Region, Uganda. Photo of habitat at (C) Imatong Foothills, and (F) Mount Kadam, Northern Region, Uganda. Photographs by D.F.H.

specimens from western Kenya and southern South Sudan also belong to this species. If confirmed, this species would have a distribution that is similar to the lacertid *Adolfus jacksoni* (Greenbaum *et al.* 2018). However, we recommend caution until molecular data become available.

Natural history: A diurnal and arboreal species that is always found on trees. UTEP 22592, a gravid female, was found in July on a tree at night. UTEP 22593–94 were found during the day on trees trunks *c*. 1 m above ground in an open clearing of grass and rocky outcrops that were surrounded by dry forest (Fig. 20F).

LYGODACTYLUS MIRABUNDUS SP. NOV. (Fig. 21; Table 3)

Zoobank registration: https://zoobank.org/F4934B38-B746-470D-B05B-BE56C1DEC7FE

Lygodactylus mirabundus sp. nov. is the last taxon within subgroup B, described above as B2. It is sister to **L. kibera sp. nov.** and **L. karamoja sp. nov.**, from which it differs by a minimum of 8.93% for the *16S* (uncorrected p-distance) mitochondrial gene (Table 2), and it lacks nuclear haplotype sharing for *RAG1* (Fig. 2B–C).

Holotype: UTEP 22585 (CFS 1142w), male without tail and with a ventral incision, collected at Katako Kombe, Sankuru Province, DRC, S03.23949, E24.25117, 551 m a.s.l. on 8 May 2015 by Wandege M. Muninga, Chifundera Kusamba, and Mwenebatu M. Aristote.

Diagnosis: Lygodactylus mirabundus sp. nov. represents a moderately sized Lygodactylus (SVL 34.8 mm), with a gular pattern that is similar to the L. gutturalis group. Seven to eight supralabials and six infralabials. Large triangular mental followed by three symmetrical postmental scales (Fig. 21). Ventral pholidosis with large, flattened, and imbricate scales. Ventral scales usually denticulated posteriorly. Digits elongated with five terminal scansors under the fourth toe (Table 3).

Like other Lygodactylus within the L. gutturalis group, this species can be easily differentiated from members of the L. angularis group by its characteristic \cap -shaped gular chevrons (vs. V-shaped gular in the L. angularis group), and from other members of the L. picturatus group based on dorsal coloration (light brown with five or six laterodorsal cream ocelli vs. usually blueish dorsum with yellow to white head in the L. picturatus group).

Lygodactylus mirabundus **sp. nov.** is a cryptic species and can be differentiated from other species within the *L. gutturalis*

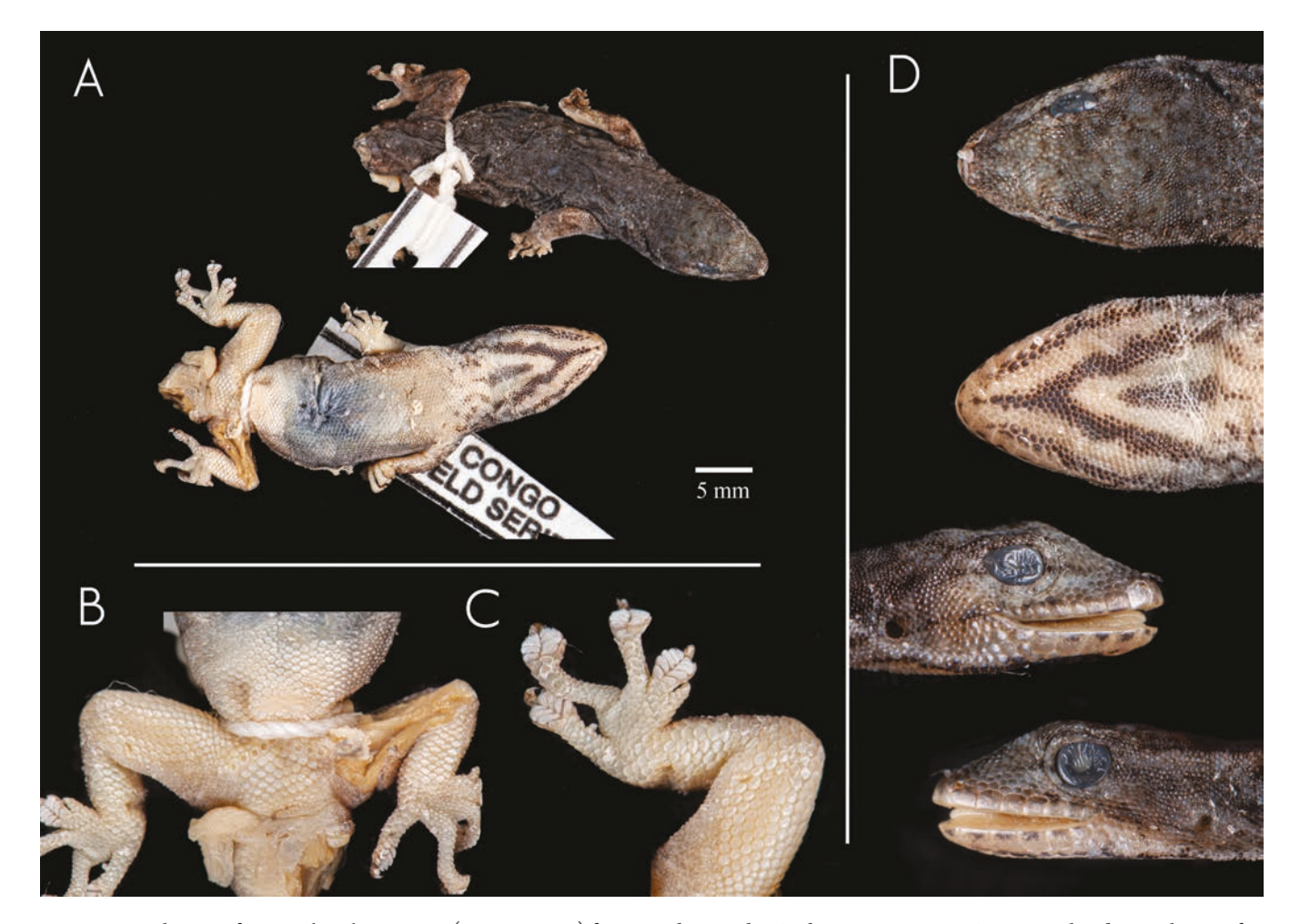


Figure 21. Holotype of *L. mirabundus* sp. nov. (UTEP 22585) from Katako Kombe, Sankuru Province, DRC. A, Dorsal and ventral view of body. B, Details of cloacal region and (C) right pes. D, Detailed view of head in dorsal, ventral, and lateral views (from top to bottom). Photos by J.L.R.

subgroup by only a few morphometric and meristic characters. It can be differentiated from other *L. gutturalis* subgroup species described above as follows: more precloacal pores [ten vs. 5–8 (in *L. gutturalis*), nine (in *L. dysmicus*), seven (in *L. depressus*), 7–8 (in *L. kibera* sp. nov.), and eight (in *L. karamoja* sp. nov.), and a unique gular pattern comprising black markings on the mandibular margin that extend to the posterior region of the jaw, an inverted *Y*-shaped chevron that converges anteriorly, and a posterior middle line between the two chevron branches (vs. a ∩-shaped pattern in all the described species above). For comparison with other species not included above, see the diagnoses in the species descriptions below.

Etymology: The name 'mirabundus' is a Latin adjective that means 'astonishing or surprising'. The species is only known from a unique location in a transition zone between dry savannah and the Congolian Rainforest.

Description of the holotype (Fig. 21): Measurements and meristic characters of the holotype are presented in. Adult male, with a snout-vent length (SVL) of 34.8 mm and a broken tail. Body slender, nape almost indistinct. Head as broad as body, and moderate head length (HW/HL 0.79). Canthus rostralis not prominent. Eye diameter 1.8 mm with circular pupil. Ear to eye distance almost double the orbit diameter (3.6 mm). Snout rounded and slightly pointed. Frontal granular scales larger than occipital scales, with 19 small granular scales between the eyes. Dorsal scales granular from rostral to tail. Rostral undivided, in contact with 1st supralabial, prenasals, and one large internasal scale. Seven to eight supralabials and six infralabials. Prenasal scale present and in contact with 1st supralabial. Nostril circular and not in contact with the rostral and surrounded by 1st supralabial, prenasal, and one supranasal. Postnasal not contacting the nostril, separated by 1st supralabial, which it contacts posteriorly. Four rows of scales between supralabials and orbit. Mental large, triangular, and posteriorly in contact with three rounded, symmetric postmental scales. Five barely symmetric post-postmental scales. Gular scales granular, rounded, and slightly smaller than ventral scales. Ventral scales large and imbricate with 21 scales rows across the venter. Body relatively robust and slightly elongated (TRL/SVL 0.44). Ten precloacal pores. Fore- and hind limbs moderately short, stout; forearm medium-sized (FL/SVL 0.14); tibia short (CL/SVL 0.17). Digits elongated and unwebbed with 5-6 terminal scansors. Thumb rudimentary with a small terminal claw. Relative length of digits: I < II = V < III < IV (manus); I < II < V < III < IV

Coloration: In life, unknown. In preservative (holotype; Fig. 21): dorsum uniform dark brown-grey with lateral black spots barely visible; black spotted marks on upper and lower lips; fore- and hind limbs slightly lighter dorsally; black line from nostril to anterior insertion of the forelimb; venter uniform light cream all along the body with gular pattern of two lines (one on each side) that do not connect anteriorly, followed by an inverted *Y*-shaped pattern with middle line between the branches of the *Y*-shaped chevron. Lamellae whitish on all digits.

Habitat and distribution (Fig. 5): Lygodactylus mirabundus sp. **nov.** is only known from the type locality in DRC. The holotype

was found on a large tree ~2 m above the ground at the edge of the transition zone between Miombo Woodland and the Congolian Rainforest. The association of this taxon with a particular biome will remain uncertain until more material is collected.

Natural history: Nothing is known about the natural history of this species.

LYGODACTYLUS LEOPARDINUS SP. NOV.

(Figs 22–23, Table 3; Supporting Information, Table S9)

Zoobank registration: https://zoobank.org/9010CCA9-953F-4091-9D1E-40BBFD0B9FF8

Lygodactylus leopardinus sp. nov. is the rainforest member within subgroup C, and the most morphologically distinguishable species within the *L. gutturalis* subgroup. It also differs by a minimum of *c.* 10.10% for *16S* uncorrected p-distance (Table 2) from related taxa, and it lacks nuclear haplotype sharing in *RAG1* (Fig. 2B–C).

Holotype: UTEP 22577 (ELI 2330), male with broken tail and ventral incision, collected at Balolombo Village, Busira River, Équateur Province, DRC, S00.25939, E19.63575, 305 m a.s.l. on 18 July 2013 by Chifundera Kusamba, Wandege M. Muninga, Mwenebatu M. Aristote, and Eli Greenbaum.

Paratype: UTEP 22596 (ELI 3584), female, collected from Katopa, ICCN Camp, Maniema Province, DRC, S02.74769, E25.10323, 450 m a.s.l. on 2 July 2015 by Eli Greenbaum.

Additional material: RMCA 1981.065.R.0004, male with original tail, collected at River Lotende (canopy), Mabali, Équateur Province, DRC, between 17 and 18 August 1955 by Raymond Laurent; RMCA R.2947, female, collected at Basongo, Kasai Province, DRC, on 27 July 1921 by Henri Schouteden; RMCA R.16752, male, collected at Yokamba (Boende), Tshuapa Province, DRC, in 1953 by J. Stevenart.

Diagnosis: This species represents a moderately sized Lygodactylus [maximum SVL 34.7 mm (mean 33.6 ± 1.3 mm)], with males having the most distinctive gular patterning of the L. gutturalis group (described below, Fig. 3). Females without gular pattern. Eight supralabials and 6–7 infralabials. Males with seven precloacal pores.

This species can be differentiated from all taxa of the angularis group taxa by the same osteological differences described above (e.g. postorbitofrontal reduced almost vestigial vs. well developed in the *angularis* group) and a unique leopard-like pattern on the dorsum. Also, it can be easily differentiated from L. angularis and L. baptistai based on the gular patterning (broken pattern vs. V-shaped pattern in *L. angularis* and the unique pattern of *L.* baptistai described above; see Fig. 5). The species can be confused with L. heeneni and L. paurospilus based on the broken gular ornamentation; however, it can be differentiated from them as follows: unique leopard-like dorsal pattern in L. leopardinus sp. **nov.** (vs. light brown dorsal background with a light cream vertebral line of blotches in L. heeneni (Fig. 7), similar to L. paurospilus (based on preserved specimens; Fig. 8; Supporting Information, Fig. S4); broken pattern that converges anteriorly (vs. a broken pattern that converges posteriorly (V-shaped) in L. heeneni and *L. paurospilus*); fewer precloacal pores than *L. heeneni* (7 vs. 9–10); and osteological features described above.

Lygodactylus leopardinus sp. nov. is the most distinctive species within the gutturalis subgroup and the only species within the picturatus group with a broken gular pattern. It can be easily distinguished from other closely related species based on its unique gular pattern and the leopard-like dorsal pattern, which is not present in related taxa. Females lack gular patterning (vs. weakly present in other members of the gutturalis subgroup). It can also be differentiated based on minor meristic differences as follows: greater number of scales between the eyes (30–36 vs. 17–24 in L. gutturalis, 25 in L. dysmicus, 19–28 in L. kibera sp. nov., 19–22 in L. karamoja sp. nov., and 19 in L. mirabundus sp. nov.); and lower number of ventral scales at midbody (14–15 vs. 15–20 in L. gutturalis, 21 in L. dysmicus, 16–19 in L. depressus, 16–18 in L. kibera sp. nov., 16–18 in L. karamoja sp. nov., and 21 in L. mirabundus sp. nov.).

Etymology: The name '*leopardinus*' is an adjective referring to the leopard-like dorsal pattern present in males of this species.

Description of the holotype (Fig. 22): Measurements and meristic characters of the holotype are presented in Supporting

Information, Table S9. Table 3. Adult male, with a snout-vent length (SVL) of 32.4 mm and a broken tail. Body slender and nape slightly distinct. Head as broad as body, and moderate head length (HW/HL 0.63). Canthus rostralis not prominent. Eye diameter 2.0 mm with circular pupil. Ear to eye distance almost twice the orbit diameter (3.4 mm). Snout rounded and moderately pointed. Frontal granular scales larger than occipital scales, with 36 small granular scales between the eyes. Dorsal scales granular from rostral to tail. Rostral undivided, in slight contact with nostril. Three small symmetrical internasals. Eight supralabials and seven infralabials. Prenasal not in contact with the 1st supralabial. Nostril circular, in narrow contact with the rostral and bordered by 1st supralabial, prenasal, one supranasal, and one postnasal. Four rows of scales between supralabials and the orbit. Mental large, triangular, and in contact posteriorly with two rounded and symmetrical postmental scales. Five smaller post-postmental scales. Gular scales granular and smaller than ventral scales. Ventrals imbricate, rounded, and larger than dorsal scales, in 14 scale rows across the venter. Body relatively robust and slightly elongated (TRL/SVL 0.41). Seven precloacal pores. Fore- and hind limbs moderately short and stout; forearm intermediate (FL/SVL 0.15); tibia short (CL/SVL 0.17). Digits elongated, unwebbed, with 5-6 terminal scansors. Thumb

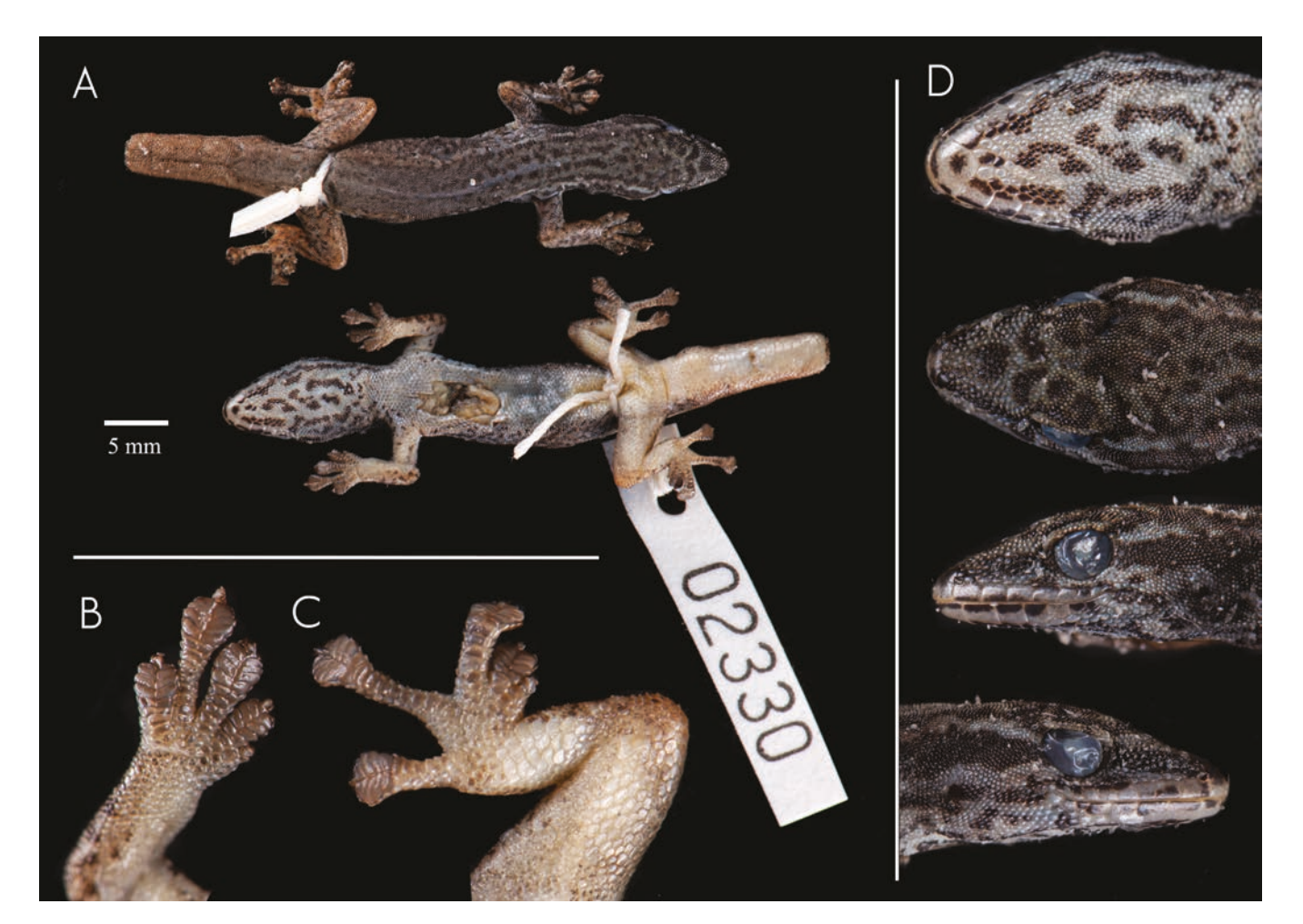


Figure 22. Holotype of *L. leopardinus* sp. nov. (UTEP 22577) from Balolombo Village, Busira River, Équateur Province, DRC. A, Dorsal and ventral view of body. B, Details of right manus and (C) pes. D, Detailed view of head in ventral, dorsal, and lateral views (from top to bottom). Photos by J.L.R.

rudimentary with a small terminal claw. Relative length of digits: I < II = V < III < IV (manus); I < II < V < III < IV (pes).

Coloration: In life (holotype; Fig. 23A–B), dorsal background colour light grey to brown, with a black reticulate dorsal pattern from snout to anterior insertion of the hind limbs; light cream blotches surrounded by black dots from eye to anterior insertion of the hind limb on each side of dorsum; tail brownish dorsally with light cream ocelli; throat white with two ∩-shaped broken dark chevrons; venter uniformly white. In preservative (holotype; Fig. 22), dorsum uniformly dark grey from snout to tail. Venter with silvery appearance, becoming brownish on tail and fore- and hind limbs; black reticulated dorsal pattern visible, with two white paravertebral lines (one on each side) from eyes to midbody; digits dark brown ventrally.

Variation: In contrast to the holotype, the female paratype has a dorsal coloration in life that is entirely black with an orangish tail and dorsolateral dots in paravertebral lines that dissipate posteriorly, without a gular pattern (Fig. 23C–D). The lack of gular pattern is corroborated *in preservative*, in the paratype, and in another female specimen (RMCA R.2947) from Basongo, DRC.

Habitat and distribution (Figs 6, 23): Lygodactylus leopardinus sp. nov. is known from Congo Basin primary rainforest at Balolombo, Katopa (Lomani River, Congo River affluent), and Basongo. This pattern suggests a large distribution in the Congo Basin like its sister taxon, *L. depressus*, which is found in sympatry at Lake Tumba and Katopa. However, it seems to be less abundant.

Natural history: A diurnal and arboreal rainforest species. The holotype was collected early in the morning on a tree about 1 m above the ground.

LYGODACTYLUS GAMBLEI SP. NOV.

(Figs 23–24, Table 3; Supporting Information, Table S10)

Zoobank registration: https://zoobank.org/411D833D-2017-4930-BD11-B783AAD6A9B7

Lygodactylus picturatus gutturalis: de Witte (1953) [part].

Lygodactylus gutturalis: Pasteur (1964) [part]; Broadley and Cotterill (2004) [part]; Röll (2005) [part].

Lygodactylus gamblei sp. nov. is a miombo-savannah form within subgroup C, described above. It also differs by a minimum of *c.* 9.96% for the *16S* mitochondrial gene (Table 2) from its sister taxon **L. leopardinus sp. nov.** (Fig. 2A) and lacks nuclear haplotype sharing in *RAG1* (Fig. 2B–C).

Holotype: UTEP 22587 (ELI 340), male with regenerated tail and ventral incision, collected at Manono, Tanganyika Province, DRC, S07.29363, E27.39472, 634 m a.s.l. on 19 January 2010 by locals and brought to Eli Greenbaum.

Paratypes (nine specimens): UTEP 22584 (ELI 293), female with original tail and ventral incision, collected at Mulongo, Haut-Lomami Province, DRC, S07.65509, E27.34027, 875 m a.s.l. on 18 January 2010 by Chifundera Kusamba, Wandege M.

Muninga, Mwenebatu M. Aristote, and Eli Greenbaum; RBINS 2721 (formerly under RBINS 6157), adult male, collected at Rivière Kande, affluent de la rive gauche de la Lupiala et sousaffluent de la rive droite de la Lufira, Upemba National Park, Haut-Katanga Province, DRC, 700-730 m a.s.l., on 4-8 October 1947; RBINS 2722 (formerly under RBINS 6160), adult male collected at Rivière Lukawe, affluent de la rive droite de la Lufira, Upemba NP, Haut-Katanga Province, DRC, 700 m a.s.l. on 28 October 1947; RBINS 2723 and RBINS 6124 (formerly under RBINS 6124), male and female, respectively, collected at Munoi, bifurcation de la rivière Lupiala, affluent de la rive droite de la Lufira, Upemba NP, Haut-Katanga Province, DRC, 890 m a.s.l. on 3 June 1948; RBINS 2725-27 (formerly in a series of nine specimens under RBINS 6122), two males and one female, respectively, collected at Munoi, bifurcation de la rivière Lupiala, affluent de la rive droite de la Lufira, Upemba NP, Haut-Katanga Province, DRC, 890 m a.s.l. on 28-31 May 1947; RBINS 2728 (formerly under RBINS 6156), collected at Kaswabilenga, région du cours inférieur de la Lupiala, affluent de la rive droite de la Lufira, Upemba NP, Haut-Katanga Province, DRC, 700 m a.s.l. on 31 January 1949. All paratype material from RBINS was collected by G.-F. de Witte during his expeditions in the former Katanga region between 1946 and 1949.

Additional material: RMCA R.8933, male, collected at Kapanga, Haut-Katanga Province, DRC, in September 1932 by G.F. Overlaet; RBINS 6121 and RBINS 20749 (formerly in RBINS 6121 series), male and female, respectively, collected at Kambi, affluent de la Grande Kafwe (Masombwe), Upemba NP, Haut-Katanga Province, DRC, on 25–27 July 1945 by G.-F. de Witte; RBINS 6139 (male) and RBINS 20748 (female) (formerly in RBINS 6139 series), collected at Mabwe, Upemba NP, Haut-Lomami Province, DRC, in August 1945 by G.-F. de Witte.

Diagnosis: A large Lygodactylus [SVL to 39.8 mm (mean 36.1 \pm 2.1 mm)] with 6–9 supralabials and 6–7 infralabials. As with other Lygodactylus within the L. gutturalis group, this species can be easily differentiated from the L. angularis group species by the gular ornamentation, dorsal pattern, and lack of terminal scansors on the tail tip, and from other members of the L. picturatus group based on dorsal coloration and gular pattern (see L. gutturalis account).

Lygodactylus gamblei sp. nov. can be differentiated from other members within the *L. gutturalis* subgroup by the following combination of characters: dorsal coloration lacking dorsolateral series of cream ocelli on flanks (present in L. gutturalis, L. karamoja sp. nov., L. kibera sp. nov., and L. dysmicus), with two parallel dorsolateral lines from head to forelimbs, the lower line extending on to the anterior side of the forelimb, reaching the cubital fossa (Fig. 25B); males usually with three \cap -shaped chevrons (vs. one or two in L. depressus; a broken chevron in L. leopardinus sp. nov.; and the exceptional inverted Y-shaped pattern in **L. mirabundus sp. nov.**) and thicker gular lines than L. gutturalis, L. dysmicus, and L. karamoja sp. nov.. Lygodactylus gamblei sp. nov. always has three postmental scales, with the lateral pair separated by a posterior extension of the mental (Fig. 25A). It can be differentiated from *L. karamoja* sp. nov., L. kibera sp. nov., and L. leopardinus sp. nov. by having a proportionally larger tibia (CL/SVL \geq 0.19 vs. CL/SVL \leq 0.17).



Figure 23. A–B, Holotype (UTEP 22577) and (C–D) paratype (UTEP 22596) of *L. leopardinus* sp. nov. in life and photo of habitat from (E) type locality at Balolombo Village, Busira River, Équateur Province, DRC. F–G, Holotype (UTEP 22587) and (H–I) paratype (UTEP 22584) of *L. gamblei* sp. nov. in life and photo of habitat from (J) type locality at Manono, Tanganyika Province, DRC. Photographs by E.G.

As in its sister taxon *L. leopardinus* sp. nov., females lack gular patterning (present in all the other members of the group, Fig. 25A). *Lygodactylus gamblei* sp. nov. can be differentiated from *L. mirabundus* sp. nov. by having a lower number of precloacal pores (7–9 vs. 10) and by subtle morphometric differences (Table 3).

Etymology: We name this new species after the American evolutionary biologist and herpetologist Tony Gamble of Marquette University, in recognition of his substantial contributions to the evolutionary biology of geckos. The name is a patronym formed in the genitive case.

Description of the holotype (Fig. 24): Measurements and meristic characters of the holotype are presented in Supporting Information, Table S10. Adult male, with a snout–vent length (SVL) of 35.0 mm and a regenerated tail of 31.0 mm. Body slender and nape slightly distinct. Head slightly broader than body, and moderate head length (HW/HL 0.66). Canthus rostralis not prominent. Eye diameter 2.51 mm with circular pupil. Ear to eye distance slightly larger than the orbit diameter (3.26 mm). Snout

rounded and moderately pointed. Granular scale of frontal larger than occipital scales, with 25 small interorbital granular scales. Dorsal scales granular from rostral to tail. Rostral undivided, in narrow contact with nostril. Two small symmetrical internasals. Seven supralabials and six infralabials. Prenasal contacts the 1st supralabial. Nostril circular and surrounded by 1st supralabial, prenasal, one supranasal, and one postnasal. Four or five rows of scales between supralabials and the orbit. Mental large, triangular, and posteriorly in contact with three rounded symmetrical postmental scales. Mental scales extending between the lateral postmentals reaching ~50% of the medial surface suture of the postmentals. Five smaller post-postmental scales. Gular scales granular, rounded, and smaller than ventral scales. Ventrals imbricate, denticulate, and larger than dorsal scales, with 19 scale rows across the venter. Regenerated tail with 30 enlarged subcaudal scales, some fragmented. Body relatively robust and slightly elongated (TRL/SVL 0.42). Eight precloacal pores. Foreand hind limbs moderately short and stout; forearm of medium length (FL/SVL 0.16); tibia moderately long (CL/SVL 0.19). Digits elongated and unwebbed with 5-6 terminal scansors.

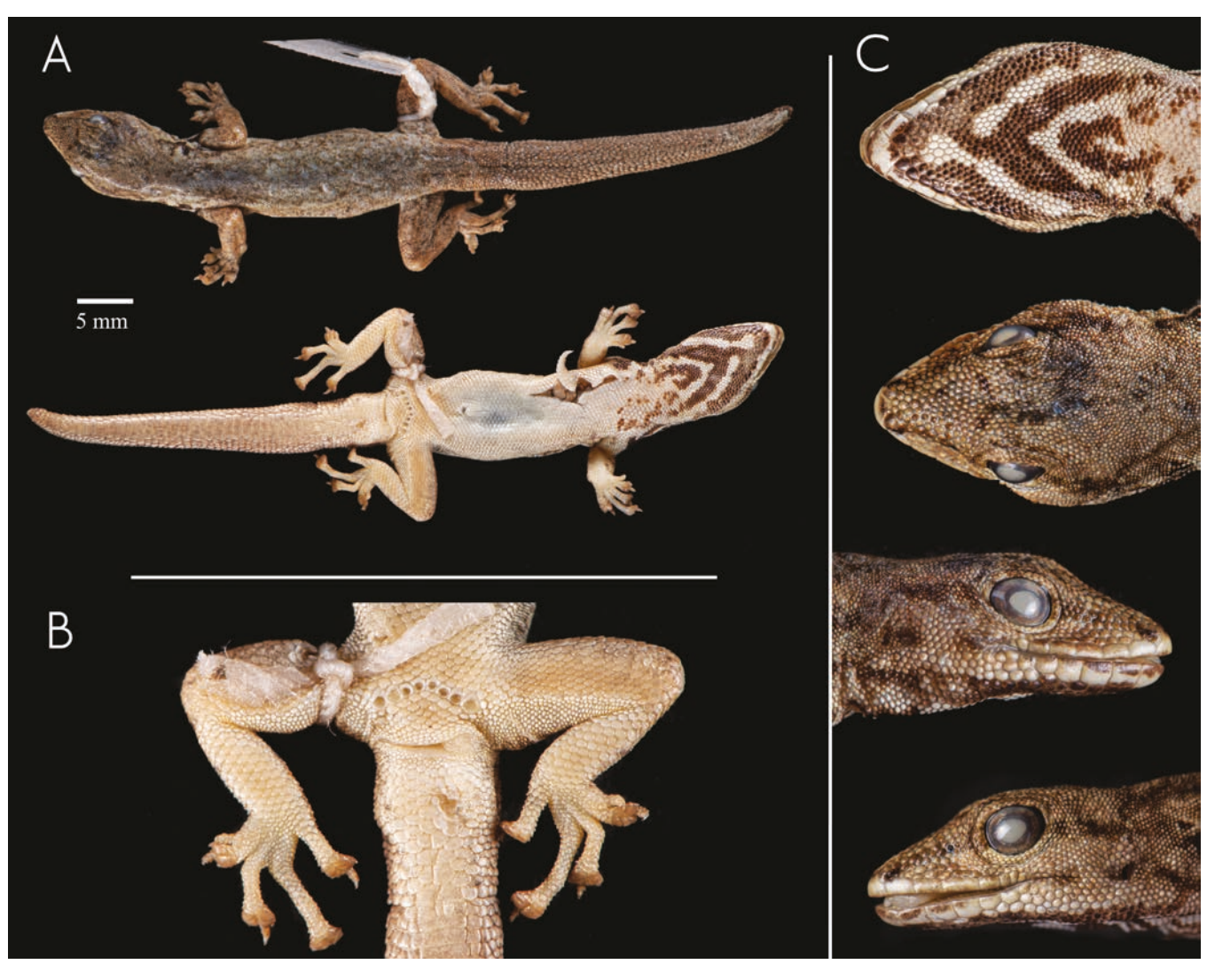


Figure 24. Holotype of *L. gamblei* sp. nov. (UTEP 22587) from Manono, Tanganyika Province, DRC. A, Dorsal and ventral view of body. B, Details of the cloacal region. C, Detailed view of head in ventral, dorsal, and lateral views (from top to bottom). Photos by J.L.R.

Thumb rudimentary with a small terminal claw. Relative length of digits: I < II = V < III < IV (manus); I < II < V < III < IV (pes).

Coloration: In life (Fig. 23A–D, F–I), dorsal colour light brown to grey, with dark brown mottled pattern in the female; male with three rows of interrupted, but conspicuous black stripes on lateral surface from head to neck, converging at the anterior insertion of the forearm, giving the impression of a single large blotch; male and female with a black-brown line from snout to ear aperture; venter uniform orange-yellowish from posterior part of gular to cloaca, and cream to white elsewhere; gular immaculate white in female, and white in male with three thick and black ∩-shaped chevrons. In preservative (holotype; Fig. 24): similar coloration as in life, slightly darker, with gular pattern more brownish.

Variation: All paratypes largely agree with the holotype, and their measurements are summarized in Supporting Information, Table S10. The specimen RBINS 6138 has a bold dorsal pattern from head to midbody. It is worth noting that all the female specimens examined from de Witte's (1953) expedition lack a gular pattern, in contradiction to de Witte's (1953) statement.

However, we noted that some young male specimens were catalogued as females, which could have misled de Witte to this conclusion.

Habitat and distribution (Figs 6, 23): Lygodactylus gamblei sp. nov. is known from Manono, Upemba National Park, and other nearby areas in south-eastern DRC. The species is associated with Miombo Woodland forest and gallery forest between 500 and ~1500 m a.s.l. This species is sympatric with *L. heeneni* in this area.

Natural history: A diurnal and arboreal species. The holotype (UTEP 22587) was collected active during the daytime with an air temperature of 45 °C and one of the paratypes (UTEP 22584) was found scampering around a tree close to the ground in an open area.

DISCUSSION

Lygodactylus is the most speciose genus of African gekkonids, with new species being described frequently (e.g. Portik et al.

2013, Travers et al. 2014, Malonza et al. 2016, 2019, Marques et al. 2020, Vences et al. 2022). However, challenges to fieldwork in many regions of Africa (Botts et al. 2011, Greenbaum 2017), together with the lack of fresh material needed for genetic purposes (Branch et al. 2006, Etard et al. 2020), have resulted in a geographic bias in our knowledge of the group, on which some regions and taxa remain more poorly studied than others. In this work, we provide an updated revision of *L. gutturalis*, which has revealed cryptic diversification. Phylogenetic reconstructions (mitochondrial and concatenated multilocus species tree, Figs 1-2) have recovered the L. gutturalis complex as a monophyletic group, sister to all other members of the L. picturatus group, in agreement with previous work (Röll et al. 2010, Gippner et al. 2021). We also place L. depressus in its phylogenetic context for the first time, demonstrating that it is related to L. gutturalis, and not L. picturatus as previously thought (Loveridge 1947, Wermuth 1965, Röll et al. 2010).

Lygodactylus gutturalis group

Based on the results of the phylogenetic reconstructions, nuclear gene networks, and biogeographic distribution, we recognize three clades within the L. gutturalis complex that include nine species as follows: L. gutturalis s.s., L. dysmicus (here elevated to full species status), L. depressus, five new species (L. kibera sp. nov., L. karamoja sp. nov., L. mirabundus sp. nov., L. leopardinus sp. nov., and L. gamblei sp. nov.), and one additional taxon that needs further study (referred to herein as Lygodactylus sp.) from Kenya and Tanzania. Many of these species are morphologically cryptic and have traditionally been regarded as conspecific with L. gutturalis; however, they have high levels of genetic divergence between one another. We have shown that the main phenotypic differences between species are related to the gular pattern of males. While females have lost the gular pattern in some species (e.g. L. gamblei sp. nov. and L. leopardinus sp. nov.), others exhibit lighter or attenuated gular patterns (L. gutturalis, L. depressus, L. karamoja sp. nov., *L. kibera* **sp. nov.**, and *Lygodactylus* **sp.**).

We have also taken the opportunity to revalidate *L. dysmicus* as a full species, although this taxonomic action lacks genetic support. Despite the morphological conservativeness of members in this group, *L. dysmicus* exhibits several characters that support its specific recognition. This species is only known from north and west of the Congo and Ubangi rivers, respectively, whereas the other two species of the *L. gutturalis* subgroup occur in the rainforest of the Congo Basin (*L. depressus* and *L. leopardinus* **sp. nov.**) and are distributed south and east of those rivers, respectively. A recent study of *Toxicodryas* snakes suggested that the Congo and Ubangi rivers are important biogeographic barriers (Allen *et al.* 2021). Future research should incorporate topotypic genetic material of *L. dysmicus* as well as intensive surveys around the northern rim of the Congo Basin to corroborate this interpretation.

Lygodactylus angularis group

Based on the molecular evidence provided by Gippner *et al.* (2021), morphological and geographical variation between *L. angularis* and *L. a. heeneni* provided by de Witte (1953), Pasteur, 1965(1964), and Broadley and Cotterill (2004), and data in this

work, we revalidate *L. heeneni* as a full species, as initially suggested by de Witte (1933).

Although Pasteur, 1965(1964) maintained that *L. paurospilus* cannot be differentiated morphologically from *L. heeneni*, we have identified some putatively diagnostic characters. Further, while *L. heeneni* was described from Kapiri, Upemba National Park, DRC, mainly dominated by Miombo Woodland savannah (Timberlake 2017), *L. paurospilus* has only been found in the Albertine Rift in Haute Lubitshako (i.e. Kabobo Plateau), between 1900–2000 m a.s.l., where the habitat is characterized by montane forest, shrubland, and grassland (Hirschfeld *et al.* 2015). These two regions are also quite distant from one another, and each has been recognised as an important region of reptile endemism (Broadley 2003, Owiunji and Plumptre 2011, Greenbaum and Kusamba 2012). Therefore, despite the lack of molecular support, we found evidence to consider *L. paurospilus* and *L. heeneni* as separate species.

Lastly, we confirmed extensive morphological and colour pattern variation within *L. angularis s.s.*, as previously reported by Pasteur, 1965(1964). Together with the molecular variation reported by Travers *et al.* (2014), it is expected that several cryptic species may be recognised within this poorly studied species in the future. However, the lack of molecular data from topotypic material from the Shire Highlands, a centre of endemism in Malawi (Dowsett-Lemaire *et al.* 2001, Branch *et al.* 2014), as well as the lack of access to the type material of *L. a. grzimeki* and the potential for overlap in habitat type between the two forms, render any taxonomic actions premature.

Evolutionary history of the Afro-American Lygodactylus

We provide a new time tree and biogeographic hypothesis for the Afro-American Lygodactylus (Clade C in Gippner et al. 2021). Our results suggest a scenario similar to that proposed by Gippner et al. (2021), adding several additional noteworthy points. Firstly, the estimated diversification dates suggest a first split that separated the L. picturatus and L. fischeri groups from the L. angularis and L. klugei groups during the Early Miocene, ~21 Mya (27.7-15.5 Mya; Fig. 2A). This result differs from that of Gippner et al. (2021), who proposed a first split of the L. klugei group from mainland Africa species around 21.9 Mya. Our BI and ML reconstructions suggest that L. klugei is sister to L. angularis and that trans-Atlantic dispersal took place in association with lineage splits between the L. angularis group and the L. klugei group, ~19.5 (26.0-14.0 Mya, Fig. 2A). However, the dating of this trans-Atlantic event agrees with the geological timeframe proposed by Gamble et al. (2011), Lanna et al. (2018), and Gippner et al. (2021) in the Mid-Miocene.

The *L. picturatus* and *L. fischeri* groups also split during the Mid-Miocene ~19 Mya (25.3–14.3 Mya). The former group experienced an extensive diversification in Central and East Africa, whereas the latter group, which extends to Cameroon and West Africa, subsequently colonized the Gulf of Guinea Islands (São Tomé, Príncipe, and Annobon). Both splits (*L. angularis-klugei* groups and *L. picturatus-fischeri* groups) coincide with the closure of the Tethys Sea in the Mid-Miocene which resulted in a period of aridification events and expansion of savannahs in Africa (Plana 2004).

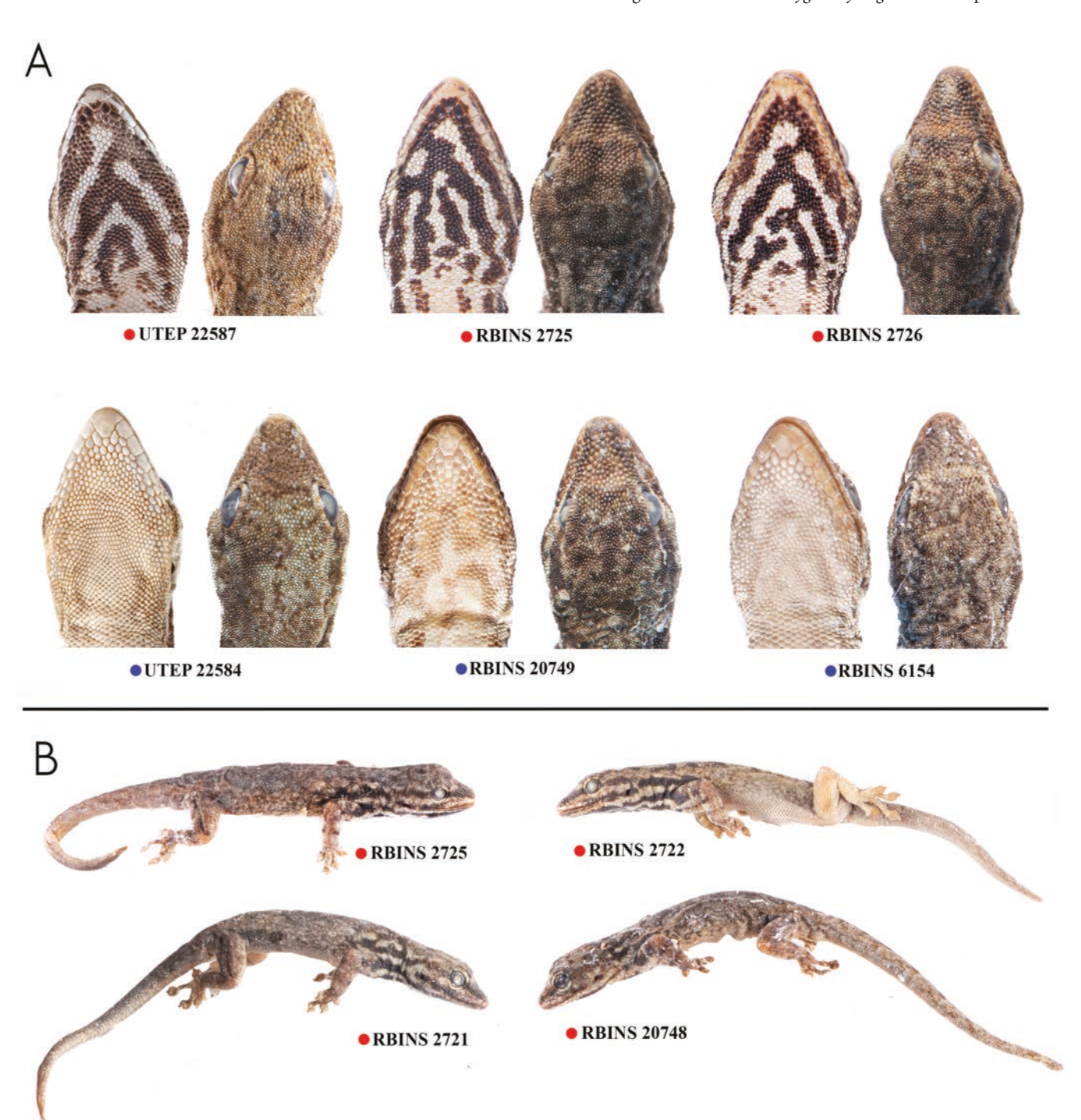


Figure 25. A, Dorsal and ventral views of head, showing gular ornamentation and pholidosis variation in **L. gamblei sp. nov.** B, Specimens of **L. gamblei sp. nov.** in lateral view, showing its characteristic scapular pattern. Red points denote males and blue points denote females. Photos by J.L.R.

Finally, the *L. picturatus* group split into two large subgroups (*L. picturatus* and *L. gutturalis* subgroups) \sim 15.0 Mya (19.9–11.0 Mya) that experienced radiations during the Late Miocene, resulting in several endemic species in the Eastern Arc Mountains and the Albertine Rift, respectively. The Late Miocene was characterized by the opening of the Rift Valley and by a period of cooling, which led to a progressive aridification in Africa, resulting in more open habitats primarily dominated by grasslands (Couvreur *et al.* 2021). This period seems to be crucial to the

evolution of tropical African biodiversity driven by climate-induced forest refugia that have promoted speciation in several groups of vertebrates, including rodents (Nicolas *et al.* 2020, Onditi *et al.* 2021), snakes (Portillo *et al.* 2018), and amphibians (Portillo *et al.* 2015, Larson *et al.* 2016). Most mainland African *Lygodactylus* species originated during this period (Travers *et al.* 2014, Gippner *et al.* 2021), probably as a consequence of the expansion of the savannah and the fragmentation of forest into climatological refugia (Plana 2004). Palaeoclimatic models also

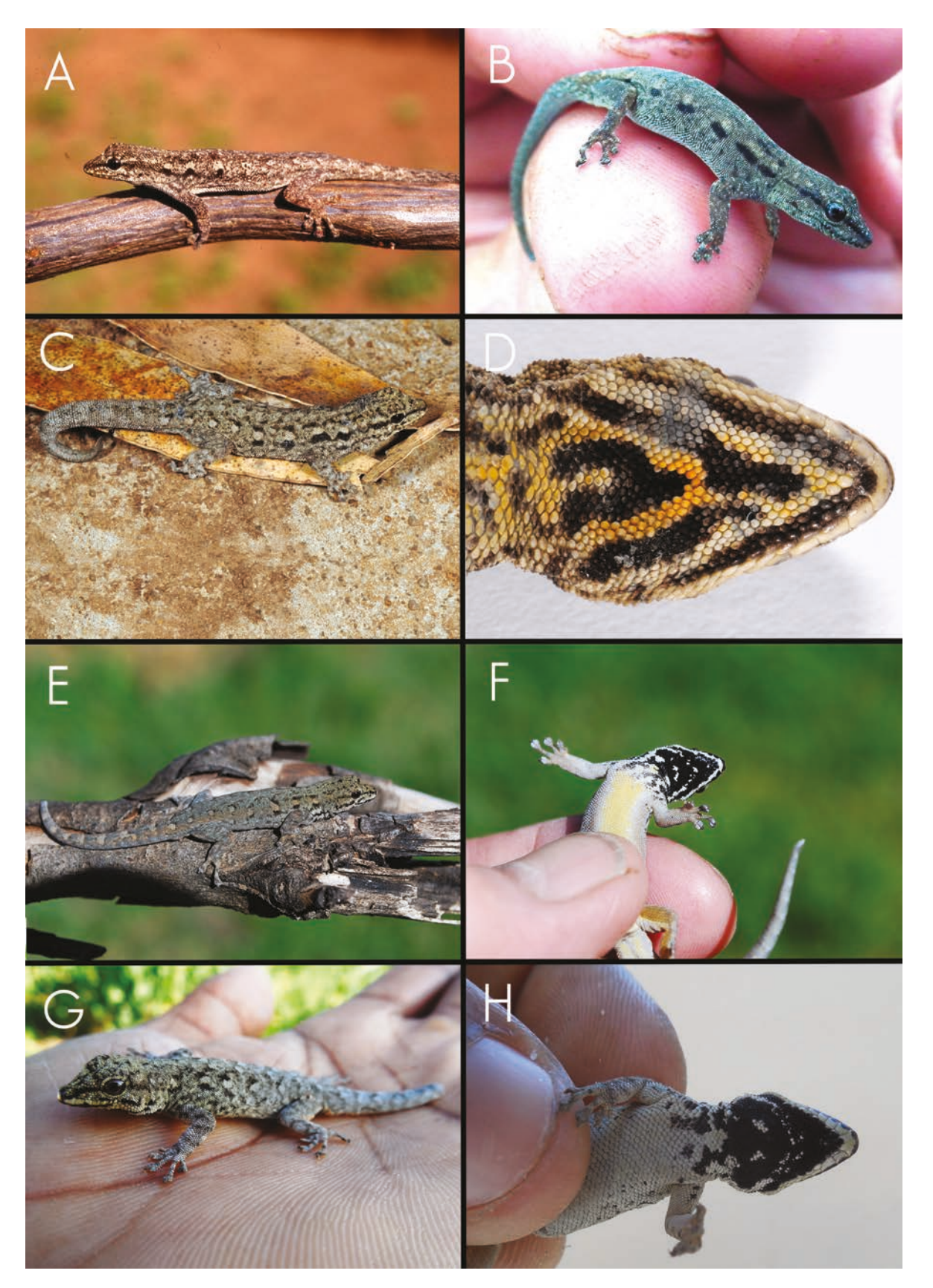


Figure 26. Photos in life of L. cf. gutturalis from (A) Jinka, South West Region, (B) Dolo Mena, Oromia Region, and (C–D) Debre Markos, Amhara Region, Ethiopia, and Lygodactylus sp. from (E–F) Maasai Mara, Rift Valley Province, Kenya and (G–H) Dodoma, Dodoma Region, Tanzania. Photos by Tim Spawls (A–B), Tomáš Mazúch (C–D), and Steve Spawls (E–H).

suggest that during the very last period of the Late Miocene and the posterior early Pliocene, the Congo Basin became humid again, leading to new dispersal events and connectivity along the Congo Basin and between the eastern and western slopes of the Albertine Rift (Couvreur et al. 2021), which may have facilitated secondary contacts between species. Such a scenario of multiple vicariance events, linked to climatic fluctuation and geological events during the Miocene between Central/West and East Africa, as suggested by Couvreur et al. (2021), seems to have contributed to the diversification of Lygodactylus.

CONCLUSION

We provide a complete integrative approach for the L. gutturalis subgroup, which revealed cryptic diversity that we rectified with the description of five new taxa, the revalidation of another, and the tentative proposal of one additional candidate species, all previously considered to be conspecific. We also revisited the L. angularis group to revalidate two additional taxa. As a consequence of this work, we elevate the number of recognized Lygodactylus species from 82 to 90. Moreover, the morphological variation found within L. angularis suggests a more extensive cryptic diversification within this group that requires further investigation. Additional work in some regions of Africa, including Ethiopia, Somalia, Kenya, and Tanzania may lead to the description of additional species. Diversification events during the Late Miocene (between 5–15 Mya) are likely linked to the expansion of African savannahs and the establishment of climatic forest refugia. This suggests that the L. gutturalis group is the result of a non-adaptative radiation, a consequence of multiple vicariance events during the Miocene that fragmented and prevented genetic connectivity between morphologically and ecologically similar taxa.

SUPPLEMENTARY DATA

Supplementary data is available at Zoological Journal of the Linnean Society Journal online.

ACKNOWLEDGEMENTS

This work was supported by National Funds through FCT-Fundação para a Ciência e a Tecnologia in the scope of the project UIDP/50027/2020. Work was co-funded by the project NORTE-01-0246-FEDER-000063 supported by Norte Portugal Regional Operational Programme (NORTE2020), under the PORTUGAL 2020 Partnership Agreement, through the European Regional Development Fund (ERDF). J.L.-R.'s visit to RMCA was possible thanks to SYNTHESYS + BE-TAF 2022. J.L.-R. is currently supported by Fundação BIOPOLIS contract BIOPOLIS 2022-18. Fieldwork by E.G. in DRC was funded by the Percy Sladen Memorial Fund, an IUCN/SSC Amphibian Specialist Group Seed Grant, research funds from the Department of Biology at Villanova University, two National Geographic Research and Exploration Grants (nos 8556-08, WW-R018-17), the University of Texas at El Paso (UTEP), and the US National Science Foundation (DEB-1145459); E.G. and C.K. thank their field companions Mwenebatu M. Aristote, Wandege M. Muninga, Maurice Luhumyo, John and Felix Akuku, and the late Asukulu M'Mema. The Centre de Recherche en Sciences Naturelles (CRSN) provided project support and permits, and we thank the Institut Congolais pour la Conservation de la Nature for permits to work in protected areas. A.M.B. was supported by National Science Foundation Grant DEB 2146654. Thanks to Instituto Nacional da

Biodiversidade e Conservação (INBC) within the Ministry of Culture, Tourism and Environment (MCTE) of Angola and especially to the Director of INBC, Albertina Nzuzi, for issuing research and export permits (no. 01/2021). We thank Fernanda Lages and Instituto Superior de Ciências da Educação da Huíla (ISCED) for logistical support. Thanks to Vladimir Russo from Fundação Kissama for critical administrative and logistical support. We also thank Centre for Molecular Analysis (CTM) workers (especially Susana Lopes, Sofia Mourão, and Patricia Ribeiro) at CIBIO for their tireless work and support in the molecular laboratory, and Fatima Linares and Alicia de Flores from Centro de Instrumentación Científica of Granada (CIC) for her incredible work on the CT scanning and SEM, respectively. The CT-scans of L. heeneni and L. paurospilus were done by Aurore Mathys of the Royal Museum for Central Africa. We thank Muofhe Tshibalanganda (Central Analytic Facilities, Stellenbosch University) for performing CT-scanning of PEM material. Select CT scans were produced as part of the open Vertebrate (oVert) project (National Science Foundation (NSF): DBI #1701714). W.C. thanks the Wild Bird Trust, which administrates the National Geographic Okavango Wilderness Project (2015-2019 National Geographic Society grant) and the Angolan Ministry of Environment Institute of Biodiversity (MINAMB) for a collecting and export permit (151/INBAC/MINAMB/2019). Alberto Sanchez-Vialas (MNCN) provided logistic support at the MNCN and photographs of type material. Nicolas Vidal (MNHN), Stevie Kennedy-Gold (MCZ), and Lauren Scheinberg (CAS) provided valuable material or CT scans for this project. Thanks to Frank Tillack (ZMB), Frank T. Burbrink (AMNH), and Lauren Vonnahme (AMNH) for providing photographs of the L. gutturalis (paratype) and L. depressus (holotype), respectively. Steve Spawls, Tim Spawls, Tomáš Mazúch, and Caspian Johnson contributed photographic records. Special thanks to the late Gerald Dunger for his photographs of L. gutturalis from Nigeria, which were donated to Steve Spawls with the hope that they would contribute to scientific knowledge.

DATA AVAILABILITY

The specimens in this study are in the collections specified in the Material and Methods section. CT scan data is available in Table S3 and Tomogram series for all scans are available on Morphosource.org. All sequences generated in this work have been deposited in GenBank. All other morphometric data are available in the Supporting Information, (Supporting Information Files S4–S11). This article and associated nomenclatural acts are registered in ZooBank.

REFERENCES

Allen KE, Greenbaum E, Hime PM et al. Rivers, not refugia, drove diversification in arboreal, sub-Saharan African snakes. Ecology and Evolution 2021;11:6133–52. https://doi.org/10.1002/ece3.7429

Auliya M, Wagner P, Böhme W. The herpetofauna of the Bijagós archipelago, Guinea-Bissau (West Africa) and a first country-wide checklist. *Bonn Zoological Bulletin* 2012;**61**:255–81.

Bannikov AG, Darevsky LS. Lygodactylus angularis grzimeki subsp. n. Bannikov et Darevsky from the Lake Manyara National Park, Tanzania. Zoologicheskii Zhurnal 1969;48:452–5. [in Russian]

Bauer AM, de Silva A, Greenbaum E et al. A new species of day gecko from high elevation in Sri Lanka, with a preliminary phylogeny of Sri Lankan Cnemaspis (Reptilia, Squamata, Gekkonidae). Zoosystematics and Evolution 2007;83:22–32. https://doi.org/10.1002/mmnz. 200600022

Bauer A, Günther R. An annotated type catalogue of the geckos (Reptilia: Gekkonidae) in the Zoological Museum, Berlin. *Mitteilungen aus dem Museum für Naturkunde in Berlin* 1991;**67**:279–310.

Bauer AM, Tchibozo S, Pauwels OSG *et al.* A review of the gekkotan lizards of Bénin, with the description of a new species of *Hemidactylus* (Squamata: Gekkonidae). *Zootaxa* 2006;**1242**:1–20.

- Bandelt HJ, Forster P, Röhl A. Median-joining networks for inferring intraspecific phylogenies. *Molecular Biology and Evolution* 1999;**16**:37–48. https://doi.org/10.1093/oxfordjournals.molbev.a026036
- Behangana M, Magala R, Katumba R *et al.* Herpetofaunal diversity and community structure in the Murchison Falls-Albert Delta Ramsar site, Uganda: Herpetofaunal diversity. *European Journal of Ecology* 2020;**6**:1–17. https://doi.org/10.17161/eurojecol.v6i2.13792
- Belluardo F, Quirós DD, Lobón-Rovira J *et al.* Uncovering the herpetological diversity of small forest fragments in south-eastern Madagascar (Haute Matsiatra). *Zoosystematics and Evolution* 2021;**97**:315–43. https://doi.org/10.3897/zse.97.63936
- Benson DA, Cavanaugh M, Clark K et al. GenBank. Nucleic Acids Research 2013;41:D36-42. https://doi.org/10.1093/nar/gks1195
- Bocage JVB. Mélanges erpétologiques. II. Sur quelques reptiles et batraciens nouveaux, rares ou peu connus d'Afrique occidentale. *Jornal de Sciencias Mathematicas, Physicas e Naturaes* 1873;4:209–27.
- Botts EA, Erasmus BFN, Alexander GJ. Geographic sampling bias in the South African Frog Atlas Project: Implications for conservation planning. *Biodiversity and Conservation* 2011;**20**:119–39. https://doi.org/10.1007/s10531-010-9950-6
- Boulenger GA. Catalogue of the Lizards in the British Museum (Nat. Hist.)

 I. Geckonidae, Eublepharidae, Uroplatidae, Pygopodidae, Agamidae.
 London: Trustees of the British Museum, 1885.
- Branch WR, Bayliss J, Tolley KA. Pygmy chameleons of the *Rhampholeon platyceps* complex (Squamata: Chamaeleonidae): Description of four new species from isolated 'sky islands' of northern Mozambique. *Zootaxa* 2014;**3814**:1–36. http://doi.org/10.11646/zootaxa.3814.1.1
- Branch WR, Cunningham M, Bauer AM, Alexander G, Harrison JA, Turner AA, Bates MF. A plan for phylogenetic studies of southern African reptiles. In: *Proceedings of a workshop held at Kirstenbosch, Biodiversity Series 5,* 48 pp. Pretoria: South African Biodiversity Institute, 2006.
- Broadley DG. The herpetofauna of northern Mwinilunga District, northwestern Zambia. *Arnoldia (Zimbabwe)* 1991;**9**:519–38.
- Broadley DG. The reptilian fauna of the Democratic Republic of the Congo (Congo-Kinshasa). In: Schmidt KP, Noble GK (eds), Contributions to the Herpetology of the Belgian Congo. Lawrence: Society for the Study of Amphibians and Reptiles, 1998, ix–xxxiii.
- Broadley DG. *Pachydactylus katanganus* de Witte 1953, a species endemic to the Upemba National Park (Sauria: Gekkonidae). *African Journal of Herpetology* 2003;**52**:69–70. https://doi.org/10.1080/21564574. 2003.9635479
- Broadley DG, Cotterill FPD. The reptiles of southeast Katanga, an overlooked 'hot spot'. *African Journal of Herpetology* 2004;**53**:35–61. https://doi.org/10.1080/21564574.2004.9635497
- Carranza S, Arnold EN. A review of the geckos of the genus *Hemidactylus* (Squamata: Gekkonidae) from Oman based on morphology, mitochondrial and nuclear data, with descriptions of eight new species. *Zootaxa* 2012;3378:1–95. https://doi.org/10.11646/zootaxa.3378.1.1
- Castiglia R, Annesi F. The phylogenetic position of *Lygodactylus angularis* and the utility of using the 16S rDNA gene for delimiting species in *Lygodactylus* (Squamata, Gekkonidae). *Acta Herpetologica* 2011;**6**:35–45. https://doi.org/10.13128/Acta Herpetol-9577
- Chirio L, Ineich I. Biogeography of the reptiles of the Central African Republic. *African Journal of Herpetology* 2006;**55**:23–59. https://doi.org/10.1080/21564574.2006.9635538
- Chirio L, LeBreton M. Atlas des Reptiles du Cameroun. Paris: Muséum national d'Histoire naturelle, IRD Éditions, 2007.
- Collyer ML, Adams DC. RRPP: An R package for fitting linear models to high-dimensional data using residual randomization. *Methods in Ecology and Evolution* 2018;**9**:1772–9. https://doi.org/10.1111/2041-210X.13029
- Conradie W, Bittencourt-Silva G, Engelbrecht HM *et al.* Exploration into the hidden world of Mozambique's sky island forests: New discoveries of reptiles and amphibians. *Zoosystematics and Evolution* 2016;**92**:163–80. https://doi.org/10.3897/zse.92.9948

- Couvreur TL, Dauby G, Blach-Overgaard A et al. Tectonics, climate and the diversification of the tropical African terrestrial flora and fauna. Biological Reviews 2021;96:16–51. https://doi.org/10.1111/brv.12644
- Davis HR, Chan KO, Das I et al. Multilocus phylogeny of Bornean bent-toed geckos (Gekkonidae: *Cyrtodactylus*) reveals hidden diversity, taxonomic disarray, and novel biogeographic patterns. *Molecular Phylogenetics and Evolution* 2020;**147**:106785. https://doi.org/10.1016/j.ympev.2020.106785
- de Lisle HF, Nazarov RA, Raw LRG, Grathwohl J. Gekkota: A Catalog of Recent Species. Winnipeg: Privately published, 2013. [First Edition]
- de Lisle HF, Nazarov RA, Raw LRG, Grathwohl J. *Gekkota: A Catalog of Recent Species*. Privately published online, 2016. [Second Edition]
- de Queiroz K. Species concepts and species delimitation. Systematic Biology 2007; 56:879–86. https://doi.org/10.1080/10635150701701083
- de Witte GF. Description de reptiles nouveaux provenant du Katanga (1930-31). Revue de Zoologie et de Botanique Africaines 1933;23:185-92.
- de Witte GF. Batraciens et reptiles. In: de Witte GF (ed.), Exploration du Parc National Albert. Mission G.F. de Witte (1933-1935). Vol. 33. Bruxelles: Institut des Parcs Nationaux du Congo Belge, 1941.
- de Witte GF. Reptiles. In: de Witte GF (ed.), Exploration du Parc National de l'Upemba, Mission G. F. de Witte en collaboration avec avec W. Adam, A. Janssens, L. Van Meel et R. Verheyen (1946–1949). Bruxelles: Institut des Parcs Nationaux du Congo Belge, vol. 6, 1953. 322 pp, pls. XLI.
- de Witte GF. Reptiles. In: de Witte GF (ed.), Exploration du Parc National de la Garamba. Mission H. D. Saeger en collaboration P. Baert, G. Demoulin, I. Denisoff, J. Martin, M. Micha, A. Noirfalise, P. Schoemaker, G. Troupin et J. Verschuren (1949–1952). Vol. 48. Bruxelles: Institut des Parcs Nationaux du Congo Belgevol. 48, 1966.100 pp.
- Dowsett-Lemaire F, Dowsett RJ, Dyer M. Malawi. In: Fishpool LDC, Evans MI (eds), Important Bird Areas in Africa and Associated Islands. Newbury and Cambridge: Pisces Publications and BirdLife International, 2001, 539–555.
- Dunger GT. The lizards and snakes of Nigeria, Part 4: Geckos of Nigeria. The Nigerian Field 1968;33:18–46.
- Etard A, Morrill S, Newbold T. Global gaps in trait data for terrestrial vertebrates. *Global Ecology and Biogeography* 2020;**29**:2143–58. https://doi.org/10.1111/geb.13184
- FitzSimons V. Preliminary descriptions of new forms of South African Reptilia and Amphibia, from the Vernay-Lang Kalahari Expedition, 1930. *Annals of the Transvaal Museum* 1932;15:35–40.
- Gamble T, Bauer AM, Colli GR et al. Coming to America: Multiple origins of New World geckos. *Journal of Evolutionary Biology* 2011;**24**:231–44. https://doi.org/10.1111/j.1420-9101.2010.02184.x
- Gippner S, Travers SL, Scherz MD et al. A comprehensive phylogeny of dwarf geckos of the genus Lygodactylus, with insights into their systematics and morphological variation. Molecular Phylogenetics and Evolution 2021;165:107311. https://doi.org/10.1016/j. ympev.2021.107311
- Greenbaum E. Emerald Labyrinth: A Scientist's Adventures in the Jungles of the Congo. Lebanon: ForeEdge, 2017.
- Greenbaum E, Dowell Beer SA, Wagner P et al. Phylogeography of Jackson's forest lizard Adolfus jacksoni (Sauria: Lacertidae) reveals cryptic diversity in the highlands of East Africa. Herpetological Monographs 2018;32:51–68. https://doi.org/10.1655/HERPMONOGRAPHS-D-18-00005.1
- Greenbaum E, Kusamba C. Conservation implications following the rediscovery of four frog species from the Itombwe Natural Reserve, eastern Democratic Republic of the Congo. *Herpetological Review* 2012;43:253–9.
- Günther A. Report on a collection of reptiles and batrachians transmitted by Mr. H. H. Johnston, C. B., from Nyassaland. *Proceedings of the Zoological Society of London* 1893;1892:555–8. https://doi.org/10.1111/j.1096-3642.1892.tb01781.x
- Håkansson NT. An annotated checklist of reptiles known to occur in the Gambia. *Journal of Herpetology* 1981;**15**:155–61. https://doi.org/10.2307/1563375

- Haagner GV, Branch WR, Haagner AJF. Notes on a collection of reptiles from Zambia and adjacent areas of the Democratic Republic of the Congo. *Annals of the Eastern Cape Museums* 2000;1:1–25.
- Hillis DM. Species delimitation in herpetology. *Journal of Herpetology* 2019;**53**:3–12. https://doi.org/10.1670/18-123
- Hirschfeld M, Rödel MO, Blackburn DC et al. Two new species of long-fingered frogs of the genus Cardioglossa (Anura: Arthroleptidae) from Central African rainforests. African Journal of Herpetology 2015;64:81–102. https://doi.org/10.1080/21564574.2015.105210
- Hoang DT, Chernomor O, Von Haeseler A et al. UFBoot2: Improving the ultrafast bootstrap approximation. Molecular Biology and Evolution 2018;35:518–22. https://doi.org/https://doi:/10.1093/molbev/msx281
- Jesus J, Brehm A, Harris DJ. Phylogenetic relationships of *Lygodactylus* geckos from the Gulf of Guinea islands: rapid rates of mitochondrial DNA sequence evolution? *Herpetological Journal* 2006; **16**(3): 291–295. https://doi.org/10.1016/j. ympey.2004.11.006.
- Kalyaanamoorthy S, Minh BQ, Wong TKF et al. ModelFinder: Fast model selection for accurate phylogenetic estimates. Nature Methods 2017;14:587–9. https://doi:/10.1038/nmeth.4285
- Kluge AG. Checklist of gekkonid lizards. Smithsonian Herpetological Information Service 1991;85:1–35. https://doi.org/10.5479/ si.23317515.85.1
- Kluge AG. Gekkonoid Lizard Taxonomy. San Diego: International Gecko Society, 1993.
- Kluge AG. Gekkotan lizard taxonomy. *Hamadryad* 2001;**26**:1–209.
- Lanna FM, Werneck FP, Gehara M et al. The evolutionary history of Lygodactylus lizards in the South American open diagonal. Molecular Phylogenetics and Evolution 2018;127:638–45. https://doi.org/10.1016/j.ympev.2018.06.010
- Lanza B. Amphibians and reptiles of the Somali Democratic Republic: Check list and biogeography. *Biogeographia* 1990;**14**:407–65. https://doi.org/10.21426/B614110318
- Largen MJ, Spawls S. Amphibians and Reptiles of Ethiopia and Eritrea. Frankfurt am Main: Chimaira, 2010.
- Largen MJ, Spawls S. Lizards of Ethiopia (Reptilia Sauria): An annotated checklist, bibliography, gazetteer and identification. *Tropical Zoology* 2006;19:21–109.
- Larson TR, Castro D, Behangana M et al. Evolutionary history of the river frog genus Amietia (Anura: Pyxicephalidae) reveals extensive diversification in Central African highlands. Molecular Phylogenetics and Evolution 2016;99:168–81. https://doi.org/10.1016/j. ympev.2016.03.017
- Laurent RF. Reptiles et batraciens nouveaux du massif du Mont Kabobo et du plateau des Marungu. Revue de Zoologie et de Botanique Africaines 1952;46:18–34.
- Leaché AD, Rödel MO, Linkem CW et al. Biodiversity in a forest island: reptiles and amphibians of the Togo Hills, Kyabobo National Park, Ghana. Amphibian & Reptile Conservation 2006;4:22–45.
- LeBreton M. A Working Checklist of the Herpetofauna of Cameroon. Amsterdam: UICN: Netherlands Committee for IUCN, 1999.
- Lobón-Rovira J, Bauer AM. Bone-by-bone: A detailed skull description of the white-headed dwarf gecko *Lygodactylus picturatus* (Peters, 1870). *African Journal of Herpetology* 2021;**70**:75–94. https://doi.org/10.1080/21564574.2021.1980120
- Lobón-Rovira J, Rocha S, Gower DJ et al. The unexpected gecko: A new cryptic species within *Urocotyledon inexpectata* (Stejneger, 1893) from the northern granitic Seychelles. *Zootaxa* 2022;**5150**:556–78. doi:https://doi.org/10.11646/zootaxa.5150.4.5
- Loveridge A. Description of a new species of gecko from Tanganyika Territory, Africa. *Proceedings of the United States National Museum* 1928;72:1-2.
- Loveridge A. New geckos of the genus Lygodactylus from Somaliland, Sudan, Kenya, and Tanganyika. Proceedings of the Biological Society of Washington 1935;48:195–200.
- Loveridge A. Revision of the African lizards of the family Gekkonidae. Bulletin of the Museum of Comparative Zoology 1947;**98**:1–469.

- Loveridge A. A startlingly turquoise-blue gecko from Tanganyika. *Journal* of the East African Natural History Society 1952; **20**:446.
- Loveridge A. Status of new vertebrates described or collected by Loveridge. Journal of the East Africa Natural History Society 1960;23:250–80.
- Maderson PFA. The epidermal glands of *Lygodactylus* (Gekkonidae, Lacertilia). *Breviora* 1968; **288**:1–35.
- Malonza PK, Bauer AM, Granthon C *et al.* A new species of gecko of the genus *Lygodactylus* (Sauria: Gekkonidae) from southeastern Kenya. *Zootaxa* 2019;**4609**:308–20. https://doi.org/10.11646/zootaxa.4609.2.6
- Malonza PK, Granthon C, Williams DA. A new species of dwarf gecko in the genus *Lygodactylus* (Squamata: Gekkonidae) from central Kenya. *Zootaxa* 2016;**4061**:418–28. https://doi.org/10.11646/zootaxa.4061.4.6
- Marlier G. Recherches hydrobiologiques au lac Tumba (Congo Belge, Province de l'Equateur). *Hydrobiologia* 1958;**10**:352–85. https://doi.org/10.1007/BF00142195
- Marques MP, Ceríaco LM, Buehler MD *et al.* A revision of the dwarf geckos, genus *Lygodactylus* (Squamata: Gekkonidae), from Angola, with the description of three new species. *Zootaxa* 2020;**4853**:301–52. https://doi.org/10.11646/zootaxa.4853.3.1
- Mezzasalma M, Andreone F, Aprea G et al. Molecular phylogeny, biogeography and chromosome evolution of Malagasy dwarf geckos of the genus *Lygodactylus* (Squamata, Gekkonidae). *Zoologica Scripta* 2017;**46**:42–54. https://doi.org/10.1111/zsc.12188
- Miller MA, Pfeiffer W, Schwartz T. Creating the CIPRES Science Gateway for inference of large phylogenetic trees. In: Gateway Computing Environments Workshop, p. 8. New Orleans: Conference Proceedings, 2010. https://doi.org/10.1109/GCE.2010.5676129
- NASA. Colored SRTM Elevation Model. Version 2000–1. 2000. https://www.jpl.nasa.gov/images. [accessed 14 October 2022]
- Nguyen LT, Schmidt HA, Von Haeseler A *et al.* IQ-TREE: A fast and effective stochastic algorithm for estimating maximum-likelihood phylogenies. *Molecular Biology and Evolution* 2015;**32**:268–74. https://doi.org/10.1093/molbev/msu300
- Nicolas V, Fabre PH, Bryja J et al. The phylogeny of the African wood mice (Muridae, Hylomyscus) based on complete mitochondrial genomes and five nuclear genes reveals their evolutionary history and undescribed diversity. Molecular Phylogenetics and Evolution 2020;144:106703. https://doi.org/10.1016/j. ympev.2019.106703
- Onditi KO, Demos TC, Kerbis Peterhans J *et al.* Historical biogeography, systematics, and integrative taxonomy of the non-Ethiopian speckled pelage brush-furred rats (*Lophuromys flavopunctatus* group). *BMC Ecology and Evolution* 2021;**21**:1–27. https://doi.org/10.1186/s12862-021-01813-w
- Owiunji I, Plumptre AJ. The importance of cloud forest sites in the conservation of endemic and threatened species of the Albertine Rift. In: Bruijnzeel LA, Scatena FN, Hamilton LS (eds), *Tropical Montane Cloud Forests: Science for Conservation and Management*. Cambridge: Cambridge University Press, 2011, 164–171.
- Palumbi SR. The polymerase chain reaction. In: Hillis D, Moritz C, Mable B (eds), Molecular Systematics. 2nd edn. Sunderland: Sinauer Associates, 1996, 205–247.
- Pasteur G. Diagnose de Lygodactylus picturatus scorteccii subsp. nov. (gekkonidés). Societe des Sciences Naturelles et Physiques du Maroc 1959;59(7):105–106.
- Pasteur G. Recherches sur l'évolution des lygodactyles, lézards Afro-Malgaches actuels. *Travaux de l'Institut Scientifique Chérifien, Zoologie* 1965(1964);**29**:1–132.
- Perret JL. Les Gekkonidae du Cameroun, avec la description de deux sous-espèces nouvelles. *Revue Suisse de Zoologie* 1963;**70**:47-60. https://doi.org/10.5962/bhl.part.117919
- Pietersen D, Verbught L, Davies J. Snakes and Other Reptiles of Zambia and Malawi. Cape Town: Struik Nature, 2021.
- Plana V. Mechanisms and tempo of evolution in the African Guineo–Congolian rainforest. *Philosophical Transactions of the Royal Society of London, Series B: Biological Sciences* 2004;**359**:1585–94. https://doi.org/10.1098/rstb.2004.1535

46

- Portik DM, Travers SL, Bauer AM *et al.* A new species of *Lygodactylus* (Squamata: Gekkonidae) endemic to Mount Namuli, an isolated 'sky island' of northern Mozambique. *Zootaxa* 2013;**3710**:415–35. https://doi.org/10.11646/zootaxa.3710.5.2
- Portillo F, Greenbaum E, Menegon M et al. Phylogeography and species boundaries of Leptopelis (Anura: Arthroleptidae) from the Albertine Rift. Molecular Phylogenetics and Evolution 2015;82:75–86. https://doi.org/10.1016/j.ympev.2014.09.024
- Portillo F, Branch WR, Conradie W et al. Phylogeny and biogeography of the African burrowing snake subfamily Aparallactinae (Squamata: Lamprophiidae). Molecular Phylogenetics and Evolution 2018;127:288–303. https://doi.org/10.1016/j.ympev.2018.03.019
- Puente M, Glaw F, Vieites DR *et al.* Review of the systematics, morphology and distribution of Malagasy dwarf geckos, genera *Lygodactylus* and *Microscalabotes* (Squamata: Gekkonidae). *Zootaxa* 2009;**2103**:1–76. https://doi.org/10.11646/zootaxa.2103.1.1
- Rambaut A, Drummond AJ, Xie D *et al.* Posterior summarisation in Bayesian phylogenetics using Tracer 1.7. *Systematic Biology* 2018;67:901–4. https://doi.org/10.1093/sysbio/syy032
- Rhen T, Sakata JT, Crews D. Effects of gonadal sex and incubation temperature on the ontogeny of gonadal steroid concentrations and secondary sex structures in leopard geckos, *Eublepharis macularius*. *General and Comparative Endocrinology* 2005;**142**:289–96. https://doi.org/10.1016/j.ygcen.2005.01.018
- Röll B. Lygodactylus gutturalis (Bocage). Sauria (Suppl.) 2005;27:645–8.
 Röll B, Pröhl H, Hoffmann KP. Multigene phylogenetic analysis of Lygodactylus dwarf geckos (Squamata: Gekkonidae). Molecular Phylogenetics and Evolution 2010;56:327–35. https://doi.org/10.1016/j.ympev.2010.02.002
- Rocha S, Vences M, Glaw F et al. Multigene phylogeny of Malagasy day geckos of the genus *Phelsuma*. Molecular *Phylogenetics and Evolution* 2009; **52**(2): 530–537. https://doi.org/10.1016/j. ympev.2009.03.032
- Ronquist F, Teslenko M, Van Der Mark P et al. MrBayes 3.2: Efficient Bayesian phylogenetic inference and model choice across a large model space. Systematic Biology 2012;61:539–42. https://doi.org/https://doi:/10.1093/sysbio/sys029
- Rösler H. Kommentierte Liste der rezent, subrezent und fossil bekannten Geckotaxa (Reptilia: Gekkonomorpha). *Gekkota* 2000;**2**:28–153.
- Rozas J, Ferrer-Mata A, Sánchez-del Barrio JC et al. DnaSP 6: DNA sequence polymorphism analysis of large data sets. Molecular Biology and Evolution 2017;34:3299–302. https://doi.org/10.1093/molbev/msx248
- Sayre RG, Comer P, Hak J, Josse C, Bow J. A New Map of Standardized Terrestrial Ecosystems of Africa. Washington DC: Association of American Geographers, 2013.
- Schätti B, Perret J. Catalogue révisé des types d'amphibiens et de reptiles du Muséum d'histoire naturelle de Genève. *Revue Suisse de Zoologie* 1997;**104**:357–70.

- Schätti B, Perret J, Mariaux J. 2002. Catalogue commenté des Types d'Amphibiens et de Reptiles du Muséum d'Histoire Naturelle de Genève. Genève: Muséum d'histoire naturelle Genève. Available from: http://www.ville-ge.ch/mhng/erpi/cat1.html [accessed 10 August 2022]
- Schlick-Steiner BC, Steiner FM, Seifert B *et al.* Integrative taxonomy: A multisource approach to exploring biodiversity. *Annual Review of Entomology* 2010;**55**:421–38. https://doi.org/10.1146/annurev-ento-112408-085432
- Schmidt KP. Contributions to the herpetology of the Belgian Congo based on the collection of the American Museum Congo Expedition, 1909-1915. Part I: turtles, crocodiles, lizards, and chamaeleons. Bulletin of the American Museum of Natural History 1919;39:385–624.
- Segniagbeto GH, Trape JF, Afiademanyo KM *et al.* Checklist of the lizards of Togo (West Africa), with comments on systematics, distribution, ecology, and conservation. *Zoosystema* 2015;37:381–402. https://doi.org/10.5252/z2015n2a7
- Spawls S, Howell K, Hinkel H, Menegon M. 2018. Field Guide to East African Reptiles. London: Bloomsbury.
- Stephens M, Smith NJ, Donnelly P. A new statistical method for haplotype reconstruction from population data. *The American Journal of Human Genetics* 2001;**68**:978–89. https://doi.org/10.1086/319501
- Struck TH, Cerca De Oliveira J. Cryptic species and their evolutionary significance. In: *Encyclopedia of Life Sciences (eLS)*, John Wiley & Sons, Ltd, 2019, 1–9 pp. https://doi.org/10.1002/9780470015902. a0028292
- Tamura K, Stecher G, Peterson D et al. MEGA6: Molecular Evolutionary Genetics Analysis V. 6.0. Molecular Biology and Evolution 2013;30:2725–9. https://doi.org/https://doi:/10.1093/molbev/mst197
- Thys van den Audenaerde DFE. Les Gekkonidae de l'Afrique centrale. Revue de Zoologie et de Botanique Africaines 1967;**76**:163–77.
- Timberlake J. Miombo Ecoregion Vision Report 2001 (rev. August 2011). Zimbabwe: Biodiversity Foundation for Africa, 2017.
- Tornier G. Die Crocodile, Schildkröten und Eidechsen in Kamerun. Zoologische Jahrbücher Abteilung für Systematik 1902; **15**(6): 663–677.
- Trape JF, Trape S, Chirio L. Lézards, Crocodiles et Tortues d'Afrique Occidentale et du Sahara. Montpellier: IRD, 2012. https://doi.org/10.4000/books.irdeditions.37699
- Travers SL, Jackman TR, Bauer AM. A molecular phylogeny of Afromontane dwarf geckos (*Lygodactylus*) reveals a single radiation and increased species diversity in a South African montane center of endemism. *Molecular Phylogenetics and Evolution* 2014;80:31–42. https://doi.org/10.1016/j.ympev.2014.07.017
- Vences M, Multzsch M, Gippner S et al. Integrative revision of the Lygodactylus madagascariensis group reveals an unexpected diversity of little brown geckos in Madagascar's rainforest. Zootaxa 2022;5179:1–61. https://doi.org/10.11646/zootaxa.5179.1.1
- Wermuth H. Liste der rezenten Amphibien und Reptilien. Gekkonidae, Pygopodidae, Xantusiidae. *Das Tierreich* 1965;**80**:I–XXIII, 1–246.